

**THE EFFECT OF TURBULENCE ON
MODELLING THE SEDIMENT
TRANSPORT IN THE SWASH ZONE**

MSc Thesis

Luuk van Weeghel | 13 July 2020

UNIVERSITY OF TWENTE.

THE EFFECT OF TURBULENCE ON MODELLING THE SEDIMENT TRANSPORT IN THE SWASH ZONE

MSc Thesis

by

LUUK VAN WEEGHEL

University of Twente
Faculty of Engineering Technology, Civil Engineering
Department of Water Engineering and Management
Marine and Fluvial Systems

To be defended the 9th of July 2020

| | | |
|-------------------|-----------------------------|-------------------------------|
| Daily supervisor: | Ir. J.W.M. Kranenburg | University of Twente |
| Thesis Committee: | Prof. Dr. S.J.H.M. Hulscher | University of Twente (Chair) |
| | Dr. ir. J.J. van der Werf | University of Twente/Deltares |
| | Dr. R. McCall | Deltares |
| | Dr. ir. G.H.P. Campmans | University of Twente |

Cover image: personal archive of the author

Abstract (English)

To better estimate whether coastal systems can withstand storms, it is important that the behaviour of the sand under the influence of the waves is understood in a higher extent. Especially for the part of the coast between the surf zone and the beach: the "swash zone" (Masselink & Puleo, 2006). How much and especially when is the sediment picked up by the water in the swash zone and when does it settle again. To model this behaviour the depth-averaged XBeach model is used. This is an open-source, depth-averaged model for hydrodynamics, sediment transport and morphology on and around the beach (Smit et al., 2009). There are three versions of XBeach, yet for this study the non-hydrostatic version was used. This research aims to investigate whether including effects of turbulence can improve the sediment transport as simulated by the model.

In order to validate the model, the results were compared with measured data from the RESIST dataset. The RESIST dataset was obtained in the CIEM flume at the Universitat Politècnica de Catalunya in Barcelona (Eichentopf et al., 2019). The XBeach model used in this study is based on the characteristics of the RESIST dataset. This means including the full-scale, a 1:15 sloped bed, a D_{50} of 0,00025 m and bichromatic waves with a period of 3,7 s and a (maximum) amplitude of 0,320 m.

Subsequently a turbulence data set has been made with a depth-dependent OpenFoam model that, unlike XBeach computes turbulence. In addition, the turbulence has also been estimated using an analytical expression (e.g., Reniers et al., 2013). Thereafter, a point-model has been made that models the sediment concentration using the Van Thiel-Van Rijn (VTVR) method (Van Thiel de Vries, 2009). In this model, both (depth-averaged) turbulent kinetic energy timeseries have been added to the hydrodynamics as modelled by XBeach. This was done by including the turbulent kinetic energy to the flow rate (Jongedijk, 2017). Finally, the new sediment concentrations have been translated into a sediment transport to see whether this modelled transport matches the measured transport to a higher extent. Subsequently, it was investigated whether some changes in the made assumptions could improve the results.

The use of this point-model has some disadvantages, such as neglecting advection and using one turbulence value. Also, the fact that the VTVR method is not intended for intra-wave models (Ruffini et al., 2020) can cause deviations in the results. However, it can be concluded that XBeach is quite good at modelling hydrodynamics in deeper water and in the swash zone but that the modelled sediment transport is quite bad. Yet, adding turbulence does not provide significant improvements in modelling the sediment concentration although it does make some small changes. Also, the transport of sediment is not improved by the inclusion of turbulence. Therefore, based on these results, it can be said that including turbulence with this approach does not significantly improve modelling sediment concentration and transport. In order to better establish these results, further research could use a 2DH model to include advection and (horizontal) diffusion which tend to be important processes (Masselink & Puleo, 2006). Another recommendation is to use a dataset that has multiple measurements in the vertical plane so that a better sediment concentration profile and depth-dependent turbulence can be used.

Abstract (Dutch)

Om beter in te kunnen schatten of kustsystemen bestand zijn tegen stormen, is het van belang dat het gedrag van het zand onder invloed van de golven beter wordt begrepen. Met name voor het deel van de kust tussen de branding en het strand: de 'swash zone' (Masselink & Puleo, 2006). Hoeveel en vooral wanneer wordt sediment opgepikt door het water in de swash zone en wanneer zakt dit weer naar de bodem? Om dit gedrag te modelleren kan het diepte-gemiddelde XBeach model gebruikt worden. Dit is een open-source, diepte-gemiddeld model voor hydrodynamica, sediment transport en morfologie op en rondom het strand (Smit et al., 2009). Er zijn drie versies van XBeach maar voor dit onderzoek is de non-hydrostatische versie gebruikt. Dit onderzoek is erop gericht om te kijken of het meenemen van effecten van turbulentie in het water het door het model gesimuleerde sediment transport kunnen verbeteren.

Om het model te kunnen verbeteren zijn de uitkomsten vergeleken met gemeten data van de RESIST-dataset. De RESIST dataset is verkregen in de CIEM stroomgoot bij de Universitat Politècnica de Catalunya in Barcelona (Eichentopf et al., 2019). Het opgezette XBeach model dat in dit onderzoek gebruikt is, is gebaseerd op de condities van de RESIST-dataset. Zoals een model op ware grootte, een initieel bodemprofiel met een 1:15 helling, een D_{50} van 0,00025 m en bichromatische golven met een periode van 3,7 s en een (maximale) amplitude van 0,320 m.

Vervolgens is er een turbulentiendataset gemaakt met een diepte-afhankelijk OpenFoam model dat, in tegenstelling tot XBeach, turbulente berekent. Daarnaast is de turbulentie ook analytisch benaderd (o.a. via Reniers et al. (2013)). Verder is er een punt-model gemaakt dat de sediment concentratie simuleert door middel van de Van Thiel-Van Rijn (VTVR) methode (Van Thiel de Vries, 2009). In dit puntmodel zijn beide (diepte-gemiddelde) turbulentie tijdreeksen toegevoegd aan de door XBeach berekende hydrodynamica. Dit is gedaan door de turbulente kinetische energie toe te voegen aan de stroomsnelheid (Jongedijk, 2017). Als laatste zijn de nieuwe sediment concentraties vertaald naar een sediment transport om te kijken of dit gemodelleerde transport beter overeenkomt met het gemeten transport. Nadien is er onderzocht of enkele wijzigingen in de gedane aannames de uitkomsten wellicht konden verbeteren.

Het gebruik van dit punt-model kent enkele nadelen zoals bijvoorbeeld het verwaarlozen van advectie en het gebruiken van één turbulentie waarde in de diepte. Ook het feit dat de VTVR-methode eigenlijk niet bedoeld is voor intra-golf modellen (Ruffini et al., 2020) kan afwijkingen in de resultaten veroorzaken. Toch kan geconcludeerd worden dat XBeach vrij goed is in het simuleren van de hydrodynamica in dieper water en in de swash zone maar dat het niet zo goed is wat betreft het sediment transport. Daarnaast levert het toevoegen van turbulentie geen aanzienlijke verbeteringen op in het modelleren van de sediment concentratie, wel resulteert het in kleine veranderingen. Het transport van sediment wordt ook niet beter met het toevoegen van turbulentie. Daarom kan op basis van deze resultaten gezegd worden dat het meenemen van turbulentie, via deze aanpak, geen significante verbeteringen oplevert in het modelleren van de sediment concentratie en transport. Om dit beter vast te kunnen stellen zou er bij nader onderzoek gebruik gemaakt kunnen worden van een 2DH model om advectie en (horizontale) diffusie wel mee te kunnen nemen aangezien dit vrij belangrijke processen lijken te zijn (Masselink & Puleo, 2006). Ook is het aan te raden om een dataset te gebruiken die meerdere metingen heeft in het verticale vlak zodat er een beter sediment concentratie profiel en diepte-afhankelijke turbulentie gebruikt kunnen worden.

Acknowledgements

Performing this research and writing this Thesis has been an exciting journey. These were my last steps of finishing my master 'River and Coastal Engineering' at the University of Twente but also my last steps of being a student. Therefore, I would like to take a moment to express my sincere gratitude to the people who helped me during this period.

First of all, I would like to thank Joost Kranenburg, my daily supervisor from the University of Twente, for his endless time, enthusiasm and guidance which helped me stay on the right track. Unless the inevitable obstacles associated with working from home due to the Coronavirus, Joost was always available for questions and digital meetings which helped me very much when I got jammed.

Likewise, I would like to thank my other supervisors, Suzanne Hulscher, Jebbe van der Werf, Robert McCall and Geert Campmans, for their time of giving my very helpful suggestions and feedback in order to improve my research. It really helped a lot!

My gratitude also goes to my fellow students who assisted me during my Thesis but as well as in the period before. They were nice sparring partners to help me when I got stuck but especially made the days at the University a lot of fun. This definitely contributed to how much I enjoyed studying.

In the end I would like to thank all my friends and family for being so supportive and patient the last months of my study. I unfortunately could not spend so much time with you, but it had to give way for the greater good: performing proper research and delivering a nice Thesis.

I hope this succeeded well and that you will enjoy reading this Thesis. Which hopefully could give you some idea of the importance of the effects of turbulence in the modelling sediment transport swash zone. If you still have any questions left, do not hesitate to contact me.

Many thanks again!

Luuk van Weeghel
Enschede, July 2020

Contents

| | |
|---|------|
| List of Figures | viii |
| List of Tables | xi |
| List of Symbols | xii |
| 1. Introduction | 1 |
| 1.1 Background | 1 |
| 1.1.1 The swash zone | 1 |
| 1.1.2 The used models and dataset | 1 |
| 1.2 Relevance of this research | 2 |
| 1.3 Objective and research questions | 2 |
| 1.4 Scope | 3 |
| 1.5 Outline of this Thesis | 3 |
| 2. Theory | 4 |
| 2.1 The swash zone | 4 |
| 2.2 The XBeach model | 4 |
| 2.3 The RESIST dataset | 5 |
| 2.3.1 Measurement equipment | 5 |
| 2.4 Sediment transport | 5 |
| 2.4.1 Suspended transport | 6 |
| 2.4.2 Equilibrium concentration | 7 |
| 2.4.3 Van Thiel-Van Rijn method | 7 |
| 2.4.4 Equations in XBeach | 8 |
| 2.4.5 Translating point measurements to depth-averaged values | 8 |
| 2.5 Turbulence | 10 |
| 2.5.1 OpenFoam modelled turbulence | 10 |
| 2.5.2 Analytical approach of turbulence | 10 |
| 2.5.3 The effect of turbulence on sediment transport | 11 |
| 2.6 Including turbulence in the sediment transport model | 11 |
| 3. Methodology | 13 |
| 3.1 Research approach | 13 |
| 3.2 The use of the dataset | 14 |
| 3.3 Setting up XBeach for this research | 14 |
| 3.3.1 The applied waves | 14 |
| 3.3.2 The initial bed | 16 |
| 3.4 Validating XBeach output with RESIST data | 17 |
| 3.4.1 Smoothing the data | 17 |

| | | |
|-----------|--|-----------|
| 3.4.2 | Validating the hydrodynamics..... | 18 |
| 3.4.3 | Spectral analysis..... | 20 |
| 3.4.4 | Suspended Sediment Concentration..... | 20 |
| 3.4.5 | Applying the Rouse profile..... | 20 |
| 3.5 | The SSC point-model..... | 21 |
| 3.5.1 | The Van Thiel-Van Rijn approach..... | 21 |
| 3.5.2 | Equilibrium sediment concentration..... | 21 |
| 3.5.3 | Calibrating the inclusion of turbulence to the SSC model..... | 22 |
| 3.6 | The OpenFoam model..... | 22 |
| 3.7 | The behaviour of turbulence in the swash zone..... | 22 |
| 3.7.1 | Evaluating the results..... | 22 |
| 3.8 | Including turbulence in the SSC calculation..... | 22 |
| 3.9 | Sediment transport rates..... | 23 |
| 3.9.1 | Calculating sediment transport..... | 23 |
| 3.9.2 | Validating the sediment transport..... | 24 |
| 3.10 | Testing other approaches..... | 24 |
| 4. | Results: validating XBeach output with RESIST data..... | 26 |
| 4.1 | Hydrodynamics..... | 26 |
| 4.1.1 | Water surface elevation..... | 26 |
| 4.1.2 | Flow velocity..... | 26 |
| 4.1.3 | Spectral analysis..... | 27 |
| 4.2 | Suspended sediment..... | 28 |
| 4.2.1 | Rouse profile..... | 29 |
| 4.2.2 | Comparing depth-averaged SSC timeseries..... | 30 |
| 4.3 | Summary..... | 31 |
| 5. | Results: the characteristics of turbulence in the swash zone..... | 32 |
| 5.1 | Validating the OpenFoam model..... | 32 |
| 5.2 | Extracting the OpenFoam turbulence data..... | 33 |
| 5.2.1 | The behaviour of the turbulence..... | 33 |
| 5.3 | The relation between the processes..... | 35 |
| 5.4 | An analytical point-model for turbulence..... | 35 |
| 5.5 | Summary..... | 36 |
| 6. | Results: including turbulence in the model..... | 37 |
| 6.1 | SSC point-model with OpenFoam turbulence..... | 37 |
| 6.1.1 | Calibrating the amount of included turbulence..... | 37 |
| 6.1.2 | OpenFoam hydrodynamics..... | 37 |

| | | |
|-----------|--|-----------|
| 6.1.3 | XBeach hydrodynamics | 38 |
| 6.1.4 | Summarizing table..... | 39 |
| 6.2 | SSC point-model with analytical turbulence | 40 |
| 6.2.1 | Summarizing table..... | 41 |
| 6.3 | Quantitative SSC results..... | 41 |
| 6.4 | Sediment transport rates..... | 42 |
| 6.4.1 | Analysis of the similarities/discrepancies | 44 |
| 6.4.2 | Net sediment transport | 45 |
| 6.5 | Validating the sediment transport | 46 |
| 6.6 | Quantitative sediment transport results..... | 46 |
| 6.7 | Testing other approaches | 47 |
| 6.7.1 | Changing the roughness coefficient in XBeach | 47 |
| 6.7.2 | Varying the OpenFoam turbulence height | 48 |
| 6.7.3 | Varying the analytical turbulence height..... | 50 |
| 6.7.4 | Assuming a vertical uniformly distributed sediment concentration | 52 |
| 6.7.5 | Using a turbulence-based equilibrium concentration | 55 |
| 6.8 | Summary..... | 56 |
| 7. | Discussion | 57 |
| 7.1 | Validating XBeach output with RESIST data..... | 57 |
| 7.2 | The characteristics of turbulence in the swash zone | 57 |
| 7.3 | Including turbulence in the sediment model..... | 58 |
| 7.3.1 | SSC calculation..... | 58 |
| 7.3.2 | Sediment transport calculation | 58 |
| 7.4 | Testing other approaches | 59 |
| 8. | Conclusion and recommendations | 60 |
| 8.1 | Conclusions | 60 |
| 8.1.1 | XBeach validation | 60 |
| 8.1.2 | Characteristics of turbulence | 60 |
| 8.1.3 | Including turbulence in sediment models | 60 |
| 8.2 | Recommendations | 60 |
| | References | 62 |
| | Appendix A | 65 |
| | Appendix B..... | 67 |

List of Figures

| | |
|--|----|
| Figure 1. Typical example of the beach and the swash zone at the Dutch coast (picture made by the author) | 1 |
| Figure 2. Schematic cross-section of the beach and the limits of the swash zone. Figure from (Elfrink & Baldock, 2002) | 4 |
| Figure 3. The difference between bed load transport and suspended transport (Métivier & Meunier, 2003) | 6 |
| Figure 4. Rouse profile of the sediment concentration over the height. With $c(z)$ and c_a depicted for the case when the Rouse number (Rou) = 0.5. The Rouse number is represented by the power in Equation 2.8. Figure after (Teles et al., 2016) | 9 |
| Figure 5. The reference sediment concentration from the old model (a) versus the newly, adapted model (b) (Van der Zanden et al., 2017b) | 12 |
| Figure 6. Schematic diagram of the approach of this research | 13 |
| Figure 7. Created wave signal for the waves by using the Linear Wave Theory and the parameter values based on the ones from the RESIST dataset | 16 |
| Figure 8. Different bed profiles as they are measured in RESIST, see Eichentopf et al., (2019). The red graph is used as the initial bed in this research | 17 |
| Figure 9. The effect of smoothing the data. The data is smoothed over the timespan of 0,5 s ... | 18 |
| Figure 10. Schematic representation of the locations of the investigated measurement equipment at the offshore location (black arrows) and the swash location (red arrow). The black line represents a perfect 1:15 sloped bed as indication. The water surface elevation (blue line) is a snapshot from the XBeach model at $t=210$ s | 19 |
| Figure 11. The offset error of the OBS sensor. At the beginning of the timeseries this value of approximately 1,2 could only be caused by other factors since there are no waves yet to bring sediment into suspension. Therefore, there has been corrected for this value. | 20 |
| Figure 12. Comparison in water surface elevation between XBeach and RESIST for the offshore location (left) and the swash location (right). The default XBeach parameter values have been used for this validation | 26 |
| Figure 13. Comparison in flow velocity between XBeach and RESIST for the offshore location (left) and the swash location (right). The default XBeach parameter values have been used for this validation | 27 |
| Figure 14. Comparison of the power spectra of the water surface elevation at the offshore location (left) and swash location (right) | 27 |
| Figure 15. Comparison of the power spectra of the flow velocity at the offshore location (left) and swash location (right) | 28 |
| Figure 16. Comparison in SSC between XBeach and RESIST for the offshore location (left) and the swash location (right). Those locations are respectively 13,5 and 0,6 m from the SWL shoreline. Note: this difference could be caused by the way it is determined (fixed height vs depth-averaged) | 28 |
| Figure 17. The sediment concentrations as directly measured in the RESIST dataset (black curve) and the translation of those into depth-averaged values (green curve) | 29 |
| Figure 18. Depth-averaged SSC values versus the observed water depth. It shows that the peaks in SSC coincide with very shallow water | 30 |
| Figure 19. Comparing the XBeach SSC with the RESIST SSC after applying the Rouse profile to convert the point measurements into depth-averaged values. This comparison is performed at the swash location, which is 0,6 m from the SWL shoreline. | 31 |
| Figure 20. OpenFoam validation with respect to RESIST and XBeach | 32 |
| Figure 21. The presence of turbulence (at 3cm above the bed versus depth-averaged) over time as modelled by OpenFoam | 33 |
| Figure 22. A wave arriving at the beach with much Turbulent Kinetic Energy (TKE) arising near the water surface, indicated by the green arrow | 34 |

| | |
|--|----|
| Figure 23. Wave propagating onto the beach (green arrow) while the turbulence propagates down the water column (green circle)..... | 34 |
| Figure 24. Backwash is starting (green arrow) while the turbulence is decaying (green circle) | 34 |
| Figure 25. New wave is arriving with again high TKE near the water surface | 35 |
| Figure 26. Overview of all timeseries to see all processes happening at the same time | 35 |
| Figure 27. The depth-averaged and the near-bed analytical turbulence (based on Reniers et al. (2013)) versus the OpenFoam turbulence over time | 36 |
| Figure 28. The SSC outputs when different values for the calibration coefficient have been used. Is plot is made based on the OpenFoam hydrodynamics and turbulence. Yet for the XBeach hydrodynamics or the analytical turbulence the same effect occurs. | 37 |
| Figure 29. Results of the point-model with the OpenFoam hydrodynamics as input with turbulence included (pink graph) and without (blue graph). In here the calibration constant was set to 6. The SSC values from XBeach (red graph) and RESIST (depth-averaged; green graph) are presented as a reference. | 38 |
| Figure 30 Results of the point-model with the XBeach hydrodynamics as input with turbulence included (pink graph) and without (blue graph). In here the calibration constant was set to 6. The SSC values from XBeach (red graph) and RESIST (depth-averaged; green graph) are presented as a reference..... | 39 |
| Figure 31. Results of the point-model with the XBeach hydrodynamics as input with the analytically computed turbulence included (pink graph) and without (blue graph). It could be seen that the inclusion of turbulence creates peaks in the SSC concentration. In here the calibration constant was set to 6. The SSC values from XBeach (red graph) and RESIST (depth-averaged; green graph) are presented as a reference. | 41 |
| Figure 32. Quantitative results of the inclusion of OpenFoam turbulence and the analytical turbulence to the sediment point-model in relation to the depth-averaged observed SSC values. The calibration for the turbulence inclusion was set to 6. | 42 |
| Figure 33. Sediment transport of the point-model based on OpenFoam hydrodynamics (top) and on the XBeach hydrodynamics (bottom). The same plots but for a wider time interval (t=150 s to t=250 s) are given in Appendix B. | 43 |
| Figure 34. Sediment transport of the point-model based on the XBeach hydrodynamics with a decreased calibration factor (now being 3). | 44 |
| Figure 35. Relation between sediment transport and the water level based on different models/measurements. It shows that peaks in SSC (both positive and negative) coincide with bore arrival..... | 45 |
| Figure 36. The nRMSE, r^2 and difference in net sediment transport of all timeseries. The difference in net sediment transport in this case is the net sediment transport of the specific timeseries minus the observed net sediment transport. | 46 |
| Figure 37. The nRMSE, r^2 and difference in net sediment transport outcomes for the different Chézy roughness coefficients as indicated in the legend of the figure. There has only been looked at the XBeach model and the point-model with XBeach hydrodynamics since the point-model with OpenFoam hydrodynamics does not change when changing XBeach .. | 47 |
| Figure 38. Sediment transport as a result of the point-model but with different Chézy roughness coefficients used in XBeach | 48 |
| Figure 39. Different turbulence datasets with the new OpenFoam turbulence (yellow graph) in relation to the old OpenFoam turbulence (black graph) and the analytical turbulence (blue graph). | 49 |
| Figure 40. Differences in the quantitative validation of using the depth-averaged OpenFoam turbulence (red bar graphs) versus the OpenFoam turbulence at 3cm from the bed (purple bar graphs). The other bar graphs (blue & yellow) did not change but are presented as a reference..... | 50 |

| | |
|--|----|
| Figure 41. Different turbulence datasets with the new (near-bed) analytical turbulence (red graph) in relation to the old analytical turbulence (blue graph) and the OpenFoam turbulence (black graph)..... | 51 |
| Figure 42. Differences in the quantitative validation of using the depth-averaged analytical turbulence (yellow bar graphs) versus the analytical turbulence at the bed (purple bar graphs). The other bar graphs (blue & red) did not change but are presented as a reference. | 52 |
| Figure 43. Different sediment transport timeseries. With the ‘old’ sediment transport based on applying the Rouse profile (black graph) versus the assumed uniformly distributed sediment concentration (red graph) | 53 |
| Figure 44. Differences in the quantitative validation of applying a Rouse profile (top) versus using a uniform sediment distribution (bottom). Changing this sediment distribution also has an effect on the validation because the validation is based on comparing experimental values to the depth-averaged observed values (which are changed). Therefore, it is chosen to present and compare all bar graphs between the top and bottom plot..... | 54 |
| Figure 45. Several SSC graphs, including the SSC modelled with the equilibrium concentration based on the near-bed turbulence only (black graph)..... | 55 |
| Figure 46. Differences in the quantitative validation of using the VTVR method (yellow bar graphs) versus the method from Reniers et. al (2013) (purple bar graphs). The other bar graphs (blue & red) did not change but are presented as an indication | 56 |

List of Tables

| | |
|--|----|
| Table 1. Wave characteristics of the studied waves. Based on the waves used in the RESIST dataset. So, after Eichertopf et al., 2019..... | 14 |
| Table 2. The distances in m from the wave paddle at which all the measurement equipment is located. As an indication: the SWL shoreline is at 77,1 m from the wave paddle..... | 19 |
| Table 3. The quantitative validation of the OpenFoam water level and flow velocity in comparison with the measured ones and the ones modelled with XBeach..... | 32 |
| Table 4. The quantitative validation of XBeach and the point-model with and without the OpenFoam turbulence effects included. These quantitative results are from the comparison between the outcomes of the sediment point-model and the depth-averaged observed SSC values. The calibration coefficient for the amount of turbulence was set to 6..... | 40 |
| Table 5. The quantitative validation of XBeach and the point-model with and without the analytical turbulence effects included. These quantitative results are from the comparison between the outcomes of the sediment point-model and the depth-averaged observed SSC values. The calibration coefficient for the amount of turbulence was set to 6..... | 41 |
| Table 6. Net sediment transport over the interval from $t=151,6$ to $t=240,4$. The positive values indicating a net sediment transport towards the shore. The calibration coefficient for the amount of OpenFoam turbulence being 6 and for the analytical turbulence being 3..... | 45 |

List of Symbols

| Symbol (Roman alphabet) | Description | Unit |
|--------------------------------|--|------------------------------------|
| a | Height of the reference concentration | m |
| A_{ss} | Suspended load coefficient | |
| c | Sediment concentration | g/l |
| C | Chézy roughness value | m ^{1/2} /s |
| c_a | Reference sediment concentration | g/l |
| c_{eq} | Equilibrium sediment concentration | g/l |
| c_R | Calibration coefficient | - |
| c_k | Calibration coefficient | - |
| (dZ / dt)_{cr} | Critical slope of the wave | m/s |
| D₅₀ | Median grain diameter | m |
| D₉₀ | Cumulative percentile value of the sediment diameter | m |
| D* | Dimensionless sediment parameter | - |
| f_s | Sampling frequency | Hz |
| f₁ | Frequency of wave component 1 | Hz |
| g | Gravitational acceleration | m/s ² |
| h | Water depth | m |
| H₁ | Wave height of wave component 1 | m |
| k | Turbulent kinetic energy | m ² /s ² |
| k_{bed} | Turbulent kinetic energy at the bed | m ² /s ² |
| K | Wave number | m ⁻¹ |
| L | Wavelength | m |
| L_o | Wavelength in deep water | m |
| N | Number of subintervals | - |
| nRMSE | Normalized Root Mean Square Error | - |
| q_{sed} | Sediment transport | kg m ⁻¹ s ⁻¹ |
| r² | Correlation coefficient | - |
| R | Roller thickness | m |
| SSC | Suspended Sediment Concentration | g/l |
| S_r | Dissipation of turbulent kinetic energy | m ³ /s ³ |
| S_w | Source term for the turbulent kinetic energy | m ³ /s ³ |
| t | Time | s |
| T_{primary} | Wave period | s |
| T_{group} | Wave group period | s |
| T_{repetition} | Period after which the waves repeat itself exactly | s |

| | | |
|------------|---|-------------------|
| T_s | Sediment adaptation time | s |
| u | Flow velocity | m/s |
| u_1 | Horizontal velocity of wave component 1 | m/s |
| u_{cr} | Critical flow velocity | m/s |
| u_{init} | Initial flow velocity | m/s |
| u_{mg} | Running mean of the flow velocity | m/s |
| u_{mod} | Modified flow velocity | m/s |
| u_{rms} | Incident wave motion | m/s |
| u_{tot} | Horizontal water motion | m/s |
| u^* | Bed shear velocity | m/s |
| ν | Viscosity of the water | m ² /s |
| w_s | Sediment fall velocity | m/s |
| z | Distance from the bed | m |
| Z | Water surface elevation | m |

| <u>Symbol (Greek alphabet)</u> | <u>Description</u> | <u>Unit</u> |
|---------------------------------------|---|--------------------|
| α | Calibration constant | - |
| β | Factor in critical slope for bore turbulence | - |
| γ | Calibration constant | - |
| Δ | Ratio between the density of the sediment and the water | - |
| Δt | Temporal resolution of XBeach | s |
| ΔX | Horizontal spatial resolution | m |
| Δz | Vertical spatial resolution | m |
| ϵ_o | Porosity of the soil | - |
| ϵ_s | Suspended load efficiency | - |
| θ_1 | Water surface elevation of wave component 1 | m |
| κ | The Von Karmann constant | - |
| ρ | Density of the water | kg/m ³ |
| ρ_{sed} | Density of the sediment | kg/m ³ |
| τ_{bed} | Bed shear stress at the bed | N/m ² |
| τ_{XBeach} | Bed shear stress as modelled by XBeach | N/m ² |
| ω | Wave angular frequency | s ⁻¹ |

1. Introduction

1.1 Background

To be able to better protect people living next to the sea from floods, it is necessary to understand the morphologic behaviour of the (nearshore) seabed (Van Thiel de Vries, 2009). For instance, it is needed to know if the beach and the dunes are strong enough to protect us when a storm surge hits and how the beach (and dunes) recovers after a period of storms. This all depends on the amount of sediment being transferred from the subaqueous domain to the dry part of the beach and vice versa (Galiforni Silva, Wijnberg, & Hulscher, 2020). In other words; does (net) sediment transport occur and if so, how much and in which direction? Because of this connection between the sea and the beach, the swash zone is a very important region for the sediment transport and eventually the change in morphology (Masselink & Puleo, 2006). To be able to make predictions about beach morphodynamics, swash zone models could be used to simulate this behaviour.

1.1.1 The swash zone

The swash zone is the part of the coast that lies between the surf zone and the beach. In other words; the swash zone is that part of the beach alternately covered and exposed by uprush and backwash (Masselink & Puleo, 2006). See Figure 1 for a typical Dutch situation of waves arriving at the shore and alternately covering and exposing the beach. The time scale of swash motion is highly variable and ranges from seconds on calm, steep and reflective beaches to minutes on energetic, low-gradient and dissipative beaches (Butt & Russell, 1999). The swash zone is characterised by strong and unsteady flows, high levels of turbulence, large sediment transport rates and rapid morphological change (Puleo, Beach, Holman & Allen, 2000).



Figure 1. Typical example of the beach and the swash zone at the Dutch coast (picture made by the author)

1.1.2 The used models and dataset

In this study the XBeach model will be used. XBeach is used widely and including Rijkswaterstaat and Deltares to evaluate the safety at the Dutch coast (Deltares, n.d.). It was first developed as a model for predicting storm impacts (Roelvink et al., 2009).

The dataset that will be used in this research is the RESIST dataset. This dataset is obtained in a waver flume in Barcelona. In such a flume, a wave paddle creates waves which travel down the flume and eventually land on an artificial made beach to measure the effect.

Besides XBeach, OpenFoam will be used in this research as well. It will be used purely hydrodynamic (so no sediment transport) and will be used to generate a turbulence dataset.

1.2 Relevance of this research

A previous study about swash zone sediment transport and XBeach did conclude that the sediment concentrations in the swash zone in XBeach are not correct, while the hydrodynamics are (Ruffini et al., 2020). Another study concluded that there are some specific swash zone processes missing in XBeach, of which turbulence tends to be the most important one (Jongedijk, 2017). But despite their efforts, neither of these researches succeeded in improving XBeach significantly by adding/changing processes. Nevertheless, both these studies concluded that XBeach models the water depth and flow velocity quite well. But when it comes to the amount of sediment transport the model output differs from the measurements. This means that some processes are not (properly) included or that a small deviation in the modelled hydrodynamics can have large consequences for the sediment transport due to the non-linearity of this relation. The error could be caused by (the absence of) multiple processes, but as Jongedijk (2017) concluded, turbulence looks to be an important process not taken into account in the modelling of sediment transport in XBeach. Additionally, Van der Zanden et al. (2017) experimentally investigated the effect of turbulence on the Suspended Sediment Concentration (SSC) and found it to be of crucial importance, but this study was about the surf zone (which is seaward of the swash zone and where wave breaking take place, generating high levels of turbulence) and so it is yet unknown how important turbulence exactly is in the swash zone dynamics. Therefore, this research will be about including the effects of turbulence to see if and to what extent this improves the sediment transport in the swash zone.

Furthermore, until now no XBeach related research is done with the most recent wave flume dataset (RESIST). For instance, Ruffini et al. (2020) used the CoSSedM dataset and Jongedijk (2017) used to Bardex II dataset. This means that it would still be useful to compare XBeach outcomes with the RESIST dataset to look for deviations and to possibly come up with XBeach improvements. This dataset will be used since it is most recent but mainly because it contains bichromatic waves so it will be possible to study the effects in a wave group-averaged way.

1.3 Objective and research questions

The main objective is

“To what extent does including turbulence to sediment transport formulations improve the XBeach model results in comparison with the RESIST dataset?”

To reach this objective, the following research questions have been formulated:

- Q1. To what extent does XBeach model the hydrodynamics and the sediment transport correctly compared to measurements in the RESIST dataset?
- Q2. How does the modelled turbulent kinetic energy behave in the swash zone?
- Q3. To what extent could the inclusion of turbulence improve modelled sediment transport?

1.4 Scope

Some things fall outside of the scope of this. For instance, this research will not touch upon longshore sediment transport but only look at sediment transport in the cross-shore direction. This means that sediment that is potentially entrained due to longshore currents will not be considered. Furthermore, there will only be looked at beaches consisting out of (fine) sand and so gravel beaches will be disregarded. Despite this exclusion, this research can still be useful for sandy beaches existing in for instance the Netherlands. Also, the morphologic change of the bed will not be considered in this research. In this study the sediment transport will be modelled in terms of the Suspended Sediment Concentration (SSC) and so the bed load transport will not be considered explicitly.

1.5 Outline of this Thesis

Chapter 2 will briefly introduce the theoretical background and is an extension of the literature search conducted in the literature study (van Weeghel, 2020). Thereafter Chapter 3 will touch upon the methodology used to execute this research, which techniques/models are used and why. The results of the research are divided into multiple chapters: Chapter 4 will cover the results of the validation of XBeach in comparison with the RESIST measurements, Chapter 5 will show the behaviour of turbulence in the swash zone. Afterwards Chapter 6 shows the results of including the effects of turbulence in the Suspended Sediment Concentration (SSC) model and how this influences the eventual sediment transport. All these results will be discussed in Chapter 7. Finally, the conclusions, leading to the answers on the research questions, and the outlook to further research are presented in Chapter 8.

2. Theory

2.1 The swash zone

In the swash zone lots of different processes are present which all interact with each other and eventually sedimentation or erosion takes place (Masselink & Puleo, 2006). See Figure 2 for a schematic representation of the swash zone.

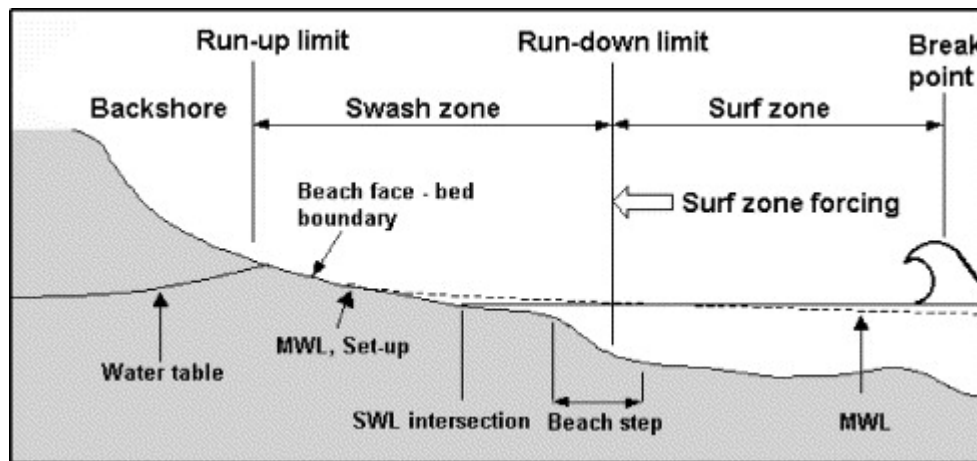


Figure 2. Schematic cross-section of the beach and the limits of the swash zone. Figure from (Elfrink & Baldock, 2002)

Following the description of Masselink & Puleo (2006) a swash event can be described by using the four stages of the hydrodynamic cycle (Kranenburg, 2020). At first there is the arrival bore, which causes high landward flow velocities at the free surface elevation. However, the underlying water is still moving in the seaward direction due to the backwash of the previous swash cycle. The uprush, which is the second stage, occurs when the bore collapses and the water is flowing onto the beach. At the start of the uprush, flow velocities, suspended sediment concentrations and suspended fluxes are at maximum (Masselink & Puleo, 2006). During this stage, the water is slowed down by the bed friction and by the gravity pulling the water seaward due to the beach slope. The decreasing flow velocities cause the sediment to settle, leaving the water clear around the time of flow reversal (Masselink & Puleo, 2006). This deceleration of the flow velocity gradually reverses the flow direction, causing the third stage to happen, namely the run-down phase. This process of reversing the flow direction happens earlier at the lower parts than at the front of the up rushing wave (O'Donoghue, Pokrajac, & Hondebrink, 2010). Again friction with the bed causes the flow velocities to decrease and so the flow velocities are lower than during the uprush (Hughes, Masselink, & Brander, 1997), however the highest back wash flow velocities occur at the end of this stage therefore also causing the highest sediment concentrations and fluxes of this stage to be at the end (Masselink & Puleo, 2006). As the back wash is interacting with the sea, the final stage is reached. This interaction even slows down the flow speeds even more. The backwash eventually interacts with the newly arriving bore, causing the cycle to be fulfilled and meanwhile a new cycle is started.

The net sediment transport of one swash cycle is relatively low compared to the uprush sediment load, which is two to three orders of magnitude larger (Masselink & Puleo, 2006). However, this net sediment transport of one event is in the same order of magnitude as the net changes over one tidal cycle (Blenkinsopp, Turner, Masselink, & Russell, 2011).

2.2 The XBeach model

XBeach is an open source, depth-averaged model for hydrodynamics, sediment transport and morphology in the nearshore, beach and dune area (Smit et al., 2009). It is a public-domain model that has been developed with funding and support by the US Army Corps of Engineers,

by a consortium of UNESCO-IHE, Deltares (Delft Hydraulics), Delft University of Technology and the University of Miami (Hoonhout, 2011).

There are three versions of XBeach, namely the stationary model, surfbeat model and the nonhydrostatic model. Only the latter two can be used to calculate swash zone sediment transport. The surfbeat model resolves the long-wave and wave-group motion but short-wave effects are parametrized. This model works well on dissipative sandy beaches but for steeper beaches (and gravel) the short waves need to be included in the model (Roelvink, McCall, Mehvar, Nederhoff, & Dastgheib, 2018). For this purpose, the nonhydrostatic version of XBeach was developed. For this reason, this research will look at the nonhydrostatic version which simulates the system in an intra-wave way.

XBeach does contain many different processes such as groundwater effects, infiltration effects and wave-breaking induced turbulence. For sediment transport it per default uses implementations based on the equilibrium concentration concept, but other sediment transport methods can be used as well. XBeach is based on the Non-Linear Shallow Water Equations (NLSWE). Especially for steeper beaches, the non-hydrostatic version of XBeach is developed, in which the short waves are also included (Kranenborg, 2020).

2.3 The RESIST dataset

The dataset that will be used in this research is the ‘influence of storm sequencing and beach REcovery on Sediment TranSPorT and beach resilience’ (RESIST) dataset (Eichentopf et al., 2019). This dataset is obtained at the Canal d’Investigació i Experimentació Marítima (CIEM). This is a large-scale wave flume at the Universitat Politècnica de Catalunya (UPC) in Barcelona. This dataset contains three waveseries: one random wave series (as benchmark), two different bichromatic erosive waves and three different bichromatic accretive waves were tested. The beach had an initial profile of 1:15 and the D_{50} of the sediment was 0,25 mm.

This dataset is chosen because of multiple reasons: 1) Van der Zanden has obtained and worked with other datasets as well (CoSSedM and Sinbad) and says that the RESIST has the best quality of data (J. van der Zanden, personal communication, January 2020). 2) It is useful to use bichromatic (instead of random) waves, in order to draw conclusions in a repetitive, wavegroup-averaged way. 3) The RESIST data has not yet been used in this typical way, comparing with and trying to improve a numerical model. Therefore, it will be an addition to the current available studies and knowledge.

2.3.1 Measurement equipment

To measure all different parameters and different locations, multiple measurement tools were installed in the flume. There were Resistive Wave Gauges (RWG), Pore Pressure Transducers (PPT) and Acoustic Wave Gauges (AWG) which could all measure the water level with a sampling frequency of $f_s = 40$ Hz (Eichentopf et al., 2019). Besides those there were Acoustic Doppler Velocimeters (ADV) installed which could measure the flow velocity with a sampling frequency of $f_s = 100$ Hz (Eichentopf et al., 2019). At last there were Optical Backscatter Sensors (OBS) co-located with the ADVs which measured the sediment concentrations with a sampling frequency of $f_s = 40$ Hz (Eichentopf et al., 2019). Both the ADVs and the OBS’s were placed at (and if needed re-adjusted to) 3 cm above the bed.

2.4 Sediment transport

Sediment transport is the movement of solid particles (sediment), typically due to a combination of gravity acting on the sediment, and/or the movement of the fluid in which the sediment is entrained. This process is frequently considered and modelled in two different ways: bedload

transport and suspended transport, see Figure 3 (Métivier & Meunier, 2003) for a schematization of both processes.

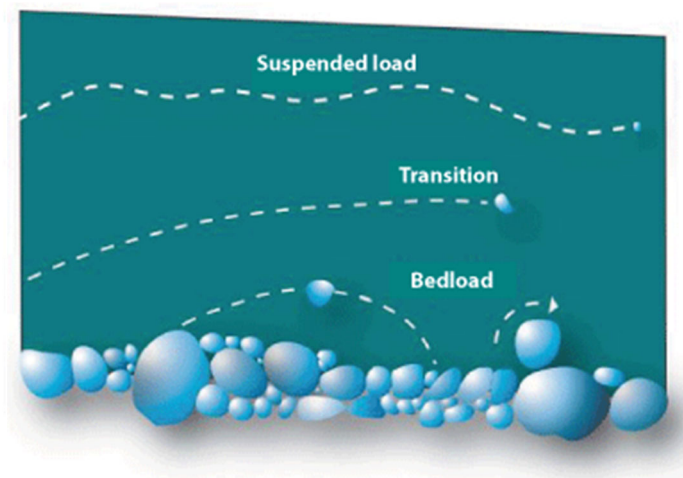


Figure 3. The difference between bed load transport and suspended transport (Métivier & Meunier, 2003)

Bedload transport is the transport of sediment particles in a thin layer with a certain thickness (order of 1 cm) close to the bed (van Rijn, 2007a). It consists of larger particles which travel in saltation on the bed. The larger and denser is the grain, the shorter its ballistics and the longer it remains on the bed. The moving sediment is in more or less continuous contact with the bottom (Rooijen, 2011).

Suspended transport on the other hand consist of fine particles which are almost transported at flow velocity and rarely touch the bed. Their trajectory is close to the flow path, in suspension in the fluid. The amount of suspended sediment is influenced by the following three processes (Fredsoe & Deigaard, 1992; Kranenborg, 2020): 1) Flow velocity, a high flow velocity could pick up a sediment particle. 2) Turbulence, small turbulence bursts could also bring sediment into suspension. 3) Gravity, this force pulls the sediment particles down again. This is especially the case when the flow velocities and the amount of turbulence decrease and so the force which brings/keeps the sediment in suspension diminishes.

Calculation methods for sediment transport also often distinguish between these two types. However, since this research is about suspended load only, this paragraph will only discuss the different, commonly used methods for suspended load. Note that sediment transport occurs in all directions but in this case only cross-shore sediment transport will be considered.

2.4.1 Suspended transport

Sediment is advected by the flow field of the water to which a sediment fall velocity is added. The diffusion of sediment typically arises from flow turbulence (Kranenborg, 2020). That is why suspended sediment is often modelled by an advection-diffusion equation. This equation describes the spatial and temporal evolution of the suspended sediment concentration. However, this could be modelled in two ways:

- Equilibrium concentration: this method calculates the difference between an equilibrium concentration and the present concentration to model if sediment is entraining or settling. An example of this method is the Van Thiel-Van Rijn method. Van Thiel de Vries changed the Van Rijn method slightly to calculate the equilibrium concentration by using wave-averaged quantities (van Rijn, 2007a, 2007b; Van Thiel de

Vries, 2009). This Van Thiel-Van Rijn method is for instance used by Ruffini et al. (2020) and is explained in further detail below in Section 2.4.3.

- Reference concentration: this method uses the concentration of sediment in the water column at a certain height above the bed to obtain the total amount of sediment in the water column. An example of this method is the one by Pritchard & Hogg (2003).

Most sediment transport methods are only valid for its own system characteristics and different system characteristics may need a different formula. But all these formulas are based on more or less the same principles and therefore contain more or less the same variables (Jenniskens, 2001). These are:

- The roughness of the bed [$m^{1/2}/s$]
- The gravitational acceleration [m/s^2]
- The volumetric weight of the sediment and of the water [kg/m^3]
- The (depth-averaged) flow velocity [m/s]
- The median grain size [m]

However, these sediment transport methods are only valid for a steady uniform flow with a horizontal bed. So, to be able to look at the sediment transport in the swash zone, where there is no steady uniform flow and horizontal bed, some other processes should be investigated. For instance Nielsen (2006) tried this by incorporating acceleration effects. Another process that is likely to have an influence on the sediment transport is turbulence.

2.4.2 Equilibrium concentration

As said, the equilibrium concentration is the concentration that would be reached in the water if the conditions remain constant for a very long time. However, since these conditions differ a lot over time this equilibrium concentration is hardly ever equal to the real concentration.

But this equilibrium concentration (c_{eq}) [g/l] can be used to compute the real concentration (c) [g/l] when including a sediment adaptation time (T_s) [s], in this research the advection-diffusion equation of Galappatti & Vreugdenhil (1985) is used. This equation looks as

$$\frac{\partial hc}{\partial t} + \frac{\partial hcu}{\partial x} + \frac{\partial}{\partial x} \left[Kh \frac{\partial c}{\partial x} \right] = \frac{hc_{eq} - hc}{T_s}. \quad (2.1)$$

Note: *the grey $\frac{\partial}{\partial x}$ terms will be neglected in this research, see Section 3.5.2.*

The used adaptation time depends on the water depth (h) [m] and the sediment fall velocity (w_s) [m/s] and could be computed with

$$T_s = \max \left(\gamma \frac{h}{w_s}; 0,01 \right) \quad (2.2)$$

with γ being a calibration constant [-] (Reniers et al., 2013). This sediment adaptation time makes sure that the equilibrium concentration is not reached instantaneously but that the system needs some time to adjust to the new circumstances.

2.4.3 Van Thiel-Van Rijn method

This research chooses to model the equilibrium sediment concentration by using the Van Thiel-Van Rijn (mostly referred to as VTVR) method (Van Thiel de Vries, 2009). This method could model the equilibrium concentration for both the bed load and the suspended load which

together make up the total load. But since this research is about suspended load only, this explanation of the VTVR approach will neglect the bed load aspects. Additionally, the VTVR method distinguishes between sediment that is mobilized due to waves and due to currents. Since this research only surveys the effects of waves, the current aspect will be neglected as well. The equilibrium concentration of the suspended load (c_{eq}) can be modelled according to

$$c_{eq} = \frac{A_{ss}}{h} \left(\sqrt{u_{mg}^2 + 0,64 u_{rms}^2} - u_{cr} \right)^{2,4} \quad (2.3)$$

with u_{mg} being the running mean of the flow velocity [m/s]; the u_{rms} being the incident wave motion [m/s]. The suspended load coefficient (A_{ss}) being

$$A_{ss} = 0,012 D_{50} \frac{D_*^{-0.6}}{(\Delta g D_{50})^{1.2}} \quad (2.4)$$

in which Δ represents the ratio between the densities of the sediment and water [-] and the dimensionless sediment parameter (D_*) [-] being

$$D_* = \left(\frac{\Delta g}{\nu^2} \right)^{\frac{1}{3}} D_{50} \quad (2.5)$$

In here ν is referred as the viscosity of the water [m²/s]. The critical velocity (u_{cr}) [m/s] in Equation 2.3, which is the velocity at which sediment starts to move, depends on the size of the sediment particles and can be modelled with

$$u_{cr} = \begin{cases} 0,24(\Delta g)^{\frac{2}{3}}(D_{50}T_{rep})^{1/3} & \text{for } D_{50} \leq 0,0005 \\ 0,95(\Delta g)^{0.57}(D_{50})^{0.43}T_{rep}^{0.14} & \text{for } D_{50} > 0,0005 \end{cases} \quad (2.6)$$

where g is the gravitational acceleration [m/s²] and T being the wave period [s].

2.4.4 Equations in XBeach

XBeach makes use of the same methods and associated equations as mentioned and explained above. So, it uses Equation 2.1 to convert the equilibrium concentration into a real occurring concentration but without neglecting the advection and diffusion terms. It even adds vertical advection and diffusion, represented by the **green** $\frac{\partial}{\partial y}$ terms. It then looks as

$$\frac{\partial hc}{\partial t} + \frac{\partial hc u}{\partial x} + \frac{\partial hc v}{\partial y} + \frac{\partial}{\partial x} \left[Kh \frac{\partial c}{\partial x} \right] + \frac{\partial}{\partial y} \left[Kh \frac{\partial c}{\partial y} \right] = \frac{hc_{eq} - hc}{T_s}. \quad (2.7)$$

Thereafter XBeach models the sediment response time by using Equation 2.2 as well.

To model the equilibrium concentration, XBeach uses exactly the same equations as presented and explained above at the section about the VTVR method. Yet, XBeach could cope with sediment transport due to currents but this was not used in this research.

2.4.5 Translating point measurements to depth-averaged values

In order to have a fair comparison between point measurements and depth-averaged measurements, a profile could be fitted to basically translate one in the other. The most common profile for this purpose is the Rouse profile, this gives technique provides a relation between the

(relative) water depth and the Suspended Sediment Concentration (SSC) (Roelvink & Reniers, 2011).

The equation to model the Rouse profile is

$$c(z) = c_a \left(\frac{z+h}{z} \frac{a-h}{a} \right)^{-\frac{w_s}{\kappa u_*}} \quad (2.8)$$

(Roelvink & Reniers, 2011). With $c(z)$ being the concentration at depth z [g/l] and c_a the (measured) reference concentration [g/l]. And z is the water depth at which the SSC is questioned [m]. The entire water depth is represented by h [m] and a is the height of the reference concentration [m]. These heights are schematically illustrated in Figure 4 (after (Teles et al., 2016)).

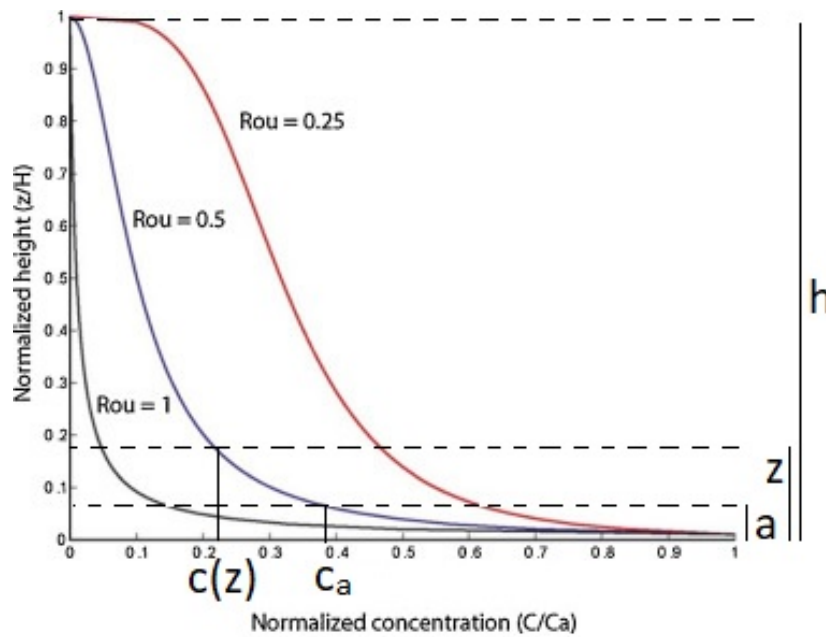


Figure 4. Rouse profile of the sediment concentration over the height. With $c(z)$ and c_a depicted for the case when the Rouse number (Rou) = 0.5. The Rouse number is represented by the power in Equation 2.8. Figure after (Teles et al., 2016)

In here w_s refers to the measured sediment fall velocity [m/s] and κ to the Von Karmann constant [-]. The bed shear velocity (u_*) [m/s] can be modelled with

$$u_* = \sqrt{\frac{\tau_{bed}}{\rho}} \quad (2.9)$$

Where ρ represents the density of the water [kg/m³] and τ_{bed} the bed shear stress at the bed [N/m²] calculated with

$$\tau_{bed} = \max(|\tau_{XBeach}|; 0,01) \quad (2.10)$$

in which τ_{XBeach} is the absolute bed shear stress [N/m²] as modelled by XBeach. The *max* operator is used to avoid values which are very small (or even zero) which will result in a very small (or impossible) u_* .

By using the Rouse profile, the SSC at each height in the water column could be modelled. In this research this was done at an interval of 1 mm with a lower boundary at 3 cm above the bed (which is the height of the OBS sensors) up to the free surface elevation. After this approximation, the depth-average value can then be calculated with

$$c_{depth\ avg} = \frac{1}{h} \sum_0^h c(z)_N \Delta z \quad (2.11)$$

where $c_{depth\ avg}$ is the depth-averaged suspended sediment concentration [g/l], h the water depth [m] and c the concentration [g/l] at depth z [m] divided into N subintervals with each subinterval representing a height (Δz) of 0,001 m. This equation has its lower limit at the bed ($h=0$). The upper limit is logically the free surface elevation, here represented by the water depth (h).

2.5 Turbulence

Turbulence is a process that is not explicitly included in the sediment transport equations, but certainly is relevant. Turbulence is the effect when inertial forces in a fluid overcome the damping viscous forces, leading to strongly and chaotically varying flow velocities. Turbulence is often described in terms of Turbulent Kinetic Energy (TKE) (e.g. Van der Zanden et al., 2017). Turbulence in the swash zone has two different causes: as generated at the bed by frictional processes and, more readily, by the churning of water in the leading edge of swash and bore motion (Masselink & Puleo, 2006). However, this bore induced turbulence is only present during uprush while the bed induced turbulence is present in both uprush and backwash (Chardón-Maldonado, Pintado-Patiño, & Puleo, 2016). Unfortunately it is hard to measure turbulence with experiments in the swash zone (Masselink & Puleo, 2006).

2.5.1 OpenFoam modelled turbulence

OpenFoam is a model which can be used for all kinds of fluid dynamics (Kranenburg, 2020). The models used in this research is based on the Reynolds Averaged Navier Stokes (RANS) equations. The turbulence is modelled with a $k-\omega$ SST model (Menter, 1993). And the waves are generated with the waves2foam toolbox (Jacobsen, Fuhrman, & Fredsøe, 2011). Yet they are implemented the same way as is in XBeach for this research. This means that based on the Linear Wave Theory two wave components are calculated which are eventually added to have the resultant wave characteristics. The model is purely hydrodynamic and so does not calculate any sediment transports.

2.5.2 Analytical approach of turbulence

In order to predict the occurrence of turbulence without making use of an extra model (and so the RANS equations), the turbulence could also be modelled by using an analytical turbulence model, after Reniers et al. (2013). This method is based on computing the roller thickness and translating that into turbulent energy. The equations this method uses are the following (after Jongedijk (2017) & Reniers et al. (2013)). The critical increase of the wave $\left(\frac{dZ}{dt}_{cr}\right)$ [m/s] could be computed with

$$\frac{dZ}{dt}_{cr} = \beta \sqrt{gh} \quad (2.12)$$

where h is the water depth [m] and β [-] is the factor in critical slope for bore turbulence. By using this critical slope, the increase (or decay) of the roller thickness (R) [m] could be computed with

$$\frac{\partial R}{\partial t} = \frac{dZ}{dt} - \frac{dZ}{dt}_{cr} \quad (2.13)$$

where Z is the surface elevation [m]. Now a source term for the turbulent kinetic energy (S_w) [m^3/s^3] can be modelled with

$$S_w = c_R R g \frac{dZ}{dt}_{cr} \quad (2.14)$$

where c_R is a coefficient [-] which could be used for calibration. Furthermore, the dissipation (S_r) [m^3/s^3] of the turbulent kinetic energy (k) [m^2/s^2] is given by:

$$S_r = c_k k^{\frac{3}{2}} \quad (2.15)$$

Where c_k is a coefficient [-] that could be used for calibration as well. All combined, the depth-averaged turbulent energy transportation equation than reads:

$$\frac{\partial kh}{\partial t} + \frac{\partial kh u}{\partial x} = S_w - S_r \quad (2.16)$$

with again the $\frac{\partial kh u}{\partial x}$ term being neglected in the point-model.

However, this calculated turbulence value is depth-averaged. So, to model the near-bed turbulence some translation needs to be included since turbulence is generated mainly at the water surface and decays in a vertical way. To account for this decay and translate this depth-averaged turbulent kinetic energy into a turbulent kinetic energy at the bed (k_{bed}) [m^2/s^2], an exponential decay function has been added, based on the distance from the free water surface (J. A. Roelvink & Stive 1989)

$$k_{bed} = k \min\left(\frac{1}{\exp\left(\frac{h}{R}\right)-1}; 1\right). \quad (2.17)$$

2.5.3 The effect of turbulence on sediment transport

The turbulent bore is a powerful mechanism that brings sediment into suspension. Since adding near bed turbulence to the calculation of the Shields number has a significant effect on the initiation of motion (Reniers et al., 2013). Turbulence associated with the collapsing bore is likely to be responsible for much of the suspended sediment that is observed in the swash zone at the start of the uprush (Butt & Russell, 1999; Puleo et al., 2000). Turbulence is also responsible for a high vertical mixing of the sediment (Masselink & Puleo, 2006).

2.6 Including turbulence in the sediment transport model

Based on observations of enhanced sand suspension in the wave breaking region, several parameterisations have been proposed to include turbulence effects on sand pickup rate and reference concentration models. Some studies related the turbulent kinetic energy either directly or indirectly as an additional parameter to increase the bed shear stress and sand suspension. However, none of these parameterisations that account for wave breaking effects on sand pickup has been widely incorporated in common morphodynamic models (Van der Zanden et al., 2017).

One of these is by adapting the bed shear velocity by adding a turbulence term (Van der Zanden et al., 2017b). To quantify this effect, they made a model in which they added wave breaking turbulence to the van Rijn (2007b) sediment transport method. The results of this model are shown in Figure 5 (Van der Zanden et al., 2017b).

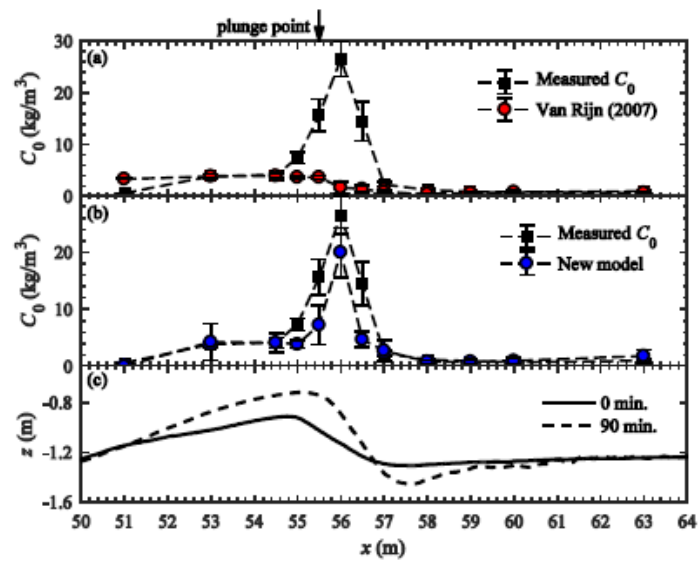


Figure 5. The reference sediment concentration from the old model (a) versus the newly, adapted model (b) (Van der Zanden et al., 2017b)

3. Methodology

3.1 Research approach

This research is generally executed in the following manner: XBeach runs are made with a modelled bed and waves as in the RESIST dataset. Then the hydrodynamic output of this XBeach model (water level and flow velocity) is quantitatively compared with the RESIST measurements. After the hydrodynamics, also the sediment concentrations are compared. This all to validate the XBeach capabilities with the RESIST dataset. After this validation, two turbulence datasets are made. The first one is done by using an OpenFoam model which is built on the same RESIST conditions. Yet OpenFoam has another way of computing the outputs and is therefore, in contrast to XBeach, capable of modelling turbulence. The second turbulence data is based on the analytical approach of the turbulence (Reniers et al., 2013). Additionally, a sediment transport point-model is set up which models the suspended sediment concentration (SSC). Eventually, in this model, the turbulence is included in the SSC calculation. This is done by adding the turbulent kinetic energy to the flow velocity. Subsequently this new SSC is compared with the RESIST measurements to investigate if the inclusion of turbulence does improve the SSC calculation sediment. Eventually this sediment concentration was used to calculate sediment transport which was also evaluated with the RESIST measurements. This general approach is schematically shown in Figure 6.

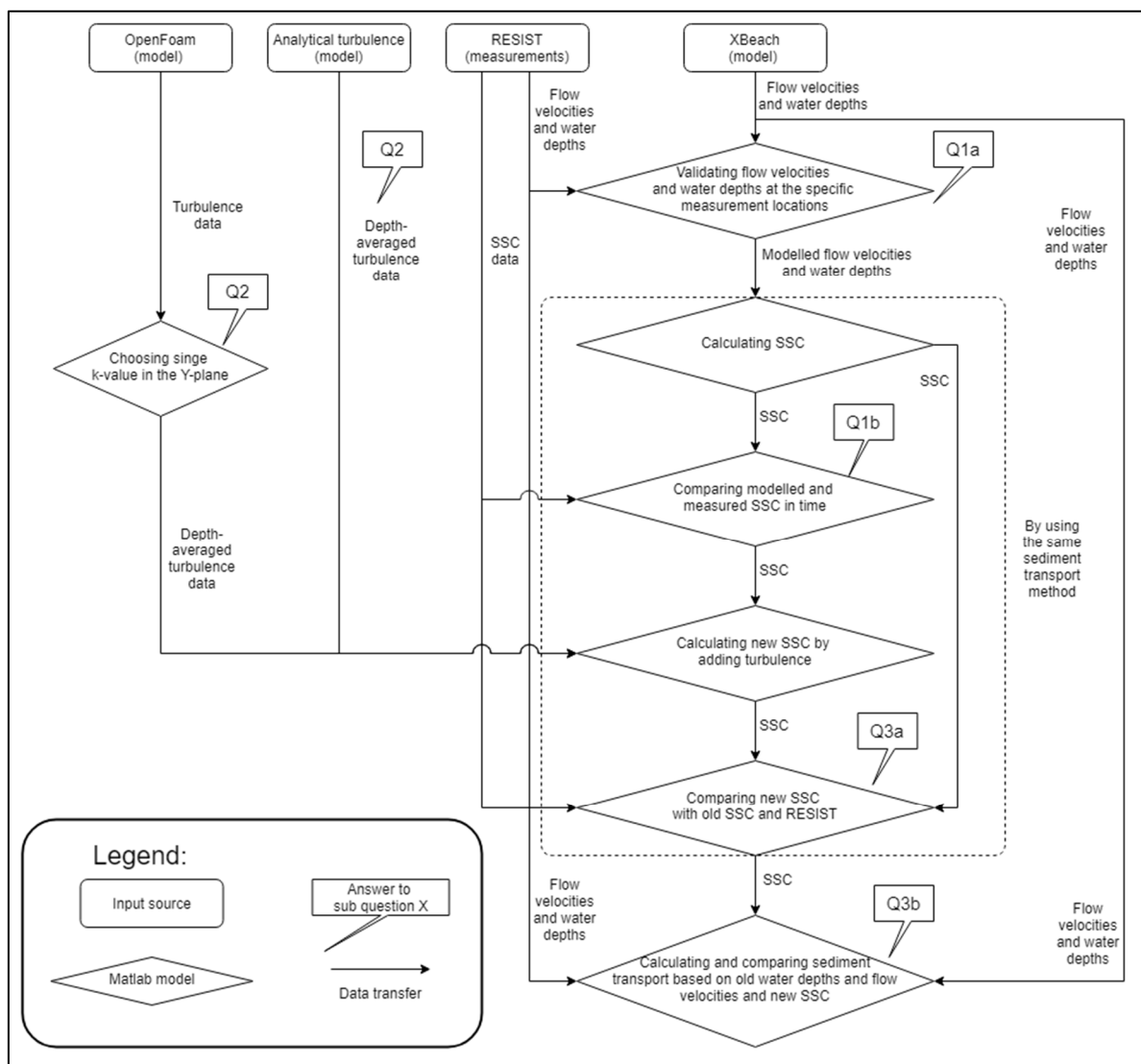


Figure 6. Schematic diagram of the approach of this research

3.2 The use of the dataset

In this research the flow velocity data from the ADVs will be used, just as the water surface elevation from the AWGs and the sediment concentration from the OBS's. The AWG was used because it showed the best correlation with the XBeach outcomes when compared to the data from the RWG's.

3.3 Setting up XBeach for this research

Although XBeach could be used to simulate in two (horizontal) dimensions, only the cross-shore dimension will be investigated in this research. This means that in this research XBeach is used as a (depth-averaged) 1DH-model. In order to do so the model was set up the following: it has a spatial resolution (ΔX) of 0,1 m (consistent with Ruffini et al., (2020)) and uses a timestep (Δt) of 0,1 s. As roughness the default value is used, which is a Chézy roughness coefficient (C) of 55 [$\text{m}^{1/2}/\text{s}$]. This value is in the same order of magnitude as in other studies, for instance Reniers et al. (2013) and Roelvink et al. (2018). In the model the same sediment distribution is used as there has been used in the RESIST dataset, which has a median grain size diameter (D_{50}) of 0,25 mm and a 90% cumulative percentile value (D_{90}) of 0,372 mm (see Eichentopf et al., (2019)). The initial bed is based on the RESIST measurements as well (see Section 3.3.2 for a more detailed description of this bed). And eventually the hydrodynamics: the boundary conditions of the surface elevation and flow velocity at the 'open end' are calculated based on the Linear Wave Theory and are subsequently implemented in XBeach. See Section 3.3.1 for the detailed explanation of this calculation. The wave parameters are again based on the ones used in the RESIST dataset, see Eichentopf et al., (2019). After this setup was complete, the model was run by using a simulation time of 30 minutes, which is also the duration of the wave sequences in the RESIST dataset. The XBeach model has not been calibrated.

3.3.1 The applied waves

The waves that are examined in this research are bichromatic. This means that the resultant waves are made up by two regular waves with different frequencies, and so wave groups are formed. The waves used in the model have the same characteristics as the waves used in the RESIST dataset. One erosive type of waves is picked from the waves tested in RESIST. In particular the waves with the highest energy (Erosive 1), since a higher energy should cause much erosion (Eichentopf, Van der Zanden, Cáceres, Baldock, & Alsina, 2020). In this case the most extreme waves are considered in this research. The used wave characteristics are shown in Table 1.

Table 1. Wave characteristics of the studied waves. Based on the waves used in the RESIST dataset. So, after Eichentopf et al., 2019.

| | Component 1 | | Component 2 | | T_{primary} [s] | T_{group} [s] | $T_{\text{repetition}}$ [s] |
|-----------------------------|-------------|------------|-------------|------------|-----------------------------|---------------------------|--------------------------------|
| | H_1 [m] | f_1 [Hz] | H_2 [m] | f_2 [Hz] | | | |
| Wave characteristics | 0,320 | 0,3041 | 0,320 | 0,2365 | 3,70 | 14,80 | 29,60 |

With the known wave height (H_i) [m], frequency (f_i) [Hz], period (T_{primary}) [s] and water depth (h) [m] the behaviour of the waves in terms of surface elevation and flow velocity could be modelled. The flow velocity could be modelled with the Linear Wave Theory. However, the Linear Wave Theory assumes a linearized description of the propagation of gravitational waves on the water surface. This implies that possible higher order relations are not considered. It also does not consider reflection of the waves. The equations the Linear Wave Theory is based on are

$$u_1(t) = \omega * \frac{1}{2} H_1 * \frac{\cosh(Kh)}{\sinh(Kh)} \cos(2\pi * f_1 * t) \quad (3.1)$$

$$u_2(t) = \omega * \frac{1}{2} H_2 * \frac{\cosh(kh)}{\sinh(kh)} \cos(2\pi * f_2 * t) \quad (3.2)$$

(Dingemans, 1994). In here u_1 and u_2 represent the horizontal velocity [m/s] of both wave components (see Table 1). H_1 and H_2 are the wave height [m] of these wave components while f_1 and f_2 represent both the frequencies [Hz]. Thereafter the time is represented by t [s]. The wave angular frequency (ω) [s^{-1}] can be computed with

$$\omega = \frac{2\pi}{T} \quad (3.3)$$

in which the wave period (T) [s] is implemented. And the wave number (K) [m^{-1}] can be calculated with

$$K = \frac{2\pi}{L} \quad (3.4)$$

In which L represents the wavelength [m]. This wavelength can be computed by using an iterating the dispersion relation

$$L_0 = \frac{gT^2}{2\pi} \quad (3.5)$$

$$L = L_0 \tanh(Kh) \quad (3.6)$$

In which g is the gravitational acceleration [m/s^2], h the water depth [m] and L_0 the wavelength in deep water [m]. In the end u_1 and u_2 together make up the resultant horizontal motion of the wave paddle (u_{tot}) [m/s] by means of

$$u_{tot}(t) = u_1 + u_2 \quad (3.7)$$

The same process of adding to wave components holds for the surface elevation (Z) (Dingemans, 1994), which is made up out of two surface elevations relative to the SWL (θ_1 and θ_2) [m]

$$\theta_1(t) = \frac{1}{2} H_1 \cos(2\pi * f_1 * t) \quad (3.8)$$

$$\theta_2(t) = \frac{1}{2} H_2 \cos(2\pi * f_2 * t) \quad (3.9)$$

$$Z(t) = \theta_1 + \theta_2 \quad (3.10)$$

The values of the wave paddle velocity (u_{tot}) and water surface elevation (Z) are then computed for a period of 30 minutes by using an interval of 0,1 s and these outcomes are loaded into XBeach as a boundary condition at the 'open end'.

The created wave signal for these waves then looks the following, see Figure 7.

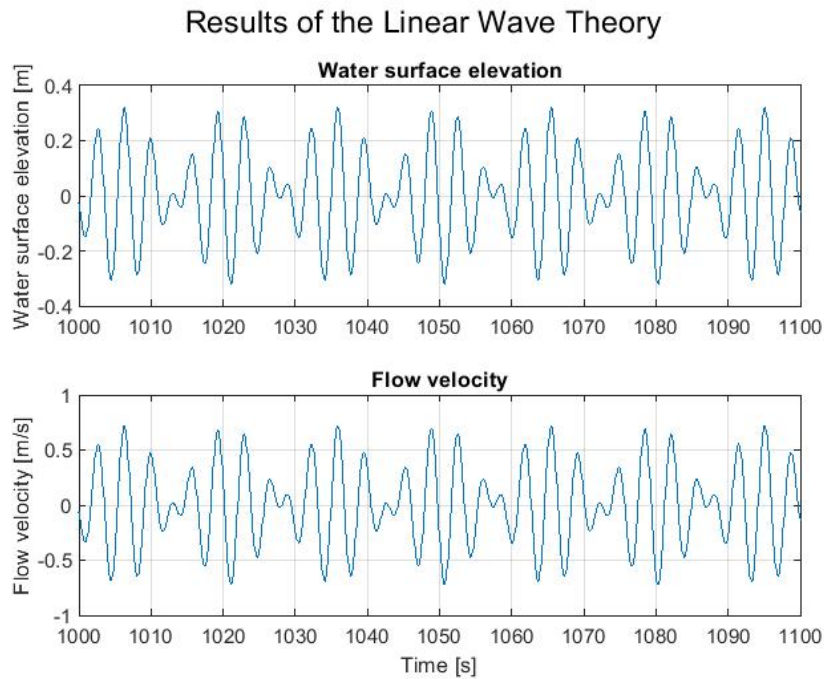


Figure 7. Created wave signal for the waves by using the Linear Wave Theory and the parameter values based on the ones from the RESIST dataset

3.3.2 The initial bed

As described in Section 3.3, a bed profile is chosen and used as the initial bed in XBeach. The profile picked is the last profile from the erosive wave sequence in RESIST, see the red graph in Figure 8. This profile is selected because it is expected to match the natural behaviour of the beach to the highest extent since the bed has already moved somewhat towards its equilibrium under those wave conditions due to the effect of the incoming waves.

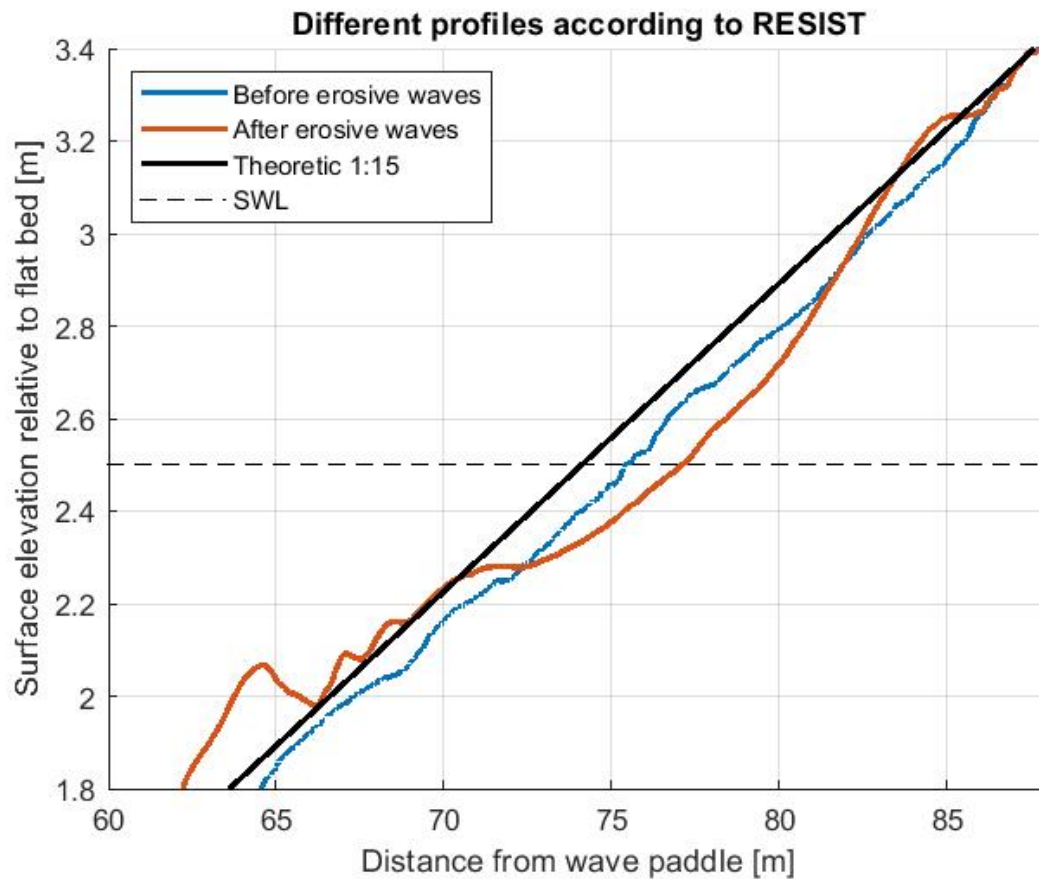


Figure 8. Different bed profiles as they are measured in RESIST, see Eichentopf et al., (2019). The red graph is used as the initial bed in this research

3.4 Validating XBeach output with RESIST data

3.4.1 Smoothing the data

The measured RESIST data was very noisy. To filter out this noise, the data was smoothed by using a moving average. See Figure 9 for this effect. It is chosen to use a timespan of 0,5 s for this moving average. A larger timespan would cancel out possibly important characteristics of the graph while a smaller width would still leave noise. Yet to have a fair comparison between RESIST and XBeach, also the XBeach data was smoothed over a timespan of 0,5 s.

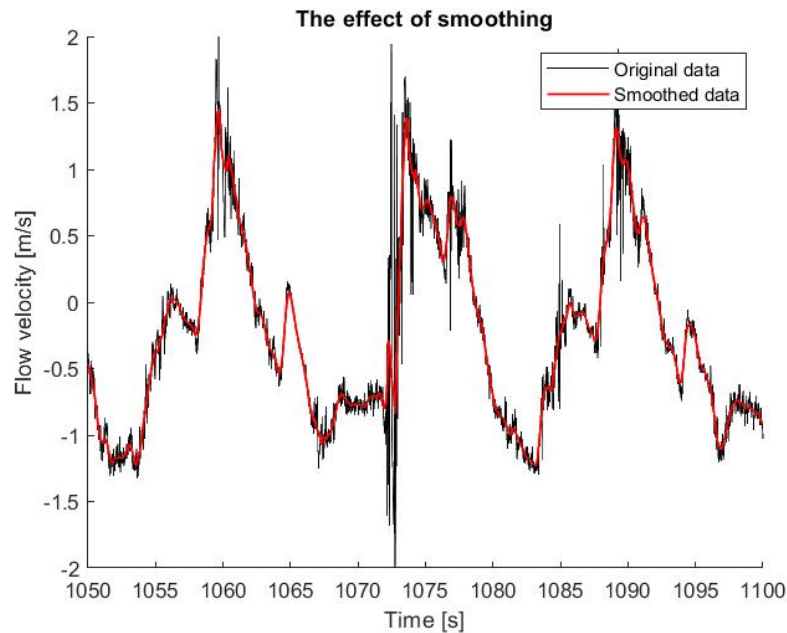


Figure 9. The effect of smoothing the data. The data is smoothed over the timespan of 0,5 s

3.4.2 Validating the hydrodynamics

To validate the XBeach hydrodynamics (i.e. water depth and flow velocity) several locations are picked at which the XBeach output is compared with the RESIST measurements. To enable a fair comparison, one location far from the beach is chosen and several locations in the swash zone to check the performance of the model at different locations in the flume. The locations at which this is evaluated differ because not all the three measurement tools are present at the same location and so multiple locations need to be investigated to include all parameters.

All the locations of measurement equipment on which the data and so the comparisons are based, are stated in Table 2 and schematically presented in Figure 10.

Table 2. The distances in m from the wave paddle at which all the measurement equipment is located. As an indication: the SWL shoreline is at 77,1 m from the wave paddle.

| Measurement equipment (measured parameter) | Distance from the wave paddle to the offshore location [m] | Distance from the wave paddle to the swash location [m] |
|---|--|---|
| AWG (water surface level) | 19,2 | 75,7 |
| ADV (flow velocity) | 63,7 | 75,5 |
| OBS (sediment concentration) | 63,6 | 75,6 |

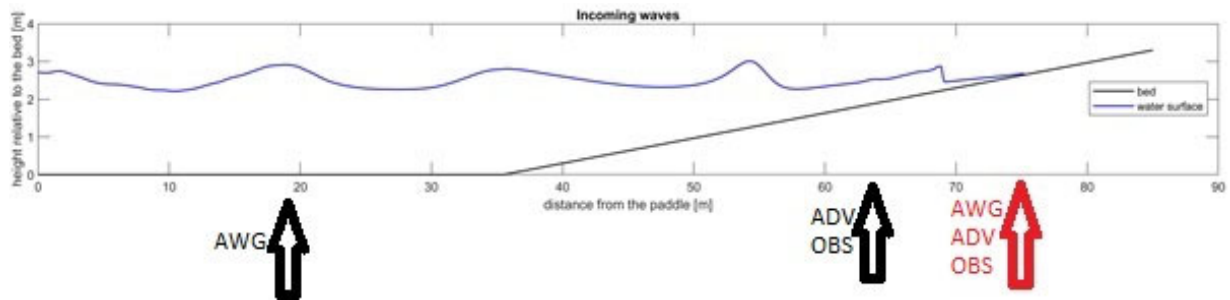


Figure 10. Schematic representation of the locations of the investigated measurement equipment at the offshore location (black arrows) and the swash location (red arrow). The black line represents a perfect 1:15 sloped bed as indication. The water surface elevation (blue line) is a snapshot from the XBeach model at $t=210$ s

The wave characteristics are translated into boundary conditions according to the method described in Section 3.3.1. Next XBeach is ran and the modelled values for the entire cross-shore section are used for this validation. Consequently, the cross-shore location corresponding to the measurement equipment is identified and the timeseries at that specific location are compared with the measured timeseries. For this validation, XBeach has not been calibrated.

XBeach timeseries have a timewise interval of 0,1 s while the RESIST timeseries have an interval of 0,025 s for the water level and 0,01 s for the flow velocities. These missing datapoints were filled by interpolating (Spline) the XBeach timeseries to the RESIST data. Furthermore, the RESIST data was in cm/s and this was translated to m/s to match the XBeach output and to be in SI units. Now both timeseries have the same frequency and units and so could be fairly compared. This comparison will be done based on the correlation coefficient (r^2) and the normalized Root Mean Square Error (nRMSE). The specific way of calculating this nRMSE is after Ruffini et al. (2020) and is

$$nRMSE = \frac{\sqrt{\frac{1}{N} \sum_i^N (y_{m,i} - y_{exp,i})^2}}{(y_{exp,max} - y_{exp,min})} \quad (3.11)$$

Where $y_{m,i}$ is the i th sample of the modelled quantity y and $y_{exp,i}$ is the corresponding experimental sample. N is the number of considered samples while $y_{exp,max}$ and $y_{exp,min}$ are respectively the maximum and minimum experimental values in the considered time interval. An nRMSE of zero would indicate a perfect fit between both timeseries, while an nRMSE of one indicates that the Root Mean Square Error (RMSE) equals the range of the measured parameter (Ruffini et al., 2020).

3.4.3 Spectral analysis

Another validation method is the spectral analysis. Spectral analysis is the process of breaking down a signal into its components at various frequencies (Randall, 2008). This is done for the water surface elevation as well for the flow velocity. This method is used to check if the frequencies of the individual wave components, of the waves itself and of the wave groups (see Table 1) indeed are present in the output.

3.4.4 Suspended Sediment Concentration

OBS sensors measure the turbidity of the water which is then translated into a sediment concentration (Curtis, 2006). So, it could happen that the sensors have a kind of offset error based on other characteristics of the water. To have a fair comparison with the XBeach results, there should be compensated for this. This error was found by looking at the beginning of the timeseries (so when the waves did not arrive at the beach already) because at that moment there was no sediment brought into suspension already so the value of the OBS could then only be caused by other factors, see the black graph Figure 11. So, to correct for other factors influencing these results, this starting value (approximately 1,2 g/l in Figure 11) was subtracted, resulting in the red graph.

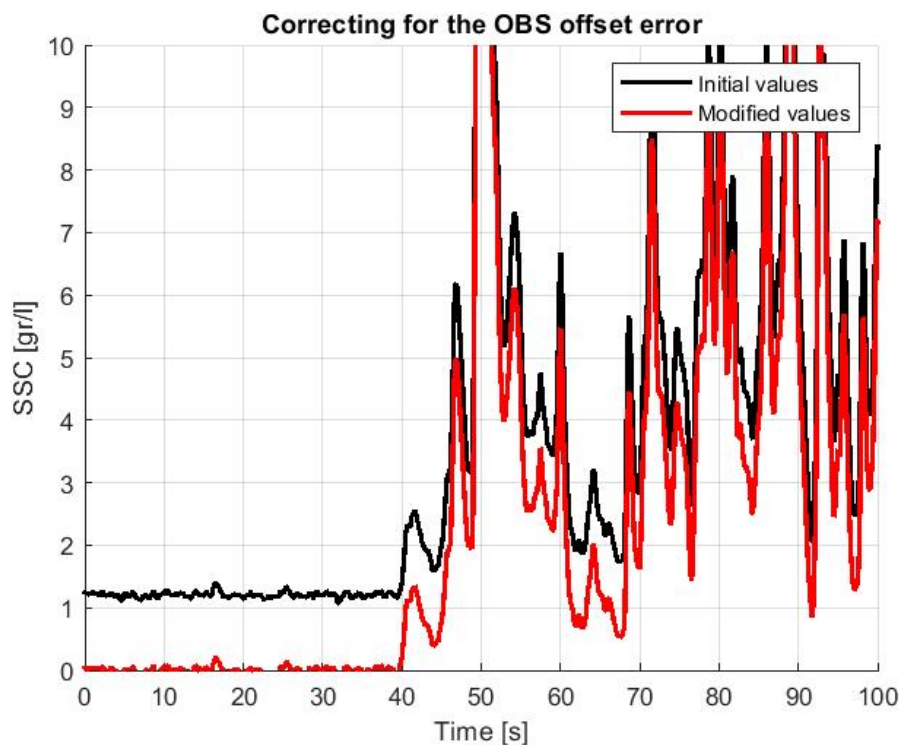


Figure 11. The offset error of the OBS sensor. At the beginning of the timeseries this value of approximately 1,2 could only be caused by other factors since there are no waves yet to bring sediment into suspension. Therefore, there has been corrected for this value.

3.4.5 Applying the Rouse profile

The theoretic background of applying the Rouse profile is described in Section 2.4.5. However, a few changes have been made in this approach in order to have a stable model such that it does not return any imaginary or enormously high values.

- Imaginary values could be the case since the used formulas are undefined for $h=0$. This is solved by implementing a minimum water depth of 0,005 m at moments in time where the water depth (h) is smaller. This is because the division by a very small h would lead to an enormous high equilibrium concentration. In other words: if some sediment

particles are present in very shallow water, the concentration will be very high, which can give a distorted view. Furthermore, this artificial change does not have a significant impact in the total amount of modelled suspended sediment transport since the water depth is almost zero so there can hardly be any sediment entrained at all.

- The enormously high values occur because the Rouse profile is not applicable for heights in the water column which are below its reference height. Those values grow exponentially and could reach values above 10^{11} . This is case for heights lower than 0,03 m, which was the reference height. Yet this sediment rich layer could not be neglected and therefor the SSC at the heights lower than 0,03 m is artificially changed to the value as there was measured at 0,03 m. In other words: the SSC between $h=0$ m and $h=0,03$ m is artificially changed to the value measured at $h=0,03$ m.

3.5 The SSC point-model

To be able to eventually make a fair comparison between SSC values without and SSC values calculated based with the influence of turbulence, the SSC should be modelled without making use of XBeach. Since it was outside the scope of this research to change (the source code) of XBeach itself. Therefore, this is done by using a standalone point-model in which (later on) turbulence could be included. This means that a new model was made which could calculate the SSC. In this research this is done by a model made in Matlab which makes use of the equilibrium sediment concentration. This is the concentration of sediment which could potentially be reached if the characteristics of the system remain constant for a long period of time, see Section 3.5.2 for a more detailed explanation. A way to model this equilibrium concentration is by using the Van Thiel-Van Rijn approach (Van Thiel de Vries, 2009), which uses the flow velocity as the main aspect of modelling the suspension of sediment. This method is explained in more detail in Section 2.4.3.

3.5.1 The Van Thiel-Van Rijn approach

This method is selected because it separates the suspension of sediment due to wave and due to currents. And since this research is about waves, this process could be isolated and focussed on best. Besides that, XBeach also supports this method, which makes the obtained results in this research more directly applicable to XBeach in the future. However, this method of modelling sediment transport works in a wave-averaged way. For this research, these outputs are converted into an intra-wave method in order to investigate the differences on a smaller timescale. This technique is also used by Jongedijk (2017) for similar research purposes.

The way this VTVR approach is used in the point-model is after Jongedijk (2017) as well. Since the non-hydrostatic version of XBeach only uses one flow velocity value, there is no distinction between the mean part of the flow velocity (u_{mg}) and the incident wave motion (u_{rms}) (see Equation 2.3 from Section 2.4.3). To solve this, a moving average is applied to the flow velocity time series in order to have a mean flow velocity. The incident wave motion is than the difference between the original flow velocity and the mean. In equation form this looks like

$$u_{rms} = u - u_{mg} \quad (3.12)$$

with u_{mg} being the newly calculated moving average over an interval of 25 s. This interval of 25 s is picked in order to retain the infragravity waves and is consistent with Jongedijk (2017).

3.5.2 Equilibrium sediment concentration

The equation used to convert the equilibrium sediment concentration to the real occurring sediment concentration is Equation 2.1 in Section 2.4.2. Yet this is the general equation and since

a point-model is used in this research, horizontal advection and diffusion will be neglected, and Equation 2.1 from Section 2.4.2 will look like

$$\frac{\partial hc}{\partial t} = \frac{hc_{eq} - hc}{T_s}. \quad (3.13)$$

with the neglected advection and diffusion terms. Yet, these terms are taken into account in XBeach. What remains now an equation that gives a relation between the real sediment concentration, the equilibrium concentration and the sediment adaptation time. By using the Forward Euler Technique (Zeltkevic, 1998) it is possible to calculate the suspended sediment concentration (c) [g/l] with Equation 3.13.

3.5.3 Calibrating the inclusion of turbulence to the SSC model

The equation to include turbulence in the SSC model is presented in Section 2.6. Yet this research calibrated the results of this inclusion by using the calibration coefficient (α). Changing this calibration coefficient determines how much the turbulence is included and so how heavily turbulence is taken into account. The goodness of fit is determined by looking at the validation parameters being the nRMSE and r^2 based on the match between the newly modelled SSC and the measured, depth-averaged SSC. This calibration and comparison were executed manually. However, most of the times a larger r^2 was associated with a larger nRMSE as well and then a compromise was picked at which the combination was optimal.

3.6 The OpenFoam model

To eventually add turbulence to the sediment transport model, it is needed to know how much turbulence is occurring in the water and when and where these turbulent effects take place. That is why my supervisor, ir. J.W.M. Kranenburg, made a turbulence dataset by using the OpenFoam model (see Section 2.5.1). The model which is used in this case has 420.000 cells and the cell size in the swash zone is 2,5 by 2,5 cm.

This model also accounts for the values in the region where the presence of water and air alternates and sometimes even a cell is partly filled with air and partly with water. This ratio is expressed in the Alpha-value. If this Alpha is 1, the cell is completely made up out of water, 0 means completely air and for instance 0,7 means 70% water and 30% air. Subsequently all model parameters are multiplied with their corresponding Alpha value to make sure only the water portion in a cell is taken into account.

3.7 The behaviour of turbulence in the swash zone

3.7.1 Evaluating the results

To check if the addition of turbulence to a sediment transport model does improve this model, again the correlation coefficient (r^2) and normalized Root Mean Square Error (nRMSE, see Equation 3.11) will be used to quantify the goodness of fit. Both these techniques will be used in the point-model including turbulence in comparison with subsequently the measured data, the XBeach output and the output of the point-model without the addition of turbulence.

3.8 Including turbulence in the SSC calculation

In this research the turbulence (i.e. the turbulent kinetic energy) will be added to the sediment transport calculation by using the point-model. The method which is used to add the turbulent kinetic energy to the sediment transport calculation is after (Jongedijk, 2017) and comes down to

$$u_{mod}^2 = u_{init}^2 + \alpha k \quad (3.14)$$

with u_{mod} and u_{init} respectively representing the modified flow velocity [m/s] and the initial flow velocity [m/s]. And α being a calibration constant [-] and k the (depth-averaged) turbulent kinetic energy [m²/s²]. This method has already been used in Van der Zanden et al. (2017) to evaluate sediment transport in the surf zone and by Jongedijk (2017) in the swash zone.

The method used to add the turbulence to the Van Thiel-Van Rijn point-model is from Jongedijk (2017) as well. This method includes the turbulence to the incident wave motion making it the modified flow velocity (u_{mod}) in the calculation of the equilibrium concentration (c_{eq}). By including the turbulent kinetic energy (k) and a calibration coefficient (α), the Van Thiel-Van Rijn equation (Equation 2.3 from Section 2.4.3) then becomes

$$c_{eq} = \frac{A_{ss}}{h} \left(\sqrt{u_{mg}^2 + 0,64 u_{mod}^2 + \alpha k} - u_{cr} \right)^{2,4} . \quad (3.15)$$

By doing this the turbulent kinetic energy is included in this calculation and taken into account by adding it to the incident wave motion.

3.9 Sediment transport rates

Now when the SSC is modelled with different methods and with and without turbulence, the translation to sediment transport could be made. By doing this the kind of effect these different approaches eventually have on the modelled sediment transport and so eventually on the morphodynamic changes of the system can be seen. In the end this morphodynamic change is what these models are for and what is used in other research.

3.9.1 Calculating sediment transport

By using a point-model, sediment transport (q_{sed}) [kg m⁻¹ s⁻¹] could be modelled as

$$q_{sed} = c * h * u \quad (3.16)$$

with c being the depth-averaged concentration [g/l], h the water depth [m] and u the flow velocity [m/s]. At first the sediment transport is modelled for the different models/datasets and with and without taking turbulence into account. Also, the (numerical) integral could be taken to have some insight in the net sediment transport over time. This is done by using the Trapezoidal method. This method uses the following equation to calculate the net sediment transport from the first moment in time (a) to the last moment in time (b) split up into N subintervals over the sediment transport graph f

$$\int_a^b f(t) dt \approx \frac{1}{2} \sum_{n=1}^N (t_{n+1} - t_n) [f(t_n) + f(t_{n+1})] \quad (3.17)$$

After this step, there is identified where and when large differences occur and how they could be caused. One of the steps to investigate this is by comparing the sediment transport as modelled by the point-model with XBeach input with both turbulent datasets (OpenFoam and analytical). By following this approach there could be checked if the deviations are caused by the hydrodynamics itself or by the OpenFoam turbulence.

Also, the nRMSE and r² values are used again to quantify these results.

3.9.2 Validating the sediment transport

All modelled sediment transport values are validated with the RESIST measurements. This is done by looking at two measured bed profiles as measured in RESIST and comparing the sediment loss or gain on specific locations. To translate this loss/gain in a sediment transport rate, the following equation is used

$$q_{sed}(i) = q_{sed}(i - 1) - \frac{(1-\epsilon_0) * [z_{final}(i) - z_{begin}(i)] * \Delta x}{\Delta t} * \rho_{sed} \quad (3.18)$$

which is after Posanski (2018). Where $q_{sed}(i)$ is the sediment transport [$\text{kg m}^{-1} \text{s}^{-1}$] on the location i ; ϵ_0 is the porosity of the soil [-], which is assumed to be 0,4 in this research. Furthermore, z_{final} and z_{begin} respectively represent the bed level [m] at the end of the measurements and at the beginning; Δx the special resolution [m] and Δt the timestep [s]. At last ρ_{sed} is the density of the sediment [kg/m^3]. In this case the sediment transport is the time-average between the times at which both bed profiles are measured.

3.10 Testing other approaches

In order to have some better understanding of the system, the effect of different approaches/assumptions will be investigated. This will be done the same way as the main research was conducted but is done afterwards to see what effect these changes have on the sediment transport.

The possibilities that will be investigated are:

- Changing the roughness coefficient in XBeach. Since XBeach has not been calibrated in this research, in this part of the research it will be investigated what effect a possible calibration would have had on the results. This could help further research by giving other researchers an indication of how much the changed roughness coefficient influences the outcomes. This main research is performed by using a Chézy roughness coefficient of $55 \text{ m}^{1/2}/\text{s}$, which is the default value in XBeach. But for this small calibration research, this default value has been changed in XBeach to 40, 50, 60 and $70 \text{ m}^{1/2}/\text{s}$ respectively. Afterwards XBeach is run again and the newly obtained XBeach outcomes have been used as input in the point-model to perform a comparison with respect to the old outcomes.
- Changing the height at which the turbulent kinetic energy was extracted from the OpenFoam model. In the main research the depth-averaged OpenFoam turbulence was used in order to have a fair comparison with the other depth-averaged parameters. But in this case other turbulence heights will be checked to see this influence. For instance, the height at which the ABS's and ADVs were installed in the RESIST dataset (3 cm) is modelled to see if this impacts the results.
- Using near-bed analytical turbulence. Approximately the same check is carried out for the analytical turbulence as for the OpenFoam turbulence, investigating what the results will be if the near-bed turbulence is used instead of the depth-averaged turbulence. The translation from depth-averaged to near-bed turbulence is made by using Equation 2.17 at Section 2.5.2.
- Assuming uniform sediment distribution. Furthermore, a vertical uniformly distributed sediment concentration will be investigated to see how the sediment transport will look like is the sediment is uniformly distributed in the water column. This means that the translation with the Rouse profile will be neglected and the measured point data is assumed to occur at every height.

- Calculating a different equilibrium sediment concentration. Reniers et al. (2013) propose a different method of calculating the equilibrium sediment concentration (c_{eq}) [g/l] based on the turbulent kinetic energy at the bed (k_{bed}) [m^2/s^2] alone instead of using both the turbulent kinetic energy and the flow velocity, which is done in the (adapted) Van Thiel-Van Rijn method (as explained in Section 2.6). The method to model the equilibrium sediment concentration based on turbulent kinetic energy alone is

$$c_{eq} = \frac{\epsilon_s k_{bed}^{\frac{3}{2}}}{w_s} * \frac{\rho_{sed}}{h} \quad (3.19)$$

and also uses the suspended load efficiency (ϵ_s) [-] and the sediment fall velocity (w_s) [m/s]. This is multiplied with the density of sediment (ρ_{sed}) [kg/m³] and divided by the water depth (h) [m] to convert the equilibrium concentration from m³/m³ to g/l. The value for the suspended load efficiency is chosen to be the same as in Reniers et al. (2013), namely 0,008.

4. Results: validating XBeach output with RESIST data

4.1 Hydrodynamics

4.1.1 Water surface elevation

As described, the water surface elevation is validated by looking at the AWG measurements at multiple locations: one close to the wave paddle (referred to as ‘offshore location’) and one in the swash zone (referred to as ‘swash location’), see Table 2 and Figure 10 at Section 3.4.1 for the exact locations. For other locations, the graphs as well as the associated quantitative validation can be found in Appendix A.

The waves match quite well at the offshore location with a r^2 of 0,93 and an nRMSE of 0,092. For the swash location however, the timeseries match slightly worse, illustrated by a correlation coefficient of 0,75 and an nRMSE of 0,226. The timeseries for both locations are depicted in Figure 12. These nRMSE values are consistent with Ruffini et al., (2020).

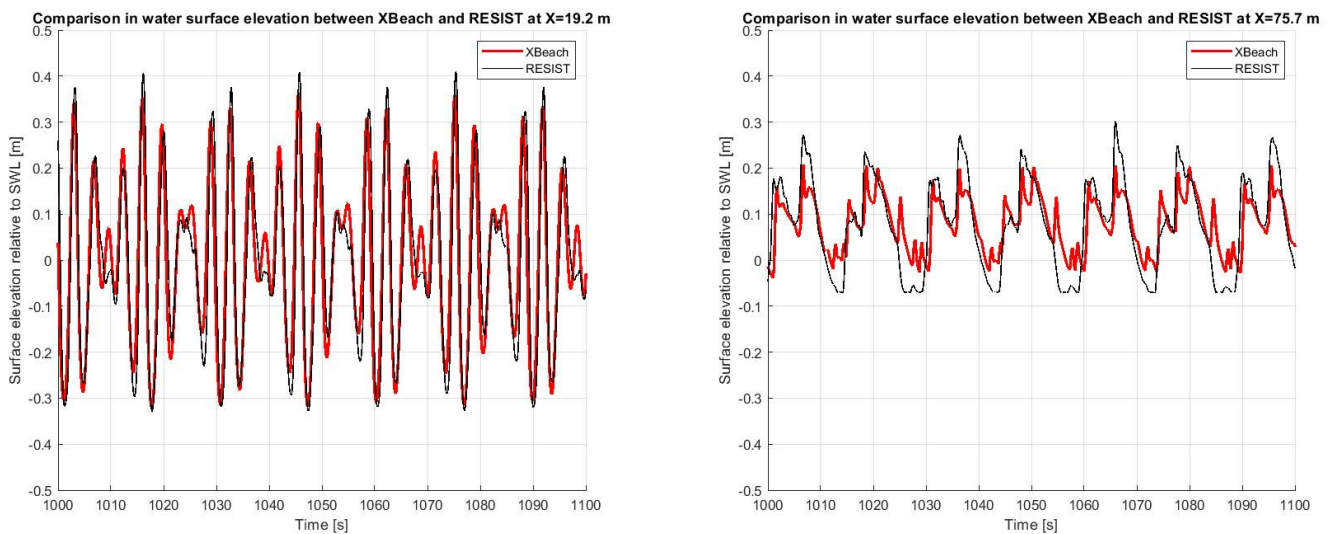


Figure 12. Comparison in water surface elevation between XBeach and RESIST for the offshore location (left) and the swash location (right). The default XBeach parameter values have been used for this validation

4.1.2 Flow velocity

The flow velocity is validated by looking at the ADV measurements at two locations as well. However, the measurement data was very noisy and in order to get a more fluent graph this data was also smoothened over the width of 0,5 s (~ 50 datapoints).

The waves match reasonable at the offshore location. The correlation coefficient has a value of 0,76 and the nRMSE is 0,144. For the swash location however, the timeseries match somewhat better, illustrated by a correlation coefficient of 0,82 and a nRMSE of 0,142. The timeseries for both locations are depicted in Figure 13. In this case it is remarkable that both the correlation coefficient as the nRMSE become better for the swash location compared to the offshore location. This is strange since in the swash more processes (shoaling, breaking, backwash etc.) are influencing the wave behaviour which could all lead to deviations.

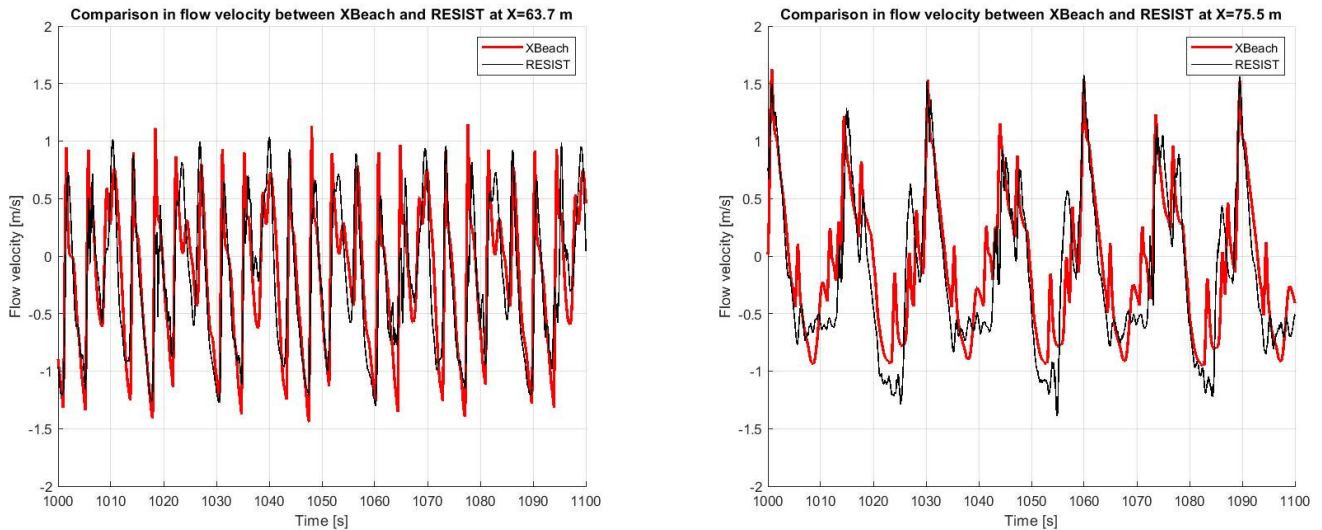


Figure 13. Comparison in flow velocity between XBeach and RESIST for the offshore location (left) and the swash location (right). The default XBeach parameter values have been used for this validation

The error between both time series for both locations could be explained by the fact that XBeach uses the depth-averaged flow velocity while the flow velocity in RESIST is measured at one vertical location (0,03 m above the bed). The height of this location could have an influence on the outcome since the velocity is lower at the bed than at the water surface.

4.1.3 Spectral analysis

The power spectra of the water surface elevation of the waves look the following, see Figure 14. It could clearly be seen that the frequencies from both the wave components are returned (at 0,24 Hz and at 0,30 Hz) at the offshore location. In the swash zone however, the highest peak is the one belonging to the resultant frequency of the wave group (0,07 Hz). This indicates that in the swash zone the specific waves are cancelled out but that the wave groups could clearly be identified.

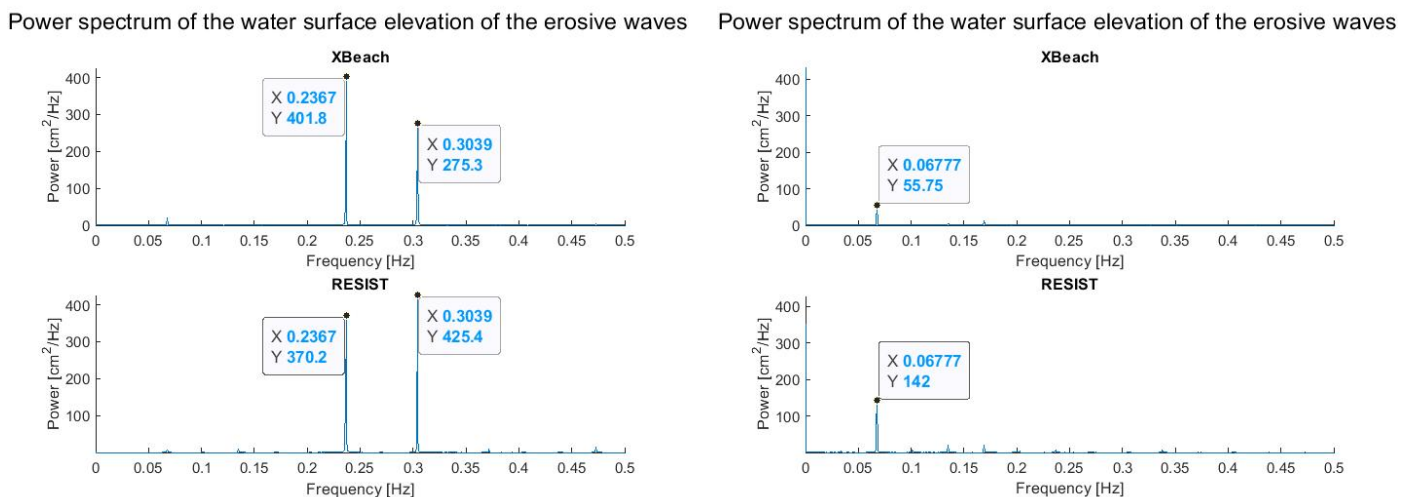


Figure 14. Comparison of the power spectra of the water surface elevation at the offshore location (left) and swash location (right)

For the flow velocity the same pattern is seen as for the water surface elevation, see Figure 15. Again, peaks are present at the bichromatic frequencies visible (at 0,24 and 0,30 Hz) at the offshore location and at the resultant frequency (at 0,07 Hz) at the swash location.

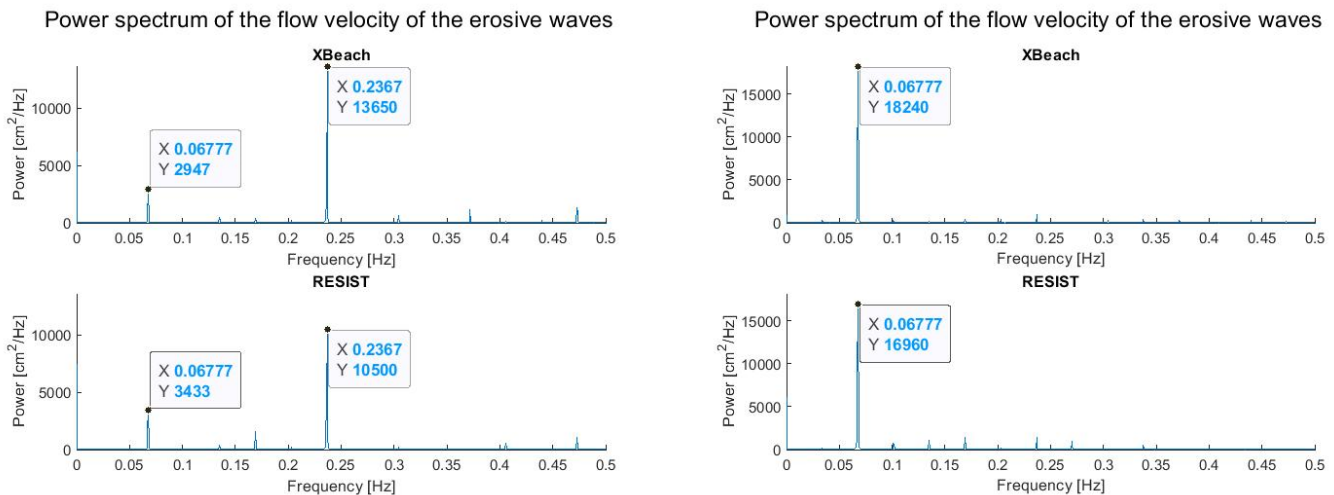


Figure 15. Comparison of the power spectra of the flow velocity at the offshore location (left) and swash location (right)

4.2 Suspended sediment

To check whether the modelled Suspended Sediment Concentration (SSC) matches the measured concentration, an initial validation should take place. This validation consists of a comparison between measured the SSC (based on OBS sensors) and modelled SSC. However, an important remark should be made here: the measured SSC is at 0,03 m from the bed while the modelled SSC is depth-averaged. This could again cause some deviations. The locations that are stated in Table 2 and Figure 10 at Section 3.4.1. Again, the RESIST data was smoothed over the timespan of 0,5 s (~20 datapoints) and this XBeach timeseries was interpolated as well to match the length and frequency of the RESIST data.

As could be seen in Figure 16, large deviations between the modelled and measured SSC are present. This applies to both locations, illustrated with a r^2 value of -,014 and 0,52 at the offshore location and the swash location respectively. The nRMSE values are respectively 0,68 and 0,50 for the offshore location and the swash location. This comparison is performed based on the measured point data versus the modelled depth-averaged data. Comparing both depth-averaged data is presented in 4.2.2.

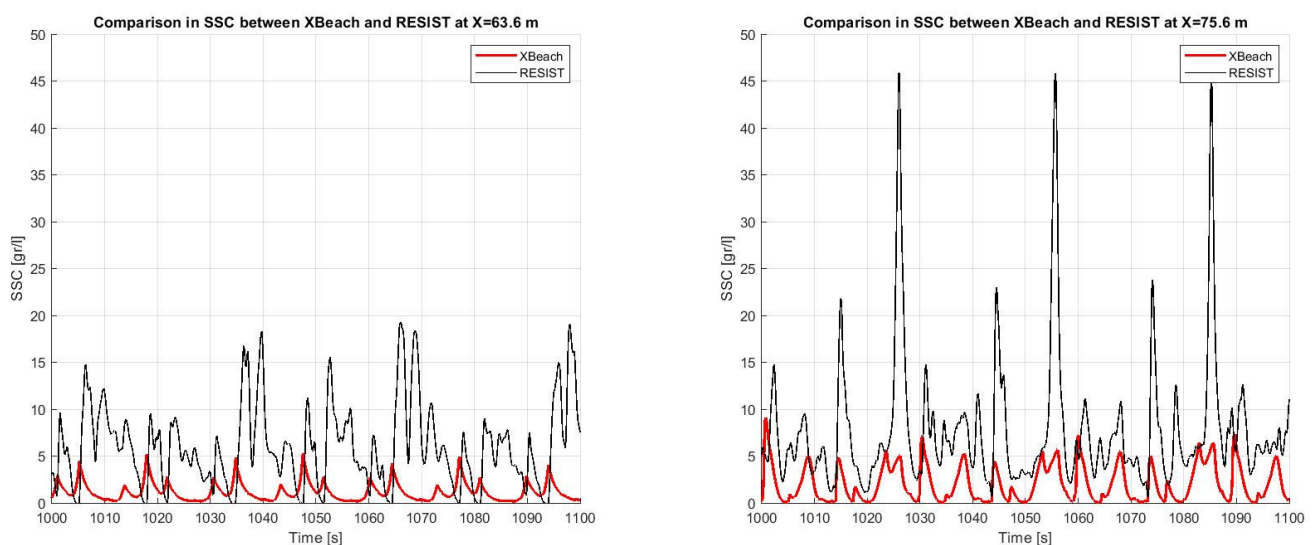


Figure 16. Comparison in SSC between XBeach and RESIST for the offshore location (left) and the swash location (right). Those locations are respectively 13,5 and 0,6 m from the SWL shoreline. Note: this difference could be caused by the way it is determined (fixed height vs depth-averaged)

In here the measured (RESIST) SSC value is higher for almost every moment in time when compared to the modelled (XBeach) value. Additionally, some peaks are present for both timeseries while at other moments in time only a peak is observed for one of the timeseries which again indicates a bad match between the two.

4.2.1 Rouse profile

As discussed in Section 2.4.5 and 3.4.5, the Rouse profile has been fitted to the data to translate the RESIST point-data into depth-averaged values. This depth-averaged concentration based on the Rouse profile and measured reference concentration is shown in Figure 17. A remark of this method is that the SSC values for water depth smaller than 0,03 m are enormously high. To compensate for this, the observed values (at 0,03 m) are filled in at those moments to get a realistic curve which clearly shows some peaks in SSC, see Figure 17.

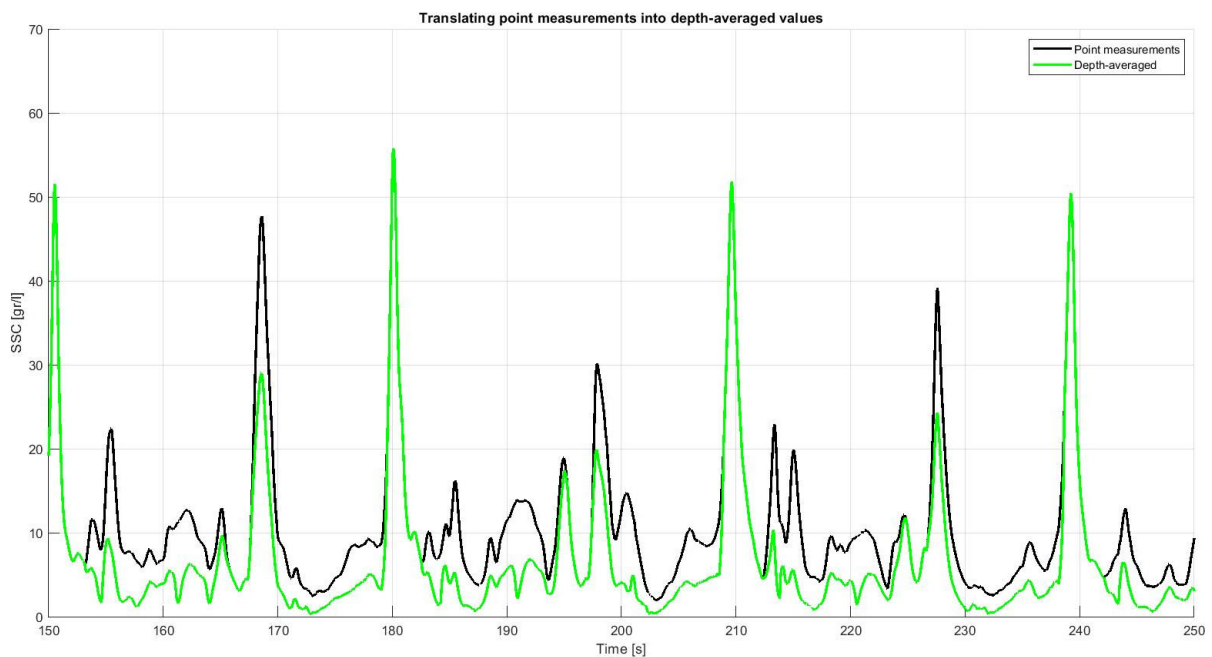


Figure 17. The sediment concentrations as directly measured in the RESIST dataset (black curve) and the translation of those into depth-averaged values (green curve).

As can be seen in Figure 17, the newly calculated depth-averaged observed SSC follows the pattern of the point measurements only some peaks to be decreased. However, as could be seen in Figure 18, the highest peaks occur when the water level is at its lowest. Which could be explained by the fact that the water depth is so minor that only the very sediment rich sheet-flow layer is taken into account at those moments since the water depth is only several centimetres or less. Another explanation is that the Rouse equation is not applicable for water depths with the same order of magnitude as the sediment particles.

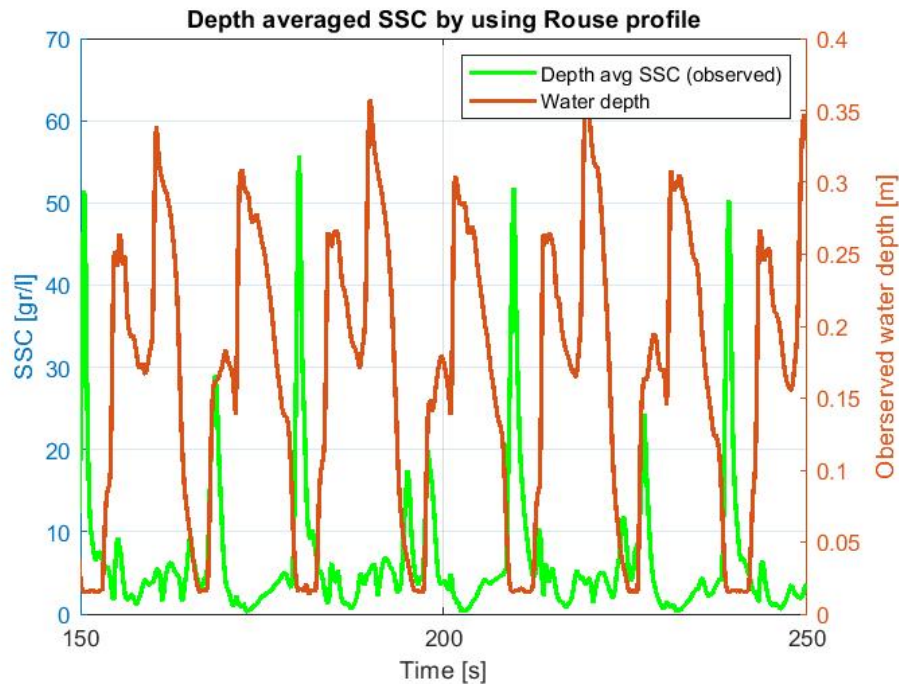


Figure 18. Depth-averaged SSC values versus the observed water depth. It shows that the peaks in SSC coincide with very shallow water

4.2.2 Comparing depth-averaged SSC timeseries

To make a fair comparison between the measured and the modelled SSC, the measured SSC is translated into a depth-averaged SSC by applying a Rouse profile, as explained above. By doing this, both SSC timeseries are now depth-averaged. This comparison is presented in Figure 19. Comparing these still results in the same pattern as it was before converting the point measurements into depth-averaged values (see therfor Figure 16). XBeach SSC peaks are approximately 5 times lower than the depth-averaged RESIST peaks and the timing is still somewhat odd. This results in a r^2 of -0,32 and an nRMSE of 0,48. These values represent quite a bad match.

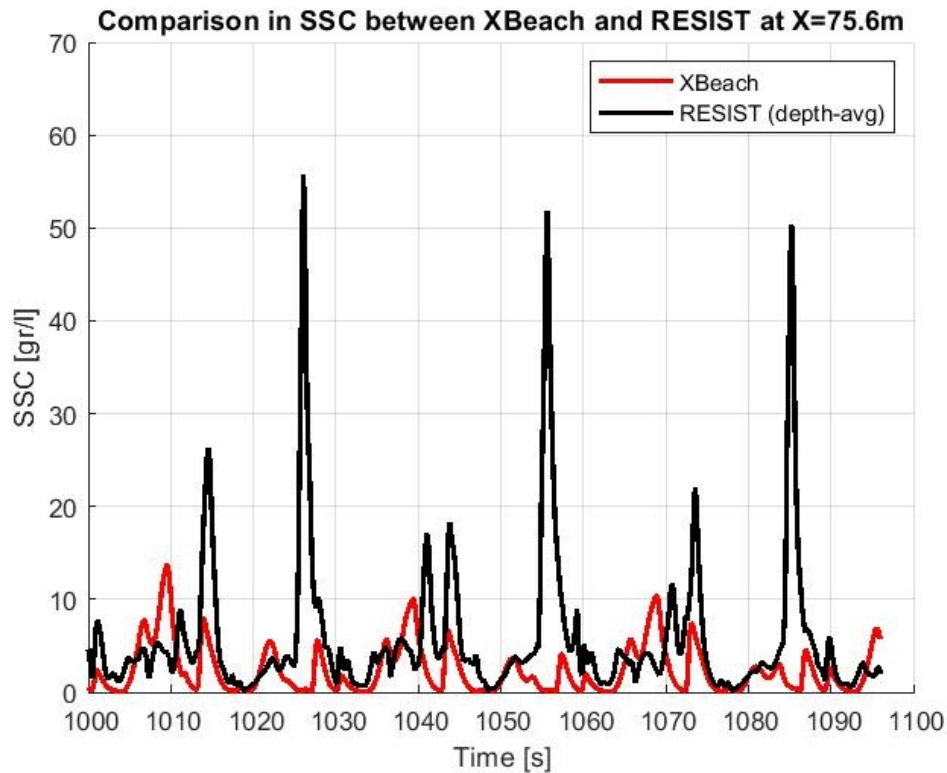


Figure 19. Comparing the XBeach SSC with the RESIST SSC after applying the Rouse profile to convert the point measurements into depth-averaged values. This comparison is performed at the swash location, which is 0,6 m from the SWL shoreline.

4.3 Summary

This chapter shows that XBeach is quite good in modelling the hydrodynamics of waves. It also shows that in deeper water the individual waves could clearly be identified. Yet this is not the case anymore in the swash zone, where the pattern is more based on the wave groups. This distinction is also proved by the spectral analyses which returns the frequencies of the individual waves and wave groups respectively in the offshore water and at the swash location.

For the sediment transport however, XBeach performs not so well. It even is not capable of matching the SSC peaks as well in amplitude as in timing. Although this chapter also shows that these peaks in the observed SSC happen at moments with very shallow water.

5. Results: the characteristics of turbulence in the swash zone

The profile chosen at Section 3.3.2 and the waves described in Section 3.3.1 are now loaded into an OpenFoam model. This type of model is capable of modelling the amount of turbulence in the water, see Section 3.6 for a more detailed explanation of this model. Yet, this model does not use depth averages, but its values are height specific. This means that the velocity, turbulence and all other parameters are computed at all heights in the water column with an Δz of 2,5 cm.

5.1 Validating the OpenFoam model

However, since this model contains values at each 2,5 cm in height, the depth-averaged value of the flow velocity should first be calculated. This was simply done by averaging all the values between the bed and the free surface elevation. After this process, it was made sure that the times were synchronized. The timeseries of the water levels and the flow velocities could then be compared and validated. This looks the following, see Figure 20.

At first the OpenFoam validation is carried out with respect to the measured timeseries. However, to make sure that there are no (large) discrepancies between the OpenFoam timeseries and the XBeach timeseries, the OpenFoam data is also compared with respect to the XBeach data. That is why the XBeach data is present in Figure 20 as well. The results of the quantitative validation are given in Table 3.

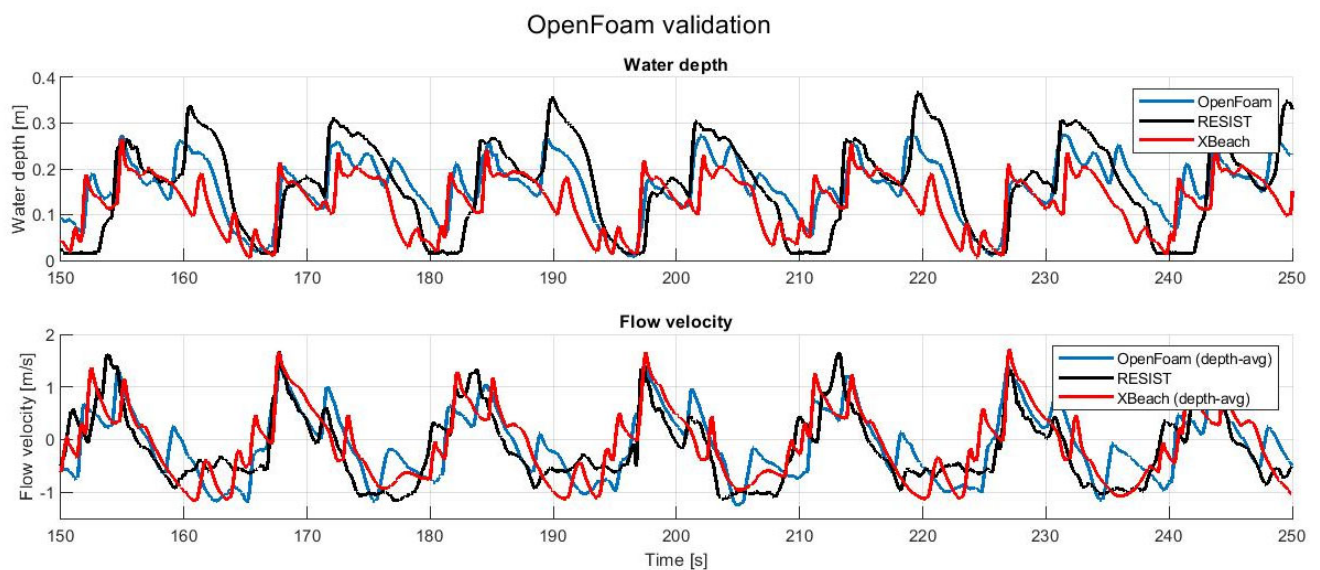


Figure 20. OpenFoam validation with respect to RESIST and XBeach

Table 3. The quantitative validation of the OpenFoam water level and flow velocity in comparison with the measured ones and the ones modelled with XBeach

| Validation timeseries | Water level [m] | | Flow velocity [m/s] | |
|-----------------------|-----------------|-----------|---------------------|-----------|
| | nRMSE [-] | r^2 [-] | nRMSE [-] | r^2 [-] |
| RESIST | 0,18 | 0,78 | 0,18 | 0,73 |
| XBeach | 0,23 | 0,70 | 0,17 | 0,70 |

It could be seen in Figure 20 that the match between the graphs is quite good, this is also illustrated by the nRMSE and r^2 values in Table 3. For instance, the peaks of the flow velocity match very well for the magnitude as well as the timing while the magnitude of the water depth

is quite a bit smaller than the one from RESIST. Although, the OpenFoam timeseries show a strange bump in the flow velocity around $t=177$ s; $t=206$ s and $t=235$ s which is not there in the other timeseries.

5.2 Extracting the OpenFoam turbulence data

After this validation, the same pre-processing of the data (described in Section 3.6 and 5.1) was carried out again but this time with the turbulence data. The results then look the following, see Figure 21. In there also the turbulence at 3 cm above the bed is plotted since this is the height at which the OBS sensors were placed in the RESIST dataset.

In this research it is decided to use the depth-averaged turbulence to do the analysis. This is mainly because all other parameters are depth-averaged as well and partly because this value could be computed for every water depth. When for instance the turbulence at a height of 3 cm was chosen, there would be no turbulence if the water surface was below this 3 cm.

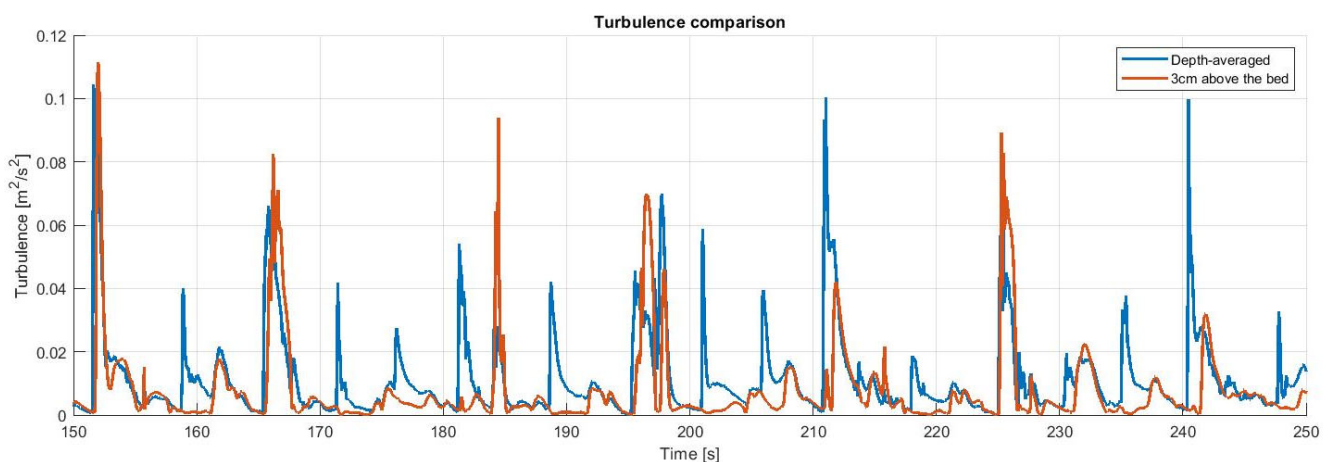


Figure 21. The presence of turbulence (at 3cm above the bed versus depth-averaged) over time as modelled by OpenFoam

Figure 21 also shows that a peak in the depth-averaged turbulence does not necessarily mean that there is a peak of the turbulence near the bed as well. In other words: the sediment at the bed is not necessarily influenced heavily when there is a peak in the depth-average turbulence. However, the other way around holds as well. Figure 21 shows some peaks of the near-bed turbulence when there is no clear peak in the depth-averaged turbulence. This both implies that using the depth-averaged turbulence could give some deviations in the eventual sediment concentration results. However, since all other parameters are depth-averaged as well, it is chosen to still use the depth-averaged turbulence in this case. Although, using the turbulence at 3 cm has also been evaluated to see this effect, see therefore Section 6.7.2.

5.2.1 The behaviour of the turbulence

To also get an insight in the way turbulence arises, propagates and eventually decays, some snapshots from the OpenFoam results are made by my supervisor, ir. J.W.M. Kranenburg. These snapshots show an intersection of the swash zone with the bed (grey), the water with the amount of turbulence indicated (blue to red) and the air above the water (dark blue). The behaviour of the turbulence is presented using four snapshots, see Figure 22 (wave arrival, arising turbulence), Figure 23 (wave propagating, turbulence propagates down), Figure 24 (Flow-reversal, turbulence decays) and Figure 25 (new wave arrival). Those snapshots are taken with a mutual time interval of 2 s.

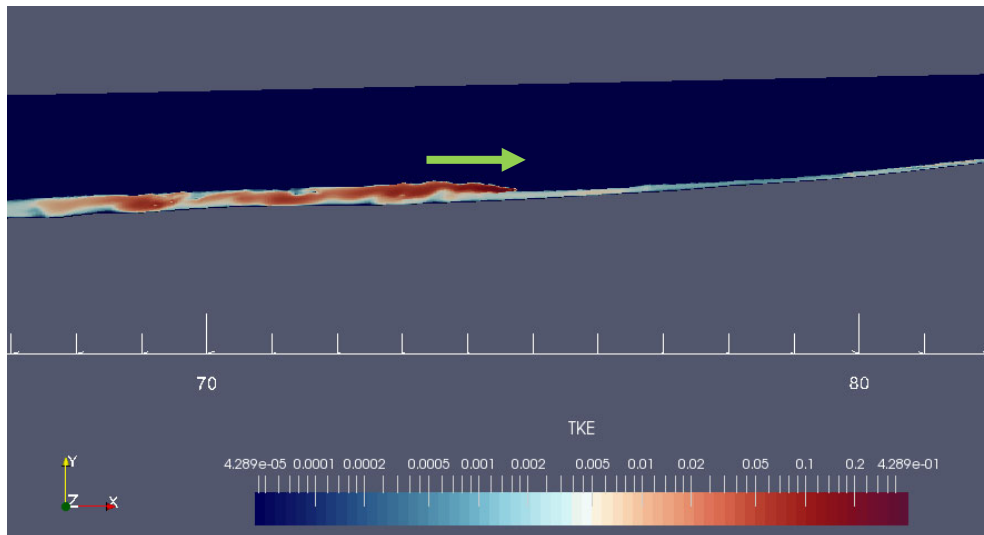


Figure 22. A wave arriving at the beach with much Turbulent Kinetic Energy (TKE) arising near the water surface, indicated by the green arrow

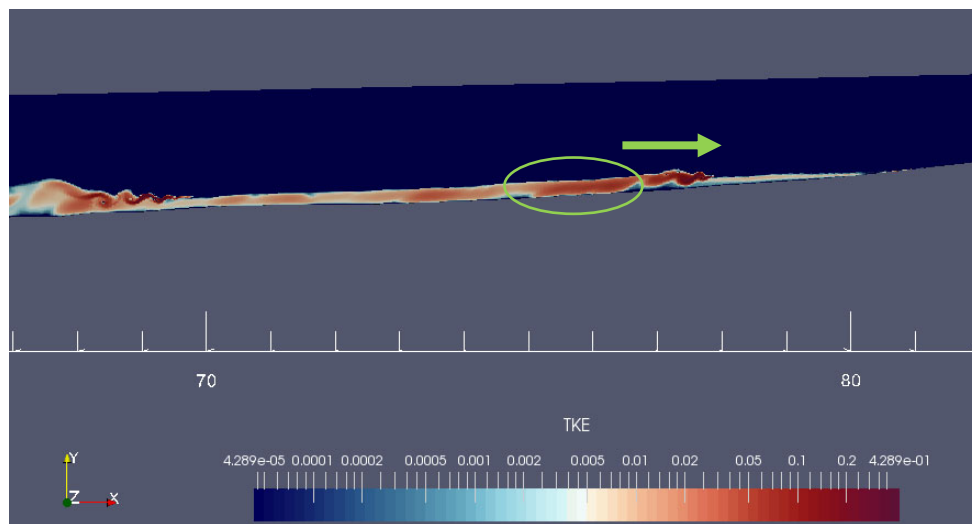


Figure 23. Wave propagating onto the beach (green arrow) while the turbulence propagates down the water column (green circle)

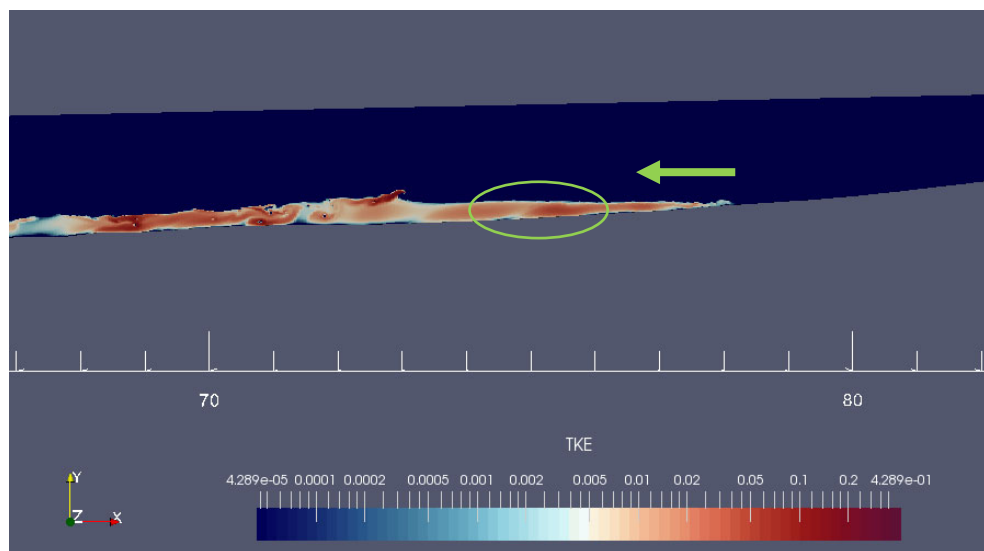


Figure 24. Backwash is starting (green arrow) while the turbulence is decaying (green circle)

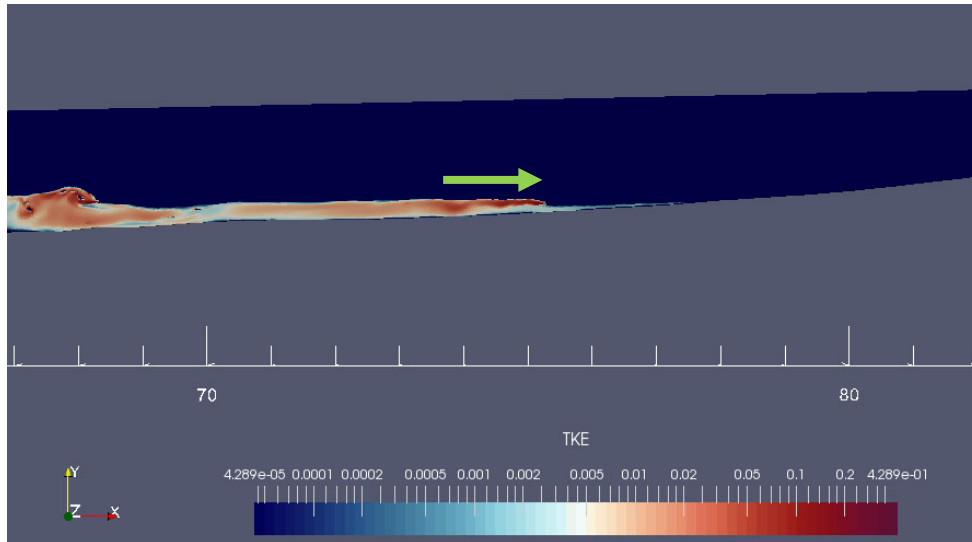


Figure 25. New wave is arriving with again high TKE near the water surface

5.3 The relation between the processes

All the available timeseries could then be plotted in one figure to see all described processes happening at the same time as an overview. This is shown below in Figure 26.

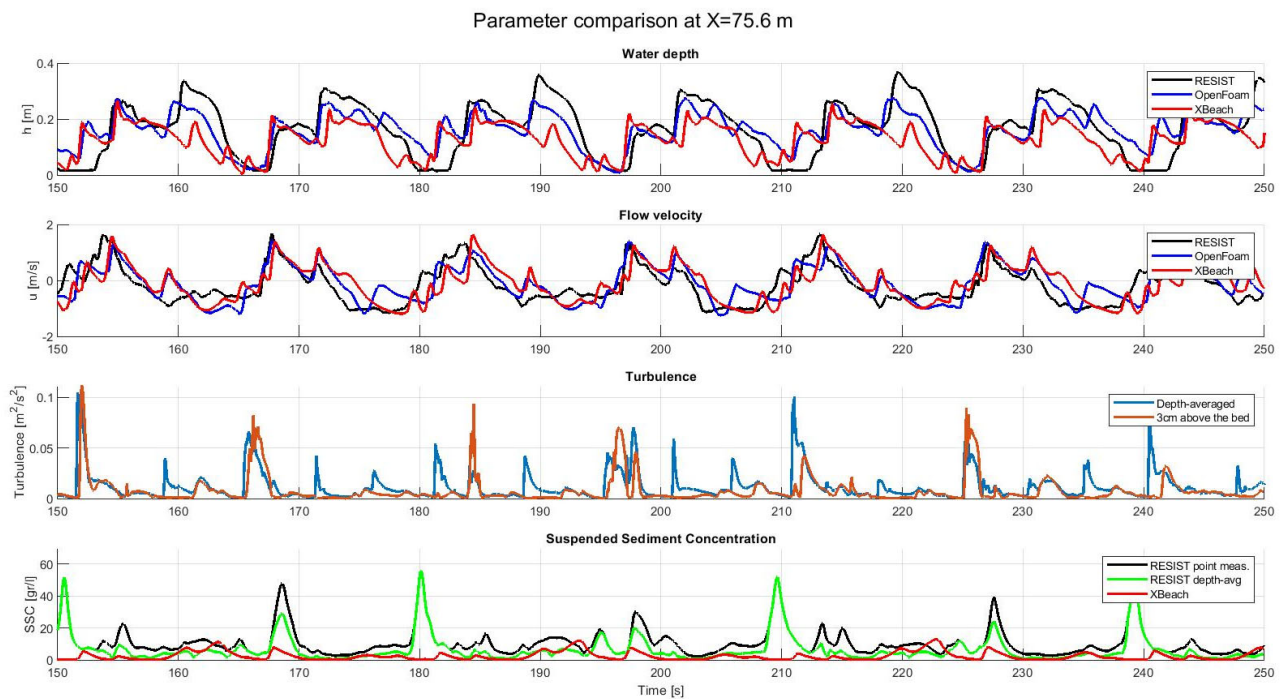


Figure 26. Overview of all timeseries to see all processes happening at the same time

5.4 An analytical point-model for turbulence

As explained in detail in Section 2.5.2 turbulence could also be modelled by following an analytical approach. This method is based on the bore-induced (depth-averaged) turbulence, which is the production of turbulence. Yet this method also takes into account the transport of turbulence over time and in space. When plotted, this then looks the following, see Figure 27.

It is remarkable that the (depth-averaged) OpenFoam turbulence is approximately a factor 5 smaller than the analytically approached depth-averaged turbulence. However, the timing and the shape of the curve are almost identical. Especially the similarity of the shape is noteworthy: both timeseries show a sudden increase (caused by bore arrival), followed by more or less exponential decay which eventually fades to zero or a new steep increase. This similar behaviour nicely shows the way turbulence arises and vanishes in the system.

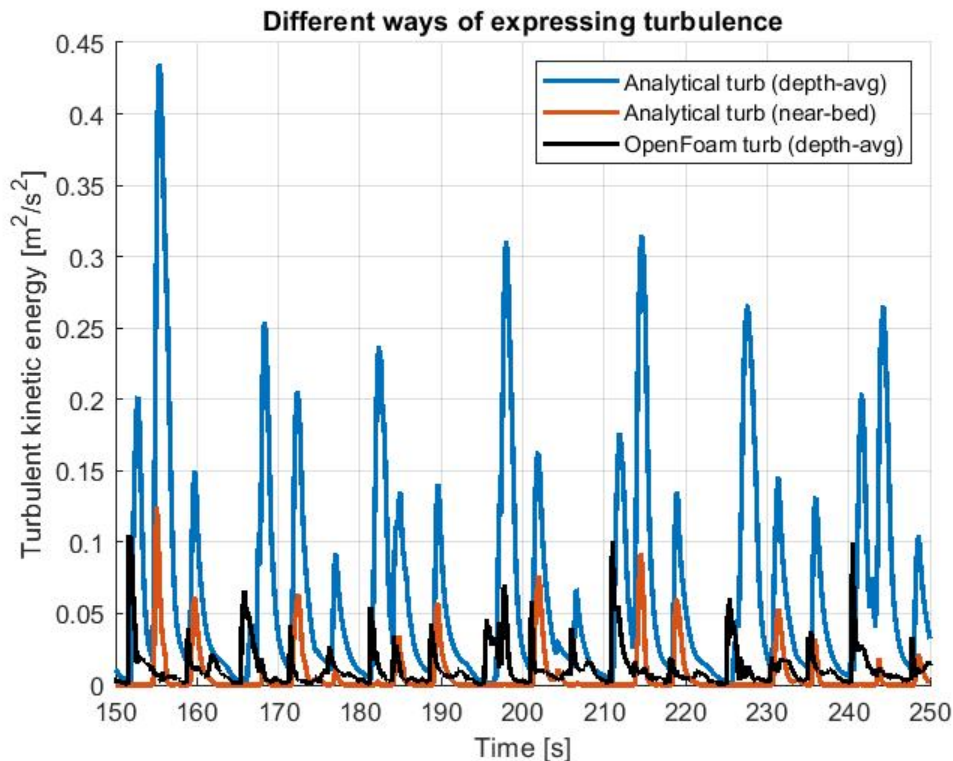


Figure 27. The depth-averaged and the near-bed analytical turbulence (based on Reniers et al. (2013)) versus the OpenFoam turbulence over time

5.5 Summary

The OpenFoam model shows quite a good match in the swash zone regarding the flow velocity as the water depth, as well as with respect to RESIST as with respect to XBeach. The turbulence dataset from this OpenFoam models shows that the turbulence is generated at the water surface and propagates horizontally with the flowing water but also propagates down to the bed. During this process dissipation takes place which eventually causes the turbulence to fade away. This process implies, and this is also showed by the dataset, that the depth-averaged turbulence is not the same as the near-bed turbulence.

Thereafter also another model for turbulence is set up which approaches the turbulence in an analytical way. The results of this model show the same timing of the occurrence of turbulence and its more or less exponential decay. Yet this turbulent kinetic energy is approximately 5 times larger than the OpenFoam turbulence.

6. Results: including turbulence in the model

6.1 SSC point-model with OpenFoam turbulence

As explained in Section 2.6, the turbulence will be added to the sediment transport calculation by basically adding the turbulent kinetic energy to the flow velocity.

6.1.1 Calibrating the amount of included turbulence

As explained in Section 3.5.3 the amount of turbulence being included to the sediment transport model could be changed by altering the calibration coefficient. In this part of the research the result of this altering is made clear. The different SSC results when altering this calibration coefficient are shown in Figure 28. The largest effect can be seen around the peaks ($t=166$ s; $t=197$ s; $t=252$ s). The results of the regular VTVR method (so no extra included turbulence) are presented with the black graph. The orange graph shows the effect of adding a small amount of turbulence and it could be seen that at those moments the SSC is slightly higher than with no turbulence included. This pattern is even more visible for the yellow graph where calibration coefficient is set to 5 and the purple graph where the calibration is set to 10. By choosing a relatively high value for the calibration coefficient, peaks in the SSC could be created at the moments in time where there was a through without any turbulence.

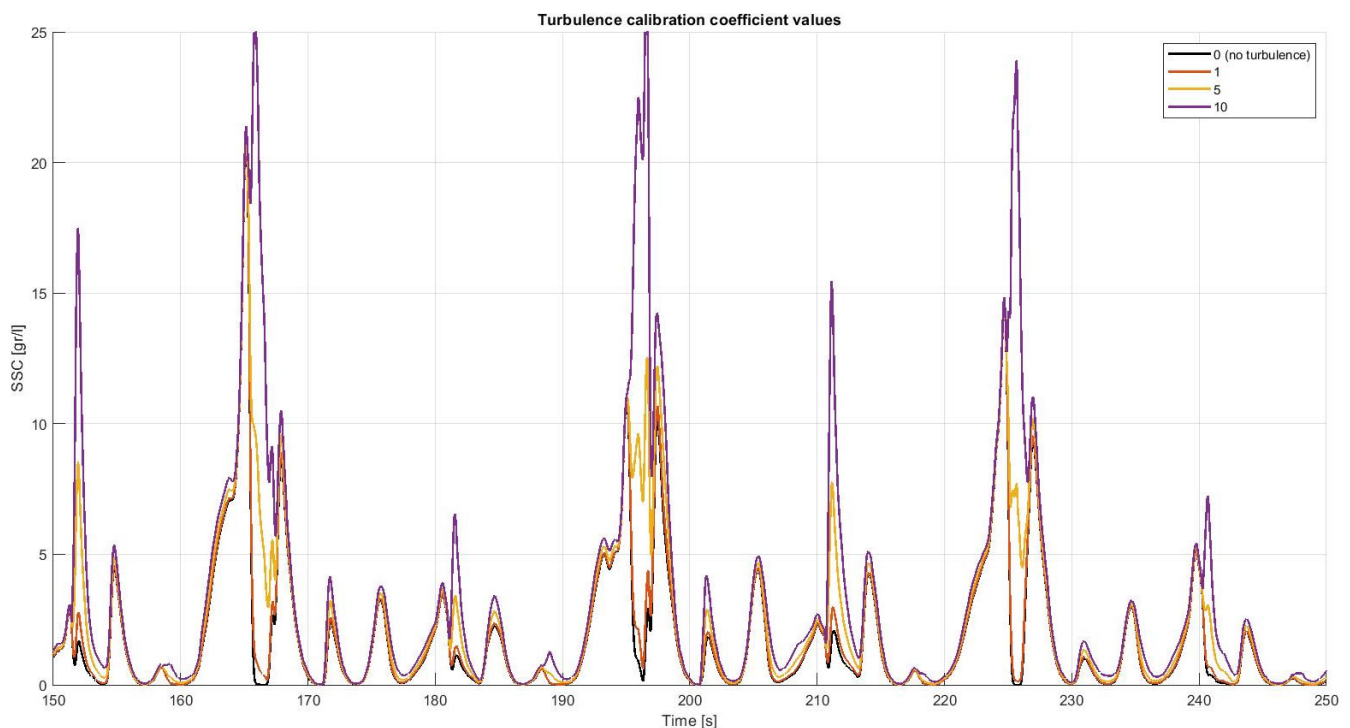


Figure 28. The SSC outputs when different values for the calibration coefficient have been used. Is plot is made based on the OpenFoam hydrodynamics and turbulence. Yet for the XBeach hydrodynamics or the analytical turbulence the same effect occurs.

Eventually a value of 6 was used in this research since these results showed the r^2 and nRMSE values when compared to the measurements.

6.1.2 OpenFoam hydrodynamics

At first this point-model will be ran by using the hydrodynamics from OpenFoam. This is to make sure the turbulence data matches the water depths and flow velocities is the most optimal way since it is the output of the same model. The results are shown below in Figure 29.

As there could be seen in Figure 29, the regular point-model matches quite well with the XBeach output but is not a perfect match. This makes sense since both the point-model and XBeach make use of the Van Thiel-Van Rijn approach but XBeach is somewhat more complex and takes for instance advection into account. However, it still differs a lot from the measured data. It can be seen as well that including turbulence in this model does make the SSC peaks already somewhat higher at some moments in time (for instance $t=196$ s and $t=211$ s). However, the curve of the point-model including turbulence does still not match well with the RESIST curve. This is also illustrated by both the nRMSE and r^2 value which also indicate a bad match, see Table 4.

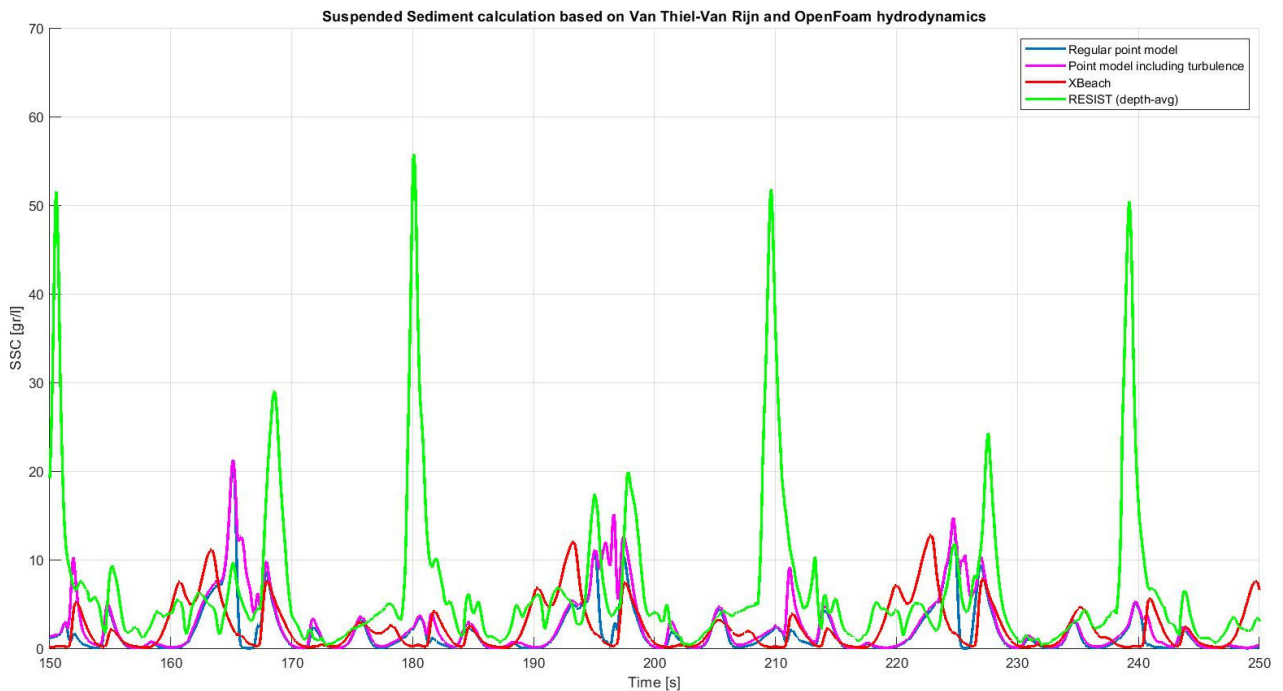


Figure 29. Results of the point-model with the OpenFoam hydrodynamics as input with turbulence included (pink graph) and without (blue graph). In here the calibration constant was set to 6. The SSC values from XBeach (red graph) and RESIST (depth-averaged; green graph) are presented as a reference.

6.1.3 XBeach hydrodynamics

To be sure that this effect is not due to the difference in hydrodynamics between XBeach and OpenFoam, the point-model is run again but now by using the XBeach hydrodynamics as input. These results are shown below, see Figure 30.

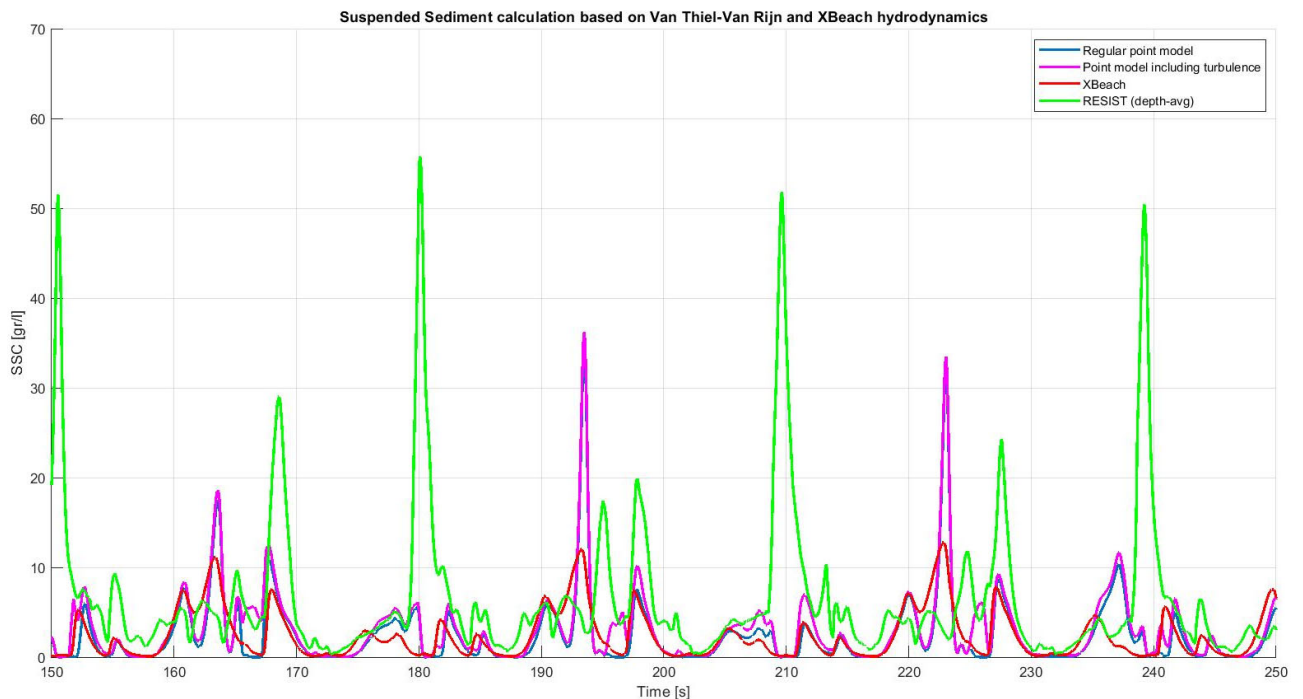


Figure 30 Results of the point-model with the XBeach hydrodynamics as input with turbulence included (pink graph) and without (blue graph). In here the calibration constant was set to 6. The SSC values from XBeach (red graph) and RESIST (depth-averaged; green graph) are presented as a reference.

As you could see in Figure 30, the same process happens with the XBeach hydrodynamic input as for the OpenFoam hydrodynamic input. The SSC peaks become slightly larger when including the turbulence, but it is still quite a bad match. This is again showed by the bad r^2 and nRMSE values, see Table 4.

6.1.4 Summarizing table

In order to have distinct quantitative comparison, the above mentioned nRMSE and r^2 are summarized below and showed again in Table 4.

Table 4. The quantitative validation of XBeach and the point-model with and without the OpenFoam turbulence effects included. These quantitative results are from the comparison between the outcomes of the sediment point-model and the depth-averaged observed SSC values. The calibration coefficient for the amount of turbulence was set to 6.

| | Hydrodynamic input | OpenFoam | XBeach |
|--------------------------|---------------------------|----------|--------|
| Sediment model | | | |
| nRMSE [-] | XBeach ¹ | - | 0,18 |
| | Point-model based on VTVR | 0,17 | 0,19 |
| | Point-model incl turb | 0,17 | 0,18 |
| r² [-] | XBeach ¹ | - | -0,03 |
| | Point-model based on VTVR | 0,26 | 0,02 |
| | Point-model incl turb | 0,20 | 0,01 |

1. Strictly seen it is unfair to show the values of the comparison of the observed values and XBeach results in this Table as well since this is not a point-model. Yet, they are just mentioned as kind of reference value showing how well XBeach performs in modelling the SSC.

As could be seen in Table 4 both the nRMSE and r² value does not change significantly when turbulence is included. It also shows that the point-model matches with the measurements to the same extent as XBeach (although it is quite low). Thereafter it shows that there is only difference in the r² values (i.e. the shape of the graph) between using the OpenFoam or the XBeach hydrodynamics while the Error of the graph does not depend on the used hydrodynamics (represented by the nRMSE).

6.2 SSC point-model with analytical turbulence

To investigate if a more sophisticated turbulence model (OpenFoam) shows better results than approaching the turbulence analytically (described in Section 2.5.2), the analytical approach will be used as an approximation of turbulence as well. When doing this, the step of using the point-model with OpenFoam hydrodynamics is skipped and it is performed with the XBeach hydrodynamics straight away. By doing that, the results of the point-model with and without turbulence are showed in Figure 31.

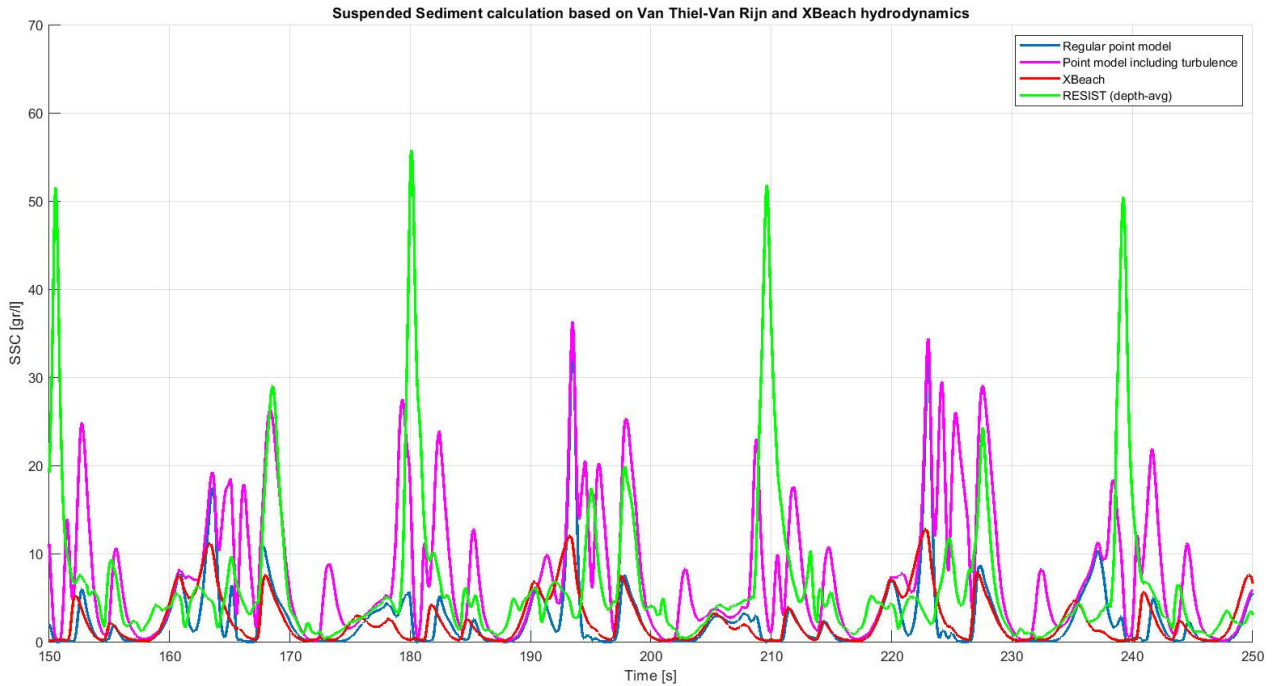


Figure 31. Results of the point-model with the XBeach hydrodynamics as input with the analytically computed turbulence included (pink graph) and without (blue graph). It could be seen that the inclusion of turbulence creates peaks in the SSC concentration. In here the calibration constant was set to 6. The SSC values from XBeach (red graph) and RESIST (depth-averaged; green graph) are presented as a reference.

Again, the results of this point-model including turbulence are does not change significantly when including turbulence although it does create some new peaks (see for instance $t=195$ s and $t=213$ s) which improves the shape of the curve slightly. This is in turn also showed with the r^2 and nRMSE values, see Table 5.

6.2.1 Summarizing table

In order to have a distinct quantitative comparison, the above mentioned nRMSE and r^2 are summarized below and showed again in Table 5.

Table 5. The quantitative validation of XBeach and the point-model with and without the analytical turbulence effects included. These quantitative results are from the comparison between the outcomes of the sediment point-model and the depth-averaged observed SSC values. The calibration coefficient for the amount of turbulence was set to 6.

| Sediment model | | Hydrodynamic input | XBeach |
|----------------|---------------------------|--------------------|--------|
| nRMSE [-] | XBeach | | 0,18 |
| | Point-model based on VTVR | | 0,19 |
| | Point-model incl turb | | 0,18 |
| r^2 [-] | XBeach | | -0,03 |
| | Point-model based on VTVR | | 0,02 |
| | Point-model incl turb | | 0,21 |

6.3 Quantitative SSC results

The quantitative validation values from Table 4 and Table 5 are also presented graphically, see therefore Figure 32. It could be seen that including turbulence in general does not change both

the validation values significantly, except for the r^2 which becomes somewhat better when including the analytical turbulence.

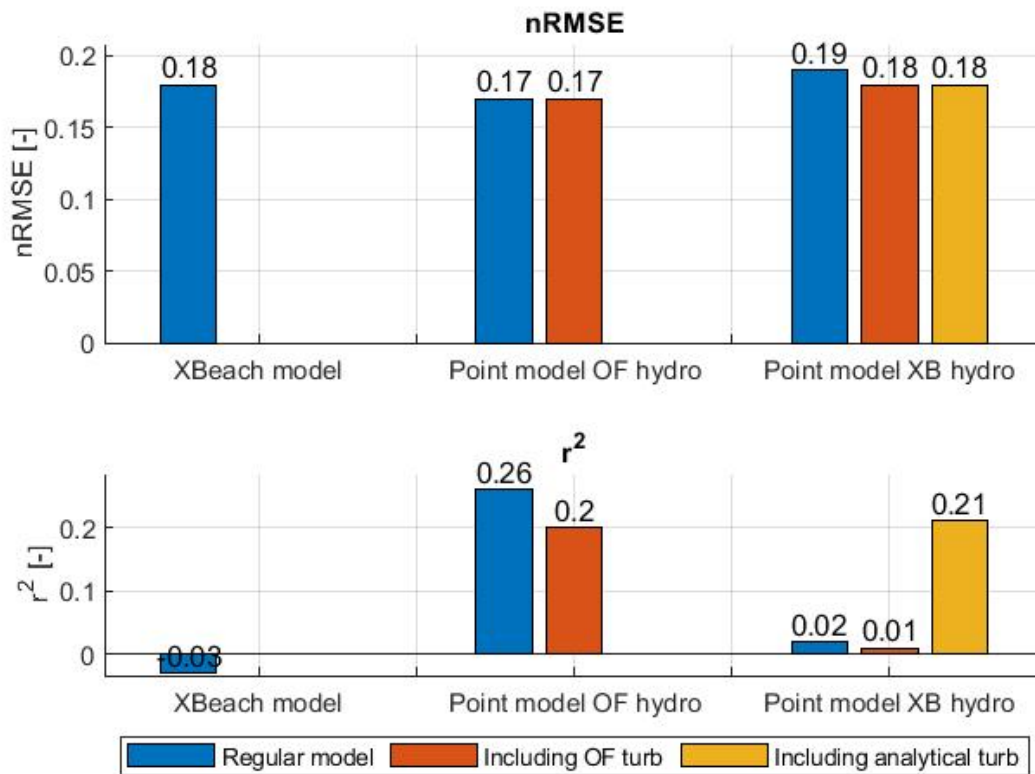


Figure 32. Quantitative results of the inclusion of OpenFoam turbulence and the analytical turbulence to the sediment point-model in relation to the depth-averaged observed SSC values. The calibration for the turbulence inclusion was set to 6.

6.4 Sediment transport rates

It is nice to have some insight in the difference the presence of turbulence makes in the amount of the Suspended Sediment Concentration, but it is more relevant to know which influence it has on the sediment transport itself. When computing the sediment transport (by using Equation 3.16 from Section 3.9.1) it looks the following, see Figure 33.

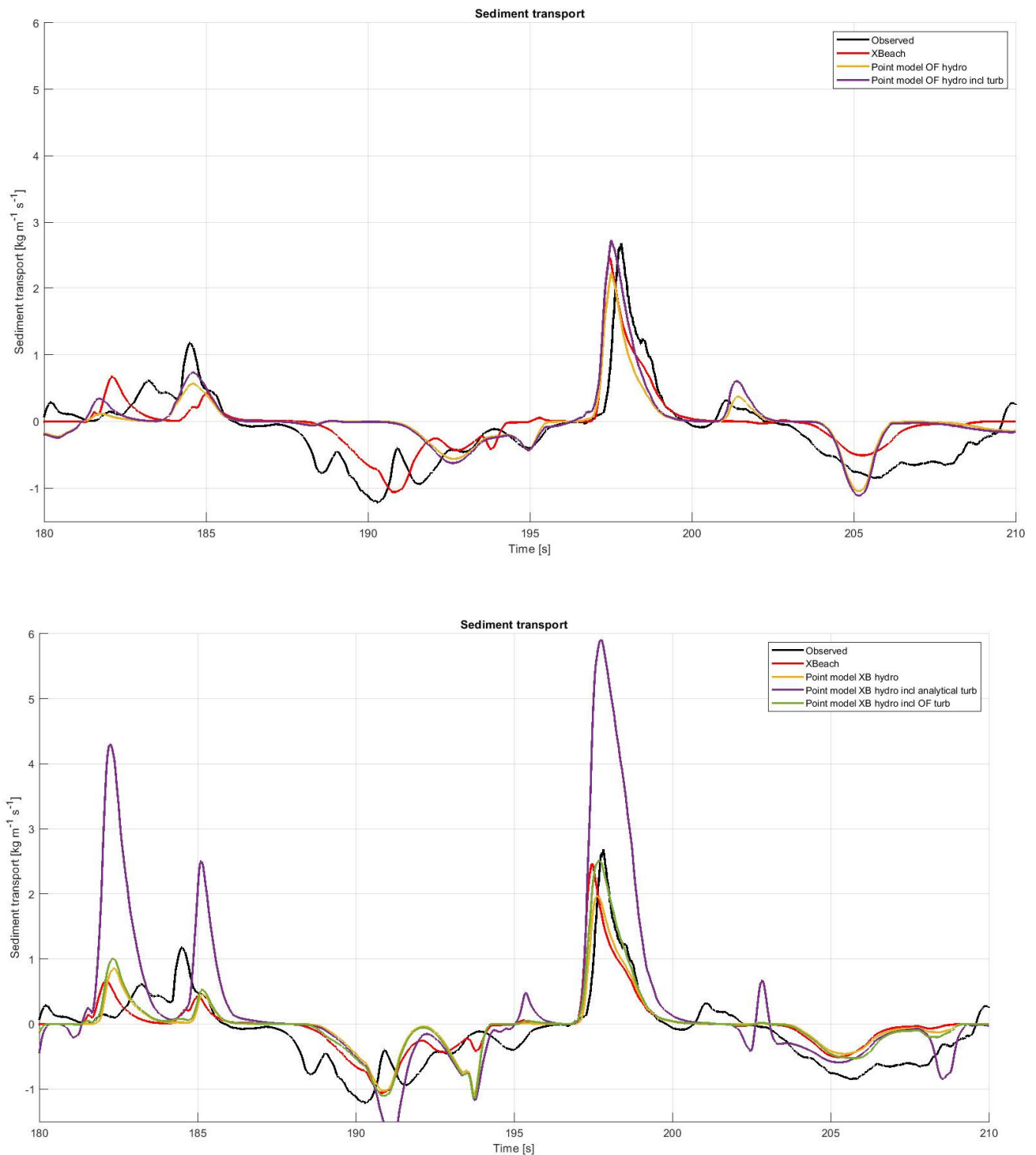


Figure 33. Sediment transport of the point-model based on OpenFoam hydrodynamics (top) and on the XBeach hydrodynamics (bottom). The same plots but for a wider time interval ($t=150$ s to $t=250$ s) are given in Appendix B.

Since the peaks of the timeseries based on XBeach hydrodynamics including the analytical turbulence are approximately 2 times higher than the peaks of other timeseries, it is determined to decrease the calibration factor for the analytical turbulence (α in Equation 3.15 in Section 3.8) with a factor 2 as well. The result of this and the comparison with the other timeseries can be seen in Figure 34.

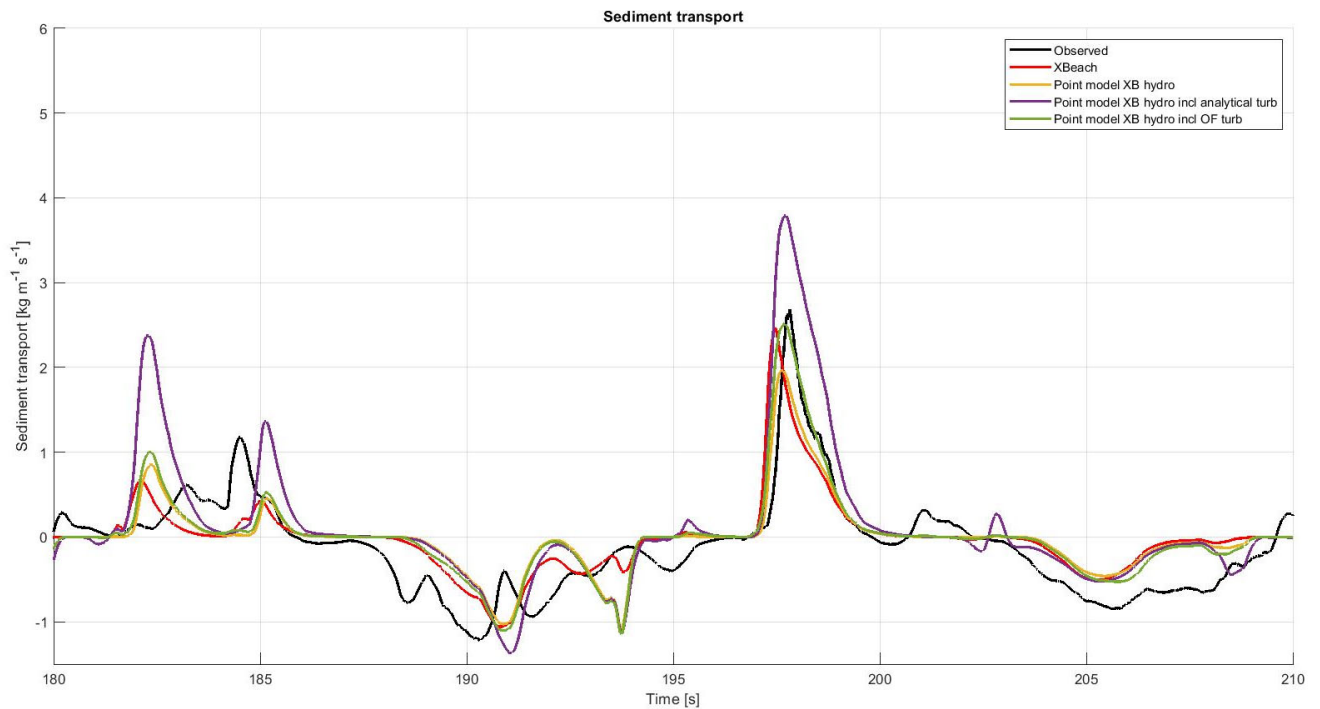


Figure 34. Sediment transport of the point-model based on the XBeach hydrodynamics with a decreased calibration factor (now being 3).

6.4.1 Analysis of the similarities/discrepancies

As seen in Figure 33 (top) and Figure 34, all modelled sediment transports graphs are more or less the same. Resulting in a positive peak around $t=182$ s to $t=185$ s and at $t = 198$ s, which (especially the latter one) matches the observed sediment transport fairly well. This also accounts for the negative sediment transport peak around $t=191$ s which is caused by the negative (offshore directed) flow velocity. Although the observed negative sediment transport is peak is a lot wider.

A possible explanation of this behaviour is that the peaks in high sediment transport (positive and negative) coincide with bore arrival, see Figure 35. This relation is also the case in Ruffini et al. (2020). They state that advection is large at bore arrival because velocity and SSC gradients are large, which is also the case in this research. This could cause inaccuracies in these results since this research uses a point-model to model the SSC in which advection (and horizontal diffusion) is/are neglected.

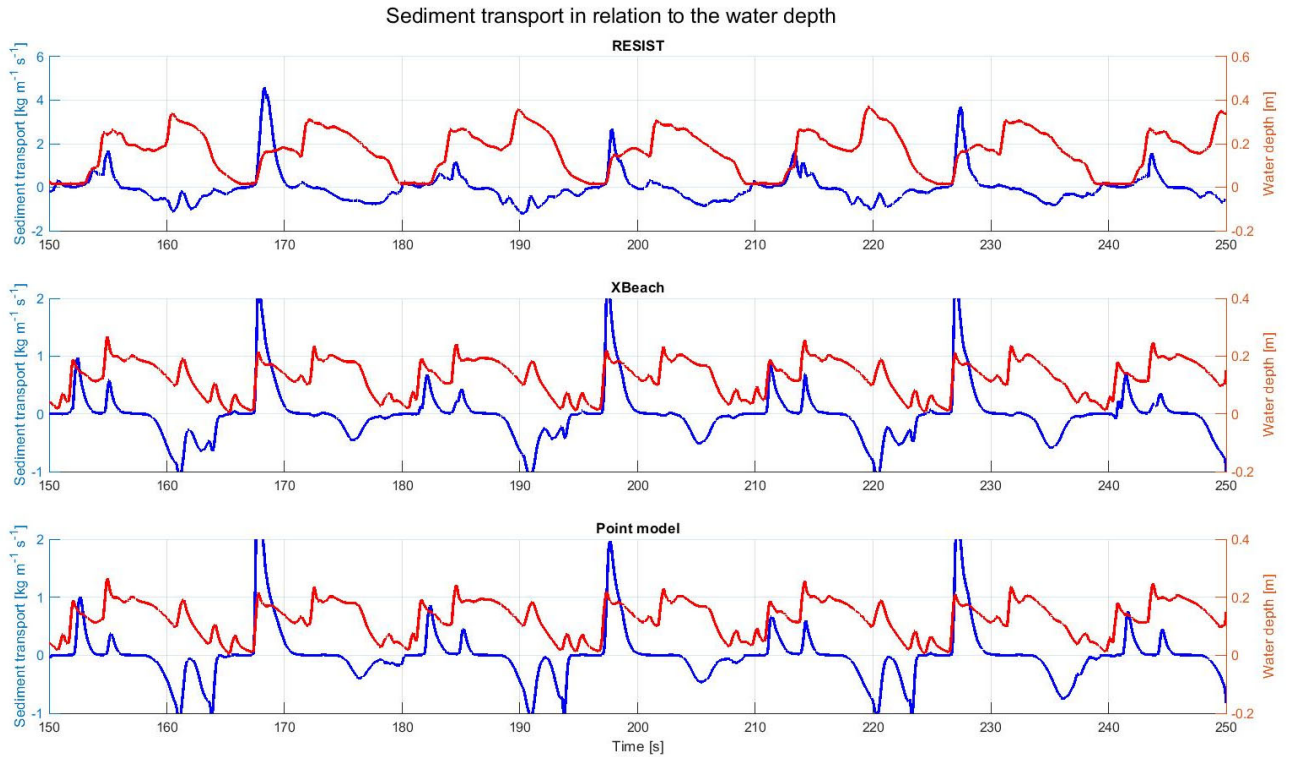


Figure 35. Relation between sediment transport and the water level based on different models/measurements. It shows that peaks in SSC (both positive and negative) coincide with bore arrival.

6.4.2 Net sediment transport

In order to know the net sediment transport over time, the (numerical) integral is taken (see Equation 3.17 from Section 3.9.1) over the timeseries ranging from $t=151,6$ s to $t=240,4$ s. These moments are chosen since those are at the same point in the wave group (just before the 1st peak, see Appendix B) and so the entire wave group is taken into account. Those results are presented in Table 6.

Table 6. Net sediment transport over the interval from $t=151,6$ to $t=240,4$. The positive values indicating a net sediment transport towards the shore. The calibration coefficient for the amount of OpenFoam turbulence being 6 and for the analytical turbulence being 3.

| Timeseries | Net sediment transport [kg m ⁻¹] |
|---|--|
| RESIST | -4,01 |
| XBeach | -0,93 |
| Point-model OF hydro | 0,38 |
| Point-model OF hydro incl OF turb | 2,26 |
| Point-model XB hydro | -0,05 |
| Point-model XB hydro incl OF turb | -1,16 |
| Point-model XB hydro incl analytical turb | 24,18 |

These results could be changed slightly by changing the calibration constant (α), which basically determines how much the turbulence is taken into account (see Equation 3.15 in Section 3.8).

6.5 Validating the sediment transport

As described in Section 3.9.2, the sediment transport is also validated by looking at the RESIST bed profiles. When executed, this resulted in a time-average sediment transport at this location of $-6,63 \text{ E-2 kg m}^{-1} \text{ s}^{-1}$. Over the time interval between $t=151,6 \text{ s}$ to $t=240,4 \text{ s}$, this results in a net sediment transport of $-5,89 \text{ kg m}^{-1}$. This is in the same order of magnitude as the *RESIST* value in Table 6. Although the values differ slightly because of the method used when calculating them.

6.6 Quantitative sediment transport results

To quantify these results, again the nRMSE and r^2 values are used. But this time in addition the net sediment transport is taken into account because not only the shape and the Error of the curve matter but also the resultant integral. These quantifications are shown in Figure 36.

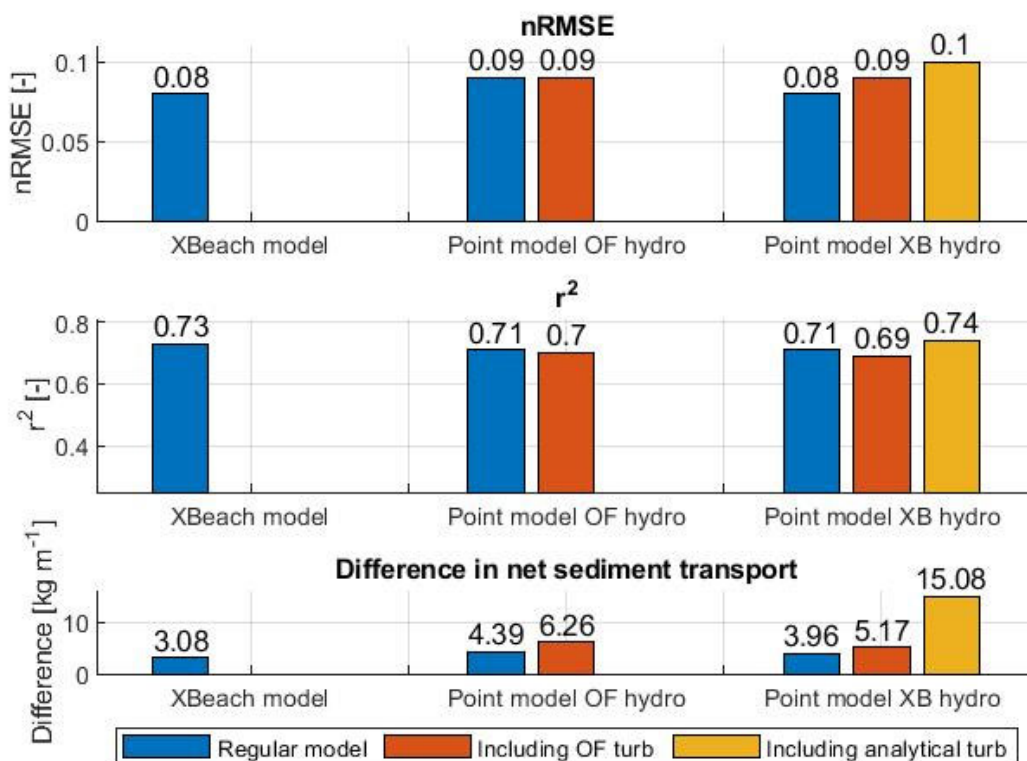


Figure 36. The nRMSE, r^2 and difference in net sediment transport of all timeseries. The difference in net sediment transport in this case is the net sediment transport of the specific timeseries minus the observed net sediment transport.

The difference in net sediment transport of the point-model with XBeach hydrodynamics and the analytical turbulence (yellow bar) in Figure 36 could be lowered by decreasing the calibration coefficient (α). However, this would have a negative influence on the r^2 value. In the end the same results as the blue bar could be achieved if the turbulence is ‘turned off’ by changing this calibration coefficient to zero. Additionally, all the nRMSE and r^2 values are quite good which means that the models could simulate the sediment transport quite well but also that the inclusion of turbulence does not make a significant difference.

6.7 Testing other approaches

To check if these results could be improved, the model was run again but with changing some parameters, which are described in Section 3.10, to see if this would improve the results. These preliminary results are shown below.

6.7.1 Changing the roughness coefficient in XBeach

Instead of using the default Chézy roughness value in XBeach ($55 \text{ m}^{1/2}/\text{s}$), this value is altered to 40, 50, 60 and $70 \text{ m}^{1/2}/\text{s}$. The results are shown below in Figure 37.

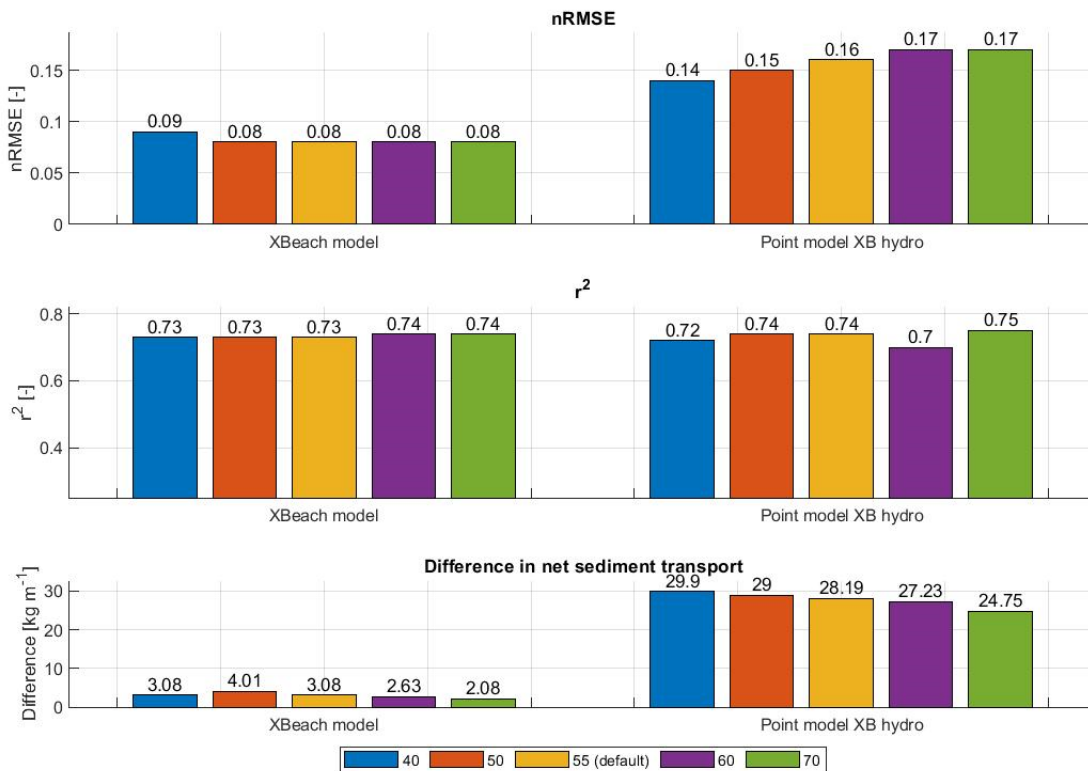


Figure 37. The nRMSE, r^2 and difference in net sediment transport outcomes for the different Chézy roughness coefficients as indicated in the legend of the figure. There has only been looked at the XBeach model and the point-model with XBeach hydrodynamics since the point-model with OpenFoam hydrodynamics does not change when changing XBeach

It shows that changing the roughness coefficient in the XBeach model does not have a significant influence in the outcomes of this research. It could be seen that all validation values for the XBeach model (left planes in Figure 37) are not influenced significantly by the change in roughness since they remain more or less constant throughout the calibration. In addition, it is remarkable that for the point-model (right planes in Figure 37) a higher Chézy roughness coefficient delivers a larger nRMSE while it also delivers a smaller difference in net sediment transport. Although the changes are relatively small. The fact that the difference is so small is also illustrated by the fact that all sediment transport graphs are very similar, see Figure 38.

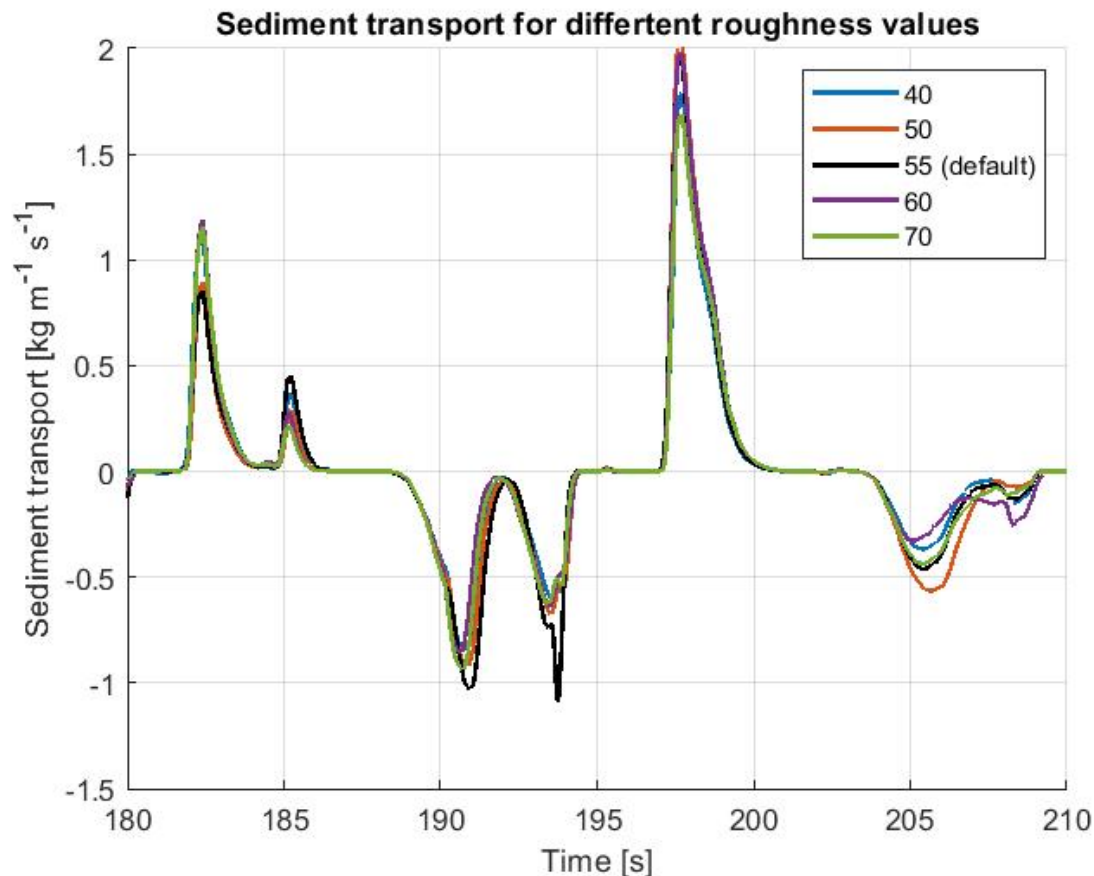


Figure 38. Sediment transport as a result of the point-model but with different Chézy roughness coefficients used in XBeach

This behaviour tells us that a calibration at forehand would not have had a large influence on the results of this research since both the validation values as well as the sediment transport graphs are quite similar.

6.7.2 Varying the OpenFoam turbulence height

Instead of taking the depth-averaged OpenFoam turbulence, the turbulence at 3 cm above the bed was taken (= the heights at which the OBS's and ADVs were installed during the RESIST measurements) to see if this would improve the results. The new OpenFoam turbulence is shown in Figure 39.

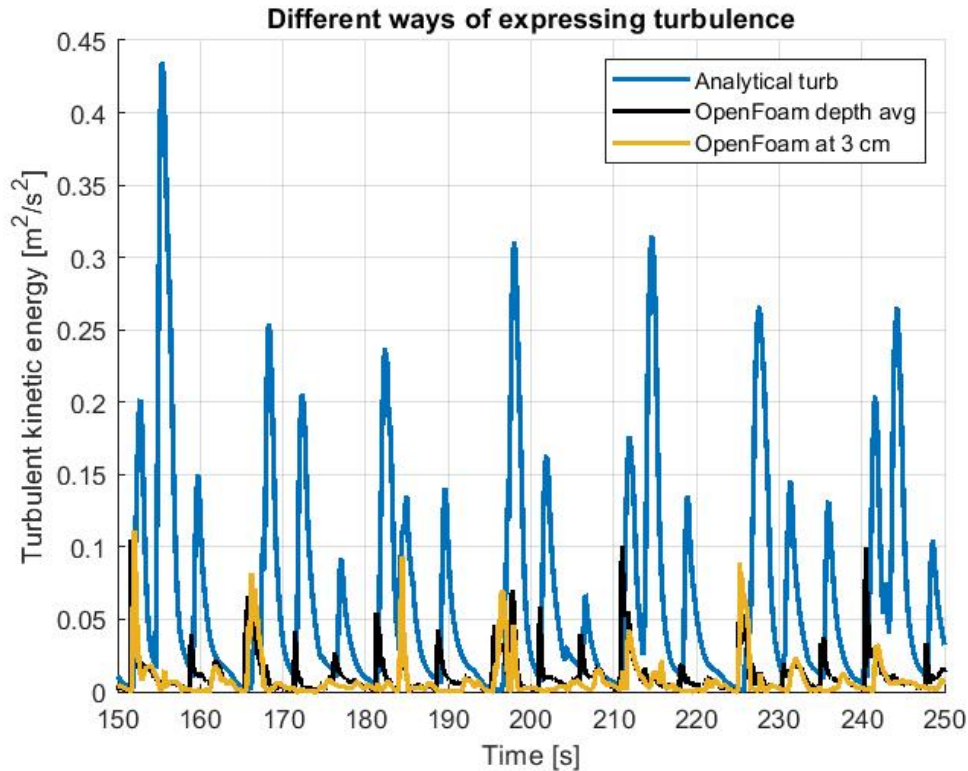


Figure 39. Different turbulence datasets with the new OpenFoam turbulence (yellow graph) in relation to the old OpenFoam turbulence (black graph) and the analytical turbulence (blue graph).

As presented in Figure 39, the turbulence at 3 cm is most of the times lower than the depth-averaged turbulence, except for those moments in time when the water depth is around 3 cm. This can be explained by the fact that the turbulence is generated around the water surface and it dissipates along the vertical distance in the water column. This is also illustrated by Figure 22 - Figure 25 about the propagation of turbulence. Therefore, it is lower at most of the times only but when the water level is around this 3 cm and the turbulence is generated nearby this level.

The way this works out throughout the model is best illustrated by the quantitative validation results. Those values regarding sediment transport as modelled with the new turbulence are shown in Figure 40. As could be seen in Figure 40, the same effect happens as which was the case with the depth-averaged turbulence: it does not really improve the sediment transport. So, the difference between using the depth-averaged or the 3cm OpenFoam turbulence turns out to be very small.

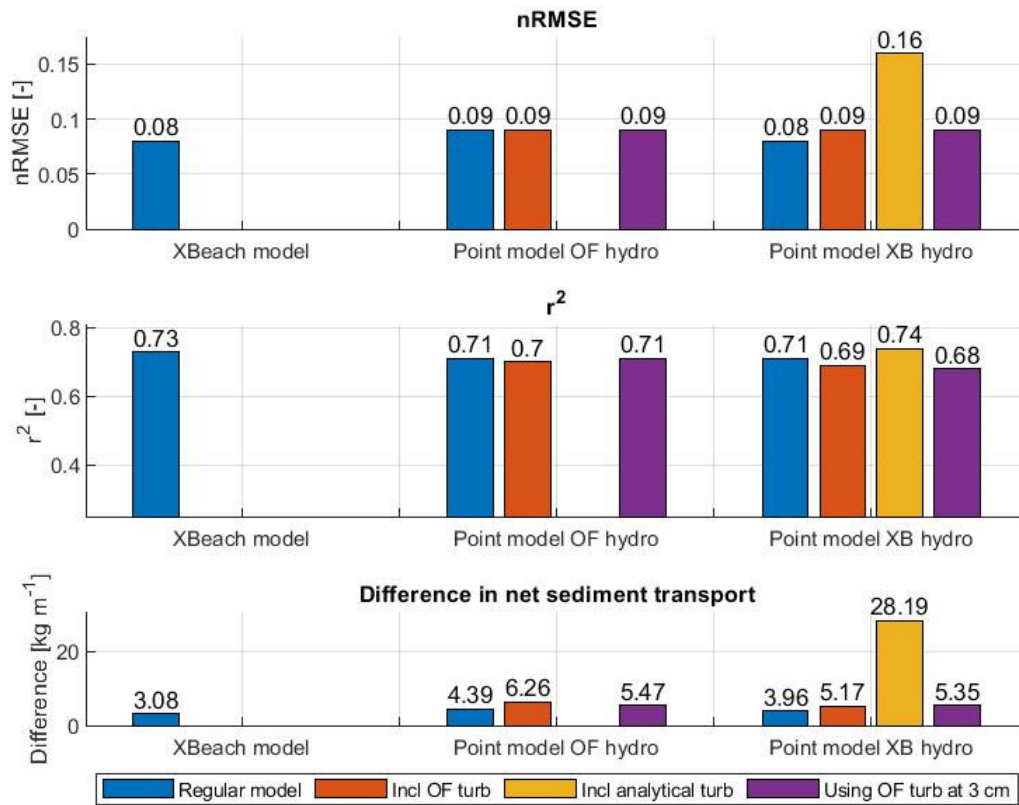


Figure 40. Differences in the quantitative validation of using the depth-averaged OpenFoam turbulence (red bar graphs) versus the OpenFoam turbulence at 3cm from the bed (purple bar graphs). The other bar graphs (blue & yellow) did not change but are presented as a reference.

6.7.3 Varying the analytical turbulence height

Another option is to vary the height at which the analytical turbulence is taken into account in the model. As proposed by Reniers et al. (2013), it could be done with the near-bed turbulence. This then looks the following, see Figure 41.

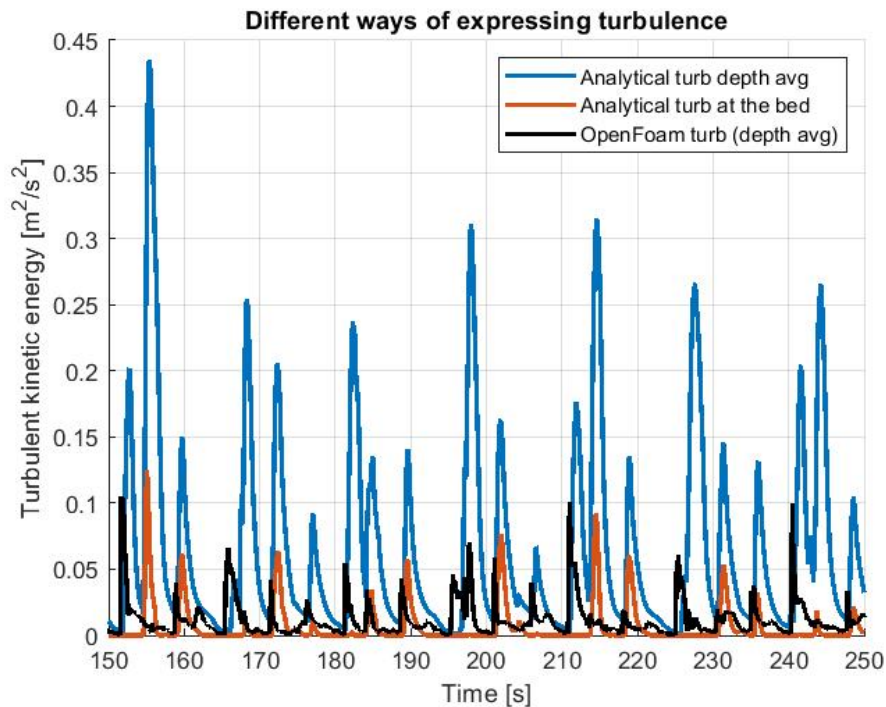


Figure 41. Different turbulence datasets with the new (near-bed) analytical turbulence (red graph) in relation to the old analytical turbulence (blue graph) and the OpenFoam turbulence (black graph).

Again, the turbulence is lower than the 'old' one (which is depth-averaged) because of the vertical dissipation of the turbulence. Also, there is some difference in the moments the peaks occur as well. This is which is probably caused by the variety in the water depths. Turbulence originates at the water surface so the deeper the water is, the more distance the turbulence has to travel to reach the bed (see Figure 22 - Figure 25). So, at some moments the turbulence is almost dissipated completely (in relatively deep water) while at other moments (in relatively shallow water) there still is quite some turbulence left which reaches the bed. To see if this change of turbulence has some effect on modelling the sediment transport, the quantitative results are presented in Figure 42.

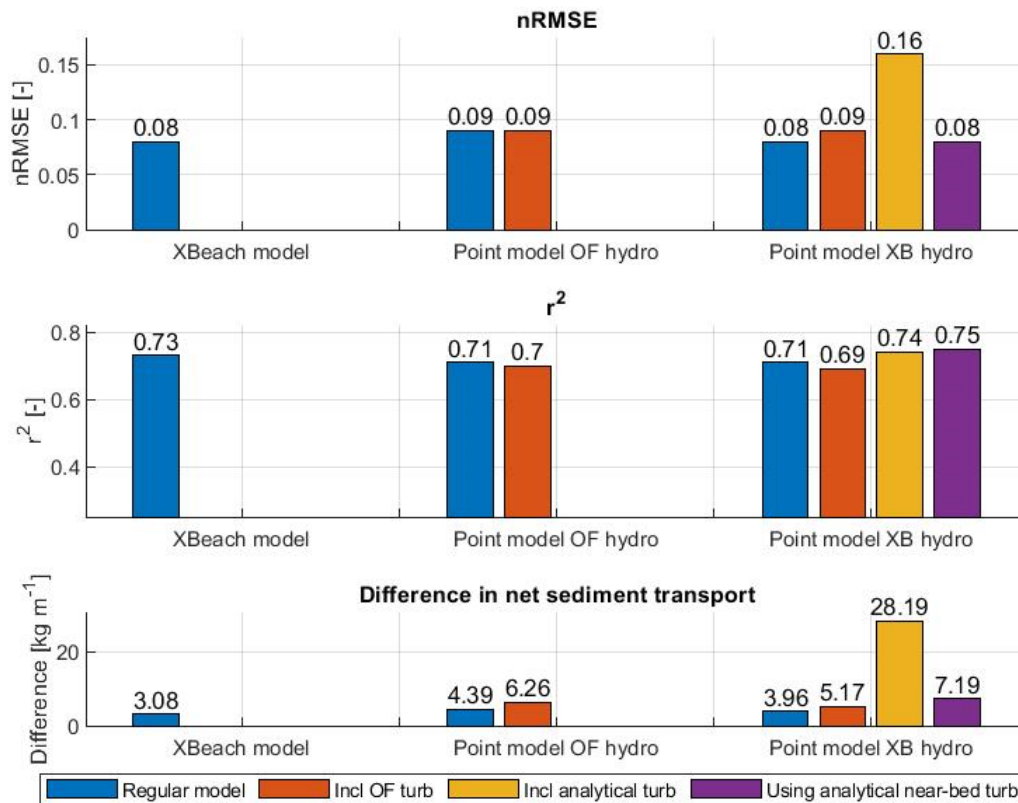


Figure 42. Differences in the quantitative validation of using the depth-averaged analytical turbulence (yellow bar graphs) versus the analytical turbulence at the bed (purple bar graphs). The other bar graphs (blue & red) did not change but are presented as a reference.

These results show that all values could be improved by using the near-bed analytical turbulence instead of the depth-averaged analytical turbulence. This is especially remarkable when looking at the nRMSE and r^2 values since these become even better than when the OpenFoam turbulence is used. Although it is still not a significant improvement when compared to the regular XBeach model.

6.7.4 Assuming a vertical uniformly distributed sediment concentration

When assuming that the sediment is distributed uniformly in the water column, it would mean that the measured SSC is present at every height in the water column and so is equal to the depth-averaged SSC. This would imply that the translation with the Rouse profile is unnecessary and that simply the measured concentration can be multiplied with the water depth and the flow velocity to obtain the sediment transport.

When doing this, the sediment transport looks the following, see Figure 43. The most striking changes are that the positive peaks as well as the negative ones increase in magnitude. As a consequence, they also become sharper which is especially the case for the negative peaks. This change is also illustrated by the net sediment transport, changing from $-4,01 \text{ kg/m}$ to $-14,41 \text{ kg/m}$. This shows that the negative aspect of the sediment transport (so offshore directed transport) is becoming stronger compared to the onshore directed transport when assuming a uniform sediment distribution.

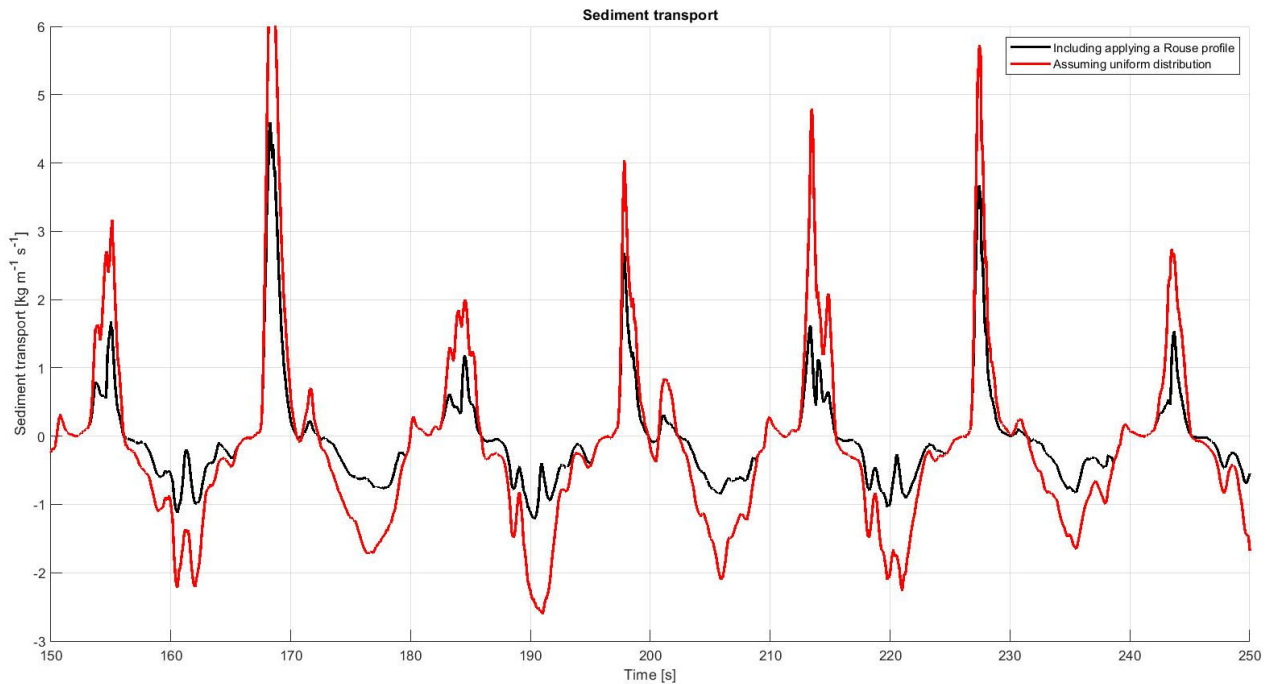


Figure 43. Different sediment transport timeseries. With the 'old' sediment transport based on applying the Rouse profile (black graph) versus the assumed uniformly distributed sediment concentration (red graph)

The way this change works through in the quantitative results, is depicted in Figure 44. It shows that all validation values become worse.

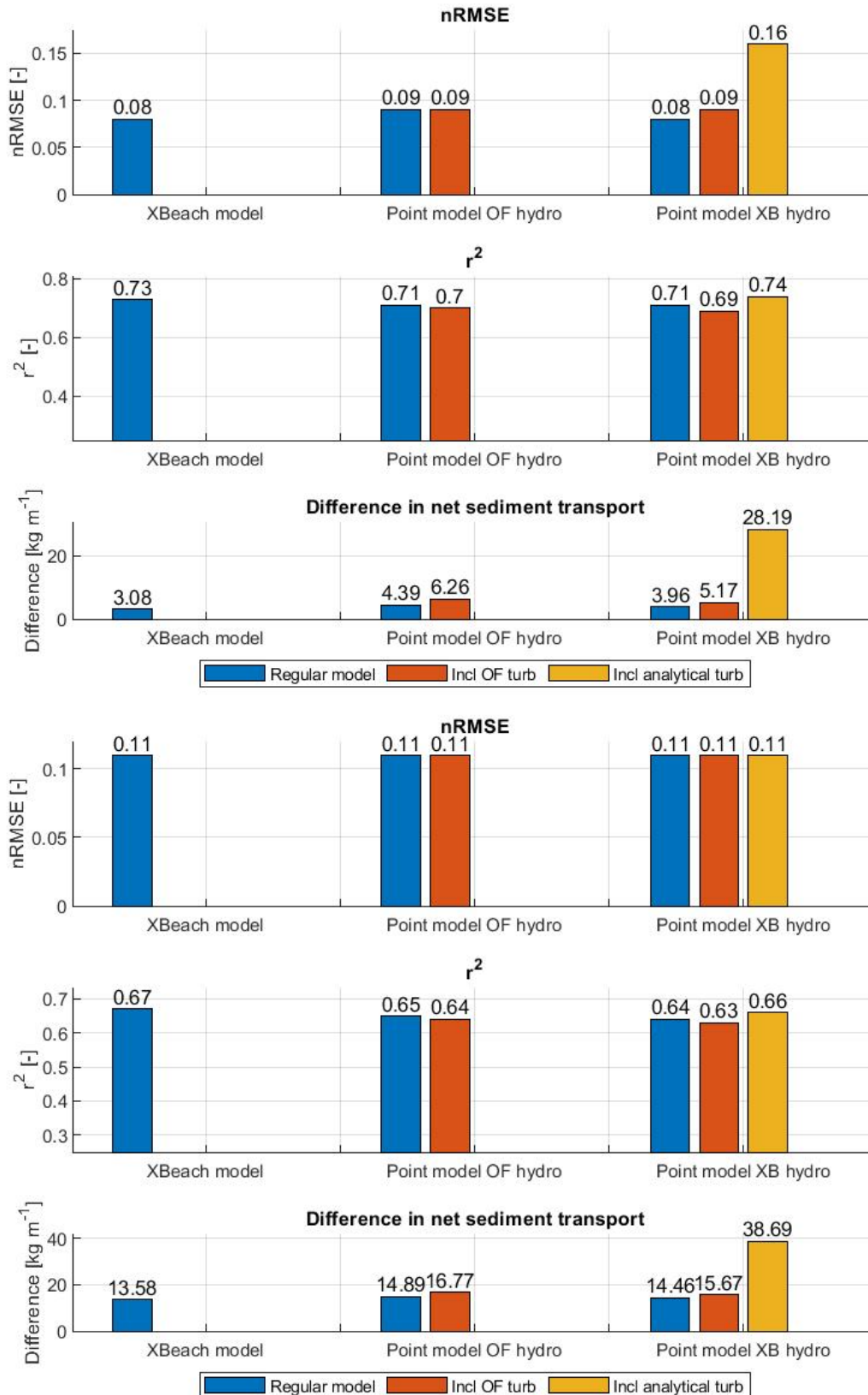


Figure 44. Differences in the quantitative validation of applying a Rouse profile (top) versus using a uniform sediment distribution (bottom). Changing this sediment distribution also has an effect on the validation because the validation is based on comparing experimental values to the depth-averaged observed values (which are changed). Therefore, it is chosen to present and compare all bar graphs between the top and bottom plot.

6.7.5 Using a turbulence-based equilibrium concentration

This turbulence based equilibrium concentration is based on the approach of Reniers et al. (2013) and is described in Section 3.10. Also, the used equation is listed there (Equation 3.19). The most remarkable influence of using this method to model the equilibrium concentration is that it creates peaks in the SSC at different moments in time than the other modelled and measured timeseries, see Figure 45. This is because this method uses the near-bed turbulence (instead of for instance the depth-averaged turbulence) and therefore peaks occur at different moments, this is also showed in Figure 27 in Section 5.4.

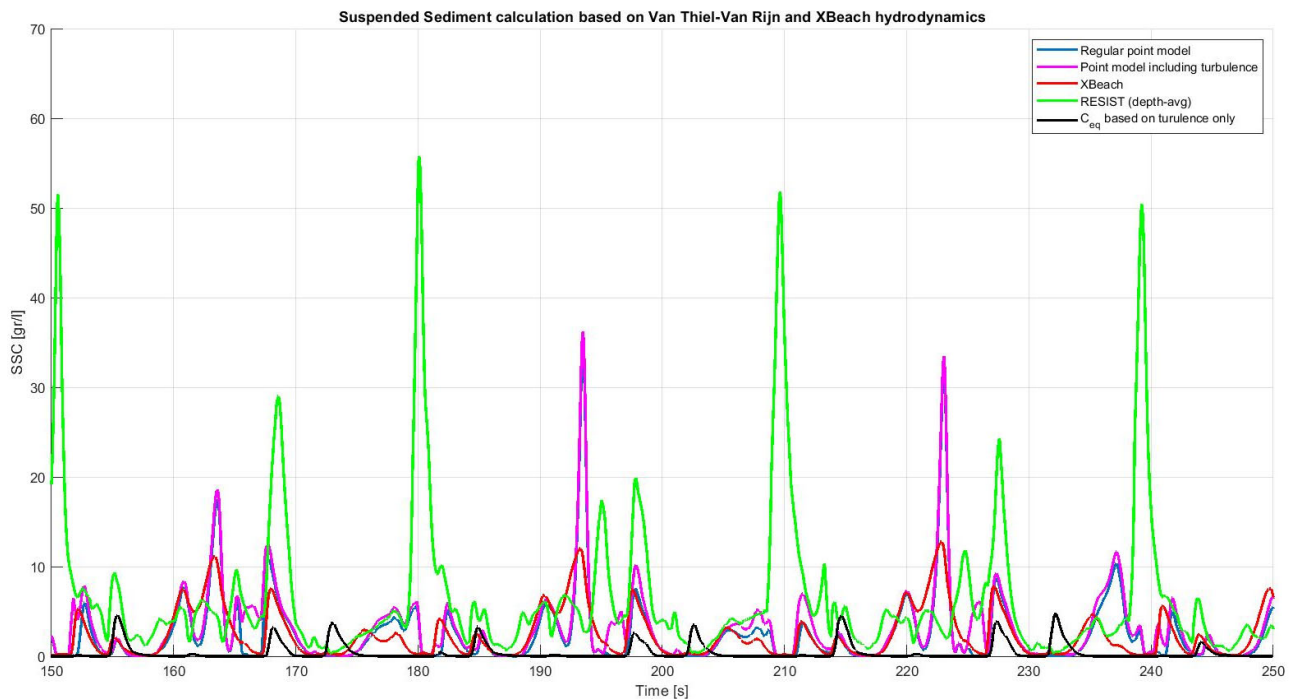


Figure 45. Several SSC graphs, including the SSC modelled with the equilibrium concentration based on the near-bed turbulence only (black graph)

This behaviour also causes the sediment transport to behave in a different way, resulting in an improving nRMSE and net sediment transport but a deteriorating r^2 value (see Figure 46) when compared to the depth-averaged analytical turbulence. However, the results are still worse than using a point-model without turbulence. The results are pretty similar to ones obtained by using the other approach with the analytical near-bed turbulence (see Figure 42).

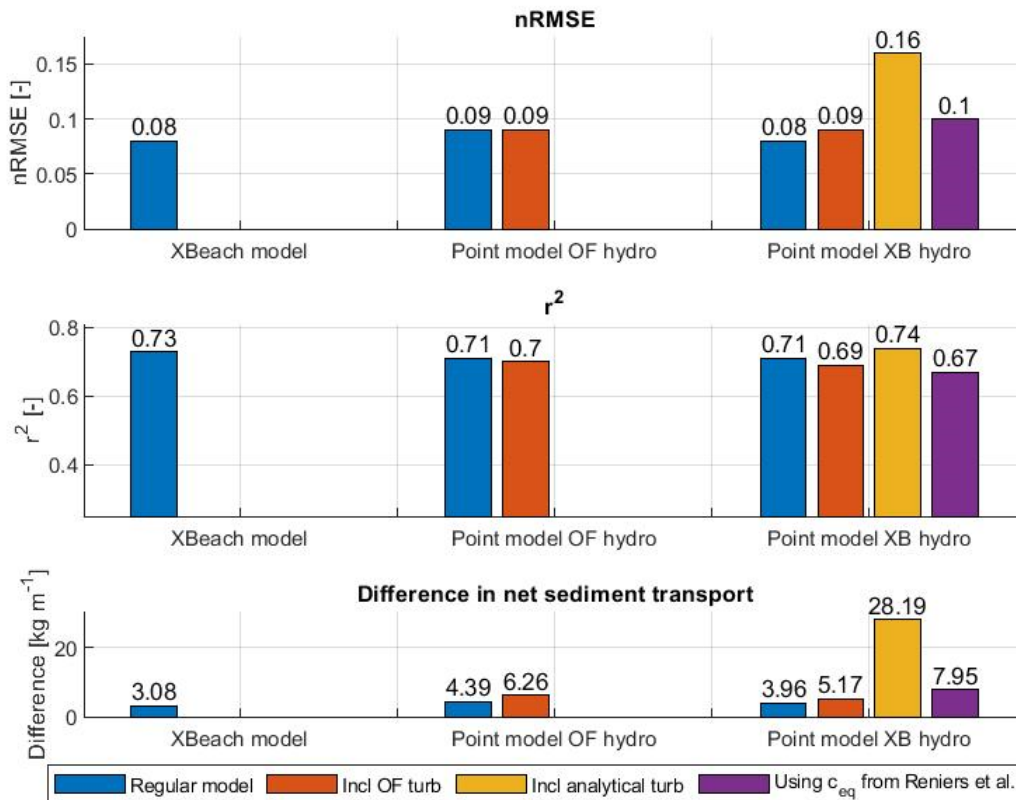


Figure 46. Differences in the quantitative validation of using the VTVR method (yellow bar graphs) versus the method from Reniers et. al (2013) (purple bar graphs). The other bar graphs (blue & red) did not change but are presented as an indication

6.8 Summary

This chapter first shows that the newly calculated sediment concentration depends pretty heavily on the value of the calibration coefficient. Thereafter it shows that, even after calibrating the model, the inclusion of sediment did not improve the modelled suspended sediment concentration significantly. This was the case for both validation values and with both turbulence datasets, expect for this slightly rising r^2 value when the analytical turbulence was included.

For the sediment transport this calibration coefficient was changed in order to have a better match with the observed transport. The overall pattern of the modelled graphs matches quite well with the observed ones. Yet, this is not the case anymore when looked at the net sediment transport over time, this really shows some other outcomes of the model when compared with the observed one. Yet the observed sediment transport was validated by calculating the sediment gain/loss based on two bed profiles and this was quite consistent. Also, the other validation values did not show any (significant) improvement of the model when including turbulence.

Thereafter some assumptions/approaches used in this research were changed in order to evaluate if the results would change as well which could maybe improve the match between the timeseries. Although some changes showed a better match than with the original assumption/approach, the inclusion of turbulence still did not improve the modelled sediment transport when looked at the validation values.

7. Discussion

7.1 Validating XBeach output with RESIST data

It is quite remarkable that both the r^2 and the nRMSE value for the flow velocity become better in the swash zone compared to the offshore location. It was expected to become worse (just as with the water level) since more processes are influencing the behaviour of the wave (breaking, shoaling etc.) in the swash zone than at the offshore location. Yet the hydrodynamics in general are modelled quite good and the validation parameters being approximately the same as in Ruffini et al. (2020).

Besides that, the intensity of the power spectra resulting from the spectral analysis seems somewhat odd. In other words, the first wave component is stronger present in the XBeach results while it is less present in the RESIST measurements. This could imply a flaw in the model set up. A possible explanation for this is the use of the Linear Wave Theory for modelling the boundary conditions of the waves which could be too straightforward. Yet the frequencies at which the wave components returned in the spectral analysis are the same as the ones used for the input and the ones which were observed in the spectral analysis of the RESIST timeseries, meaning the time interval between the arrival of the waves is modelled correctly by XBeach. This is consistent with (Ruffini et al., 2020).

Another remark is the use of the Rouse profile. Since this method is not able to calculate the sediment concentration below the reference height and therefore the SSC values for the lowest 3 cm (which contains most of the sediment) are assumed in a very conservative way. Meaning that the depth-averaged concentration as used in this research is probably lower than the real occurring depth-averaged concentration, as well as in absolute values as in the variation over time. Some researchers even suggest the concentration in the swash zone even to be uniformly distributed over the water depth (e.g. Masselink & Puleo, 2006), which results in an even higher depth-averaged concentration. That is why that approach is also tested in this research.

7.2 The characteristics of turbulence in the swash zone

At first the results of the OpenFoam model are not a perfect representation of the reality. This means that a difference exists between the real occurring turbulence and the turbulence as modelled by OpenFoam. Which in turn could mean that the real occurring turbulence is more/less or is happening at other moments in time than the modelled one. This could have had an influence on the outcomes of this research.

Furthermore, OpenFoam shows a strange bump in the graph of the water depth and the flow velocity (see Figure 20 at Section 5.1). This bump is not present in the RESIST nor the XBeach graph and could therefore point to an error in the setup of the OpenFoam model or in the way OpenFoam models the hydrodynamics.

Since the point-model used in this research could only cope with one value in height, one value for turbulence should be picked representing the turbulence in the entire water column. In this research the depth-averaged turbulence is used since all other parameters are depth-averaged as well. However, the vertical variation or the sensitivity of this are just preliminary investigated in this research. The characteristics of the turbulence even showed that the depth-averaged turbulence is different than the near-bed turbulence (see Figure 21 in Section 5.2).

A striking result of comparing the OpenFoam turbulence with the analytical one was that the shape of both curves look pretty similar (see Figure 27 at Section 5.4). Both curves start with a steep increase (due to bore arrival), followed by a more or less exponential decay which eventually fades to zero or a new steep increase. This similar behaviour shows the way

turbulence arises and vanishes in the system. This implies that using the analytical approach of computing the turbulence is quite a good representation of the turbulence as calculated by OpenFoam.

7.3 Including turbulence in the sediment model

In general, making use of a point-model is obviously a simplification of the real system and of the XBeach model. For instance, advection is neglected (see Equation 2.1 at Section 2.4.2) but also other variations in the horizontal and the vertical plane are not taken into account. Yet it did succeed to add turbulence to the point-model and therewith to the method of modelling the suspended sediment concentration. The way this was performed also showed some differences in the SSC concentration with and without turbulence at moments in time where there was much turbulence present.

7.3.1 SSC calculation

The calculation of the amount of sediment that is brought into suspension depends mainly on the squared flow velocity. This means that a small deviation in the modelled flow velocity could have quite a large influence in the amount of suspended sediment. Additionally, the amount of turbulence and therewith the nRMSE and the r^2 values directly depend on the value of the calibration coefficient α (see Equation 3.15 at Section 3.8). This means that the results are very sensitive to this value and could therefore not be trusted completely, although this value has been calibrated to come to the best quantitative fit.

Furthermore, the nRMSE and r^2 values turned out to be quite sensitive to SSC peaks, while this research also showed that these peaks occur when the water is very shallow. This together makes that matching these peaks is not so relevant since this very shallow water could not transport lots of sediment in an absolute manner.

The final remark about the SSC calculation is the use of the Van Thiel-Van Rijn method to model the suspension of sediment. This methods and underlying equations have been derived and validated in the framework of wave-averaged models (Ruffini et al., 2020). Since this research used this method to evaluate the SSC in an intra-wave way, it might cause some inaccuracies as well. On the other hand this method was already successfully used by Jongedijk (2017) for more or less the same research purposes.

7.3.2 Sediment transport calculation

If the sediment concentration is converted to sediment transport (by multiplying the concentration with the water depth and the flow velocity), the formerly seen changes in SSC due to turbulence diminish because of the very low water depths at those times. In other words: a change in SSC does not necessarily lead to a change in sediment transport because the transport also depends on the water depth and flow velocity. When there is a large SSC but very shallow water, the sediment transport is still very minor. Therefore, the sediment transport looks to depend more on the moments when the flow velocity is high and when the water depth is relatively large than at moments with a high SSC.

Furthermore, this method used to calculate the sediment transport (concentration times flow velocity times water depth) is somewhat simplistic and could deviate from the real occurring sediment transport. For instance, advection and diffusion are not considered which could influence the results. Because sediment is brought into suspension mostly at bore arrival, but it settles somewhere else due to advective processes (Butt & Russell, 1999; Puleo et al., 2000). This means that only focussing at one location neglects the in- or outgoing sediment due to advection and diffusion. Yet when this relatively simplistic method was executed for the observed values,

it did come out in the same order of magnitude as the validation based on different bed profiles, indicating that this method is still tolerable trustworthy.

In addition to the assumptions in the horizontal plane, there are some assumptions in the vertical plane as well that could have influenced the result. For instance, only using one depth-dependent value for the turbulence is not realistic since turbulence originates at the water surface and propagates down while dissipating as well. This research tried to cope with this by using different turbulence values (depth-averaged and near-bed) but this both did not succeed in improving the sediment concentration. Although the comparison between depth-averaged and near-bed turbulence showed some difference between the timing of the peaks, which could be explained by the time it takes the turbulence to propagate downward. This small difference in timing could lead to different results when this turbulence is included in the SSC model. Furthermore, this research does not consider differences in the flow velocity in the vertical plane which are there in reality (Hughes et al., 1997; Masselink & Puleo, 2006) although these differences are likely to be relatively minor in the swash zone, due to the strong mixing and relatively shallow water.

Besides that, all sediment transport graphs look more or less the same and show peaks, positive as well as negative, at approximately the same moments in time. Yet, the net sediment transport of most timeseries turned out to be quite bad when compared to the observed one. Jongedijk (2017) concluded that turbulence is an important process (see also Section 1.2) and that with including it in the sediment transport method, the model predicts accretion instead of erosion. This statement is supported by the results from this research, but this behaviour does not match the observed behaviour and so this is not considered an improvement.

7.4 Testing other approaches

Testing other approaches did show some slightly improving results in the r^2 values but these were associated with an increasing difference in the net sediment transport as well. These results are conflicting and making it hard to draw some firm conclusions. Except for using the near-bed analytical turbulence and the turbulence-based equilibrium concentration, which did improve all validation values significantly. This is probably because of the timing of the near-bed turbulence (see Figure 27 and Figure 39 respectively at Section 5.4 and 6.7.5). But it still did not perform better than the point-model without turbulence, so it is not seen as an improvement.

8. Conclusion and recommendations

8.1 Conclusions

8.1.1 XBeach validation

“To what extent does XBeach model the hydrodynamics and the sediment transport correctly compared to measurements in the RESIST dataset?” – Research question 1

Based on the used techniques and validation values, there can be concluded that XBeach is capable of modelling the hydrodynamics in the deep water and in the swash zone quite well. The water depths and flow velocities show a decent match with the measured ones in the RESIST dataset. Also, the frequencies of the surface elevation and the flow velocities of the wave(s) (groups) does match quite well with the measured ones, as showed with the spectral analysis. However, the sediment concentration is simulated far from good and can be greatly improved. This is consistent with Ruffini et al. (2020).

8.1.2 Characteristics of turbulence

“How does the modelled turbulent kinetic energy behave in the swash zone?” – Research question 2

The turbulence dataset from the OpenFoam model shows that the turbulence originates at the water surface and propagates to the bed afterwards. During this process dissipation takes place which eventually causes the turbulence to fade away. The turbulence also propagates horizontally due to the flowing water. These both effects cause the near-bed turbulence to be smaller in amplitude and occur a few seconds later than the depth-averaged turbulence.

8.1.3 Including turbulence in sediment models

“To what extent could the inclusion of turbulence improve modelled sediment transport?” – Research question 3

Including turbulence to the calculation of the suspended sediment concentration (SSC) does not significantly improve the outcomes of this point-model, as indicated by the nRMSE and r^2 values. The inclusion of turbulence does create some higher SSC values, which were not present in the regular point-model, but this does not contribute to a better match.

According to these results, the transport of sediment is not improved by the inclusion of turbulence as well. The amount of transport sediment looks to depend more on high flow velocities and relatively deep water than at a large SSC.

Even when changing something in the used assumptions/approach of this research, the conclusion that the inclusion of turbulence does not improve the sediment transport still stands. So based on these tests, there could be concluded that using another calibration coefficient in XBeach or assuming uniformly distributed sediment does not have a significant influence on the way sediment transport is modelled. Although using the near-bed analytical turbulence and using the turbulence-based equilibrium concentration, showed better results than the original approach, it still was not better than the point-model without turbulence. Indicating that the results look promising to use in further research but that based on this research these changes do not contribute to a better sediment transport model.

8.2 Recommendations

As stated by Masselink & Puleo (2006), advection is a very important process in sediment transport. Yet this process is not considered in this research since this research made use of a

point-model. The strongest recommendation would therefore be that a 2DH-model should be used to include advection (and horizontal diffusion) in the way sediment transport is modelled. Logically it would be best to do this with XBeach straight away, but a different 2DH-model will probably also improve the outcomes greatly.

By doing this it will also be beneficial to use a turbulence dataset which is measured instead of modelled. As seen OpenFoam is quite a good but not a perfect representation of reality and therefore deviations are present in the dataset which could have had an influence on the results. Besides that, the preliminary results of using the near-bed analytical turbulence or the turbulence-based equilibrium concentration show a better match with the observed values than the original approach, meaning that it could help to use these in further research.

Another remark is that it would be nice to perform such a research by using a reference concentration model instead of a model based on the equilibrium concentration. Since this research used a quite conservative way of applying the Rouse profile, a reference concentration model would probably be more accurate.

The last recommendation is about the data, it would be beneficial for the comparison to have more measurements of the sediment concentration and flow velocity in the vertical plane. This would improve the depth-averaged sediment concentration and the velocity profile which are both very important in the sediment transport model. By doing so, a better model could be used, with height-dependent values for the flow velocity and sediment. Consequently, the turbulence could vary over the height as well. Resulting in a more truthful turbulence profile by which especially the near-bed turbulence value could be improved.

References

- Blenkinsopp, C. E., Turner, I. L., Masselink, G., & Russell, P. E. (2011). Swash zone sediment fluxes: Field observations. *Coastal Engineering*, 58(1), 28–44. <https://doi.org/10.1016/j.coastaleng.2010.08.002>
- Butt, T., & Russell, P. (1999). Suspended sediment transport mechanisms in high-energy swash. *Marine Geology*. [https://doi.org/10.1016/S0025-3227\(99\)00043-2](https://doi.org/10.1016/S0025-3227(99)00043-2)
- Chardón-Maldonado, P., Pintado-Patiño, J. C., & Puleo, J. A. (2016). Advances in swash-zone research: Small-scale hydrodynamic and sediment transport processes. *Coastal Engineering*, 115, 8–25. <https://doi.org/10.1016/j.coastaleng.2015.10.008>
- Curtis, J. A. (2006). *Summary of Optical-Backscatter and Suspended-Sediment Data, Tomales Bay Watershed, California, Water Years 2004, 2005, and 2006*. Retrieved from <http://www.usgs.gov/pubprod>
- Deltares. (n.d.). XBeach - Deltares. Retrieved January 2, 2020, from <https://www.deltares.nl/nl/software/xbeach-2/>
- Dingemans, M. W. (1994). Water wave propagation over uneven bottoms. *TU Delft*, PHD Thesis.
- Eichentopf, S., Baldock, T. E., Cáceres, I., Hurther, D., Karunarathna, H., Postacchini, M., ... Alsina, J. M. (2019). Influence of storm sequencing and beach REcovery on Sediment TransporT and beach resilience (RESIST). In *HYDRALAB+ Joint User Meeting*.
- Eichentopf, S., Van der Zanden, J., Cáceres, I., Baldock, T. E., & Alsina, J. M. (2020). Influence of storm sequencing on breaker bar and shoreline evolution in large-scale experiments. *Coastal Engineering*. <https://doi.org/10.1016/j.coastaleng.2020.103659>
- Elfrink, B., & Baldock, T. E. (2002). Hydrodynamics and sediment transport in the swash zone: A review and perspectives. *Coastal Engineering*. [https://doi.org/10.1016/S0378-3839\(02\)00032-7](https://doi.org/10.1016/S0378-3839(02)00032-7)
- Fredsøe, J., & Deigaard, R. (1992). *Mechanics of coastal sediment transport. Journal of Chemical Information and Modeling* (Vol. 3). World Scientific. <https://doi.org/10.1017/CBO9781107415324.004>
- Galappatti, G., & Vreugdenhil, C. B. (1985). A depth-integrated model for suspended sediment transport: Journal of Hydraulic Research: Vol 23, No 4. *Journal of Hydraulic Research*, 23(4), 359–377. Retrieved from <https://www.tandfonline.com/doi/abs/10.1080/00221688509499345>
- Galiforni Silva, F., Wijnberg, K. M., & Hulscher, S. J. M. H. (2020). Storm-induced sediment supply to coastal dunes on sand flats, (2006), 335–350.
- Hoonhout, B. (2011). XBeach - XBeach - Deltares Public Wiki. Retrieved January 2, 2020, from <https://publicwiki.deltares.nl/display/XBEACH/XBeach>
- Hughes, M. G., Masselink, G., & Brander, R. W. (1997). Flow velocity and sediment transport in the swash zone of a steep beach. *Marine Geology*, (138), 91–103.
- Jacobsen, N. G., Fuhrman, D. R., & Fredsøe, J. (2011). A wave generation toolbox for the open-source CFD library: OpenFoam. *International Journal for Numerical Methods in Fluids*, 65(October 2010), 236–253. <https://doi.org/10.1002/flid>
- Jenniskens, M. J. J. (2001). Comparison of the sediment transport formulae according to Bijker and Van Rijn. *TU Delft*, Thesis.
- Jongedijk, C. E. (2017). Improving XBeach non-hydrostatic model predictions of the swash morphodynamics of intermediate-reflective beaches. *TU Delft*, MSc Thesis.
- Kranenburg, J. W. M. (2020). Numerical modelling of intraswash processes (Literature report). *University of Twente*, (in preperation).
- Masselink, G., & Puleo, J. A. (2006). Swash-zone morphodynamics. *Continental Shelf Research*, 26(5), 661–680. <https://doi.org/10.1016/j.csr.2006.01.015>
- Menter, F. R. (1993). Fluid Dynamics, Plasmadynamics, and Lasers Conference. In *23rd Fluid Dynamics, Plasmadynamics, and Lasers Conference*.
- Métivier, F., & Meunier, P. (2003). Input and output mass flux correlations in an experimental

- braided stream. Implications on the dynamics of bed load transport. *Journal of Hydrology*, 27(1–4), 22–38. Retrieved from http://www.geologie.ens.fr/~meunier/Geo_3c.html
- Nielsen, P. (2006). Sheet flow sediment transport under waves with acceleration skewness and boundary layer streaming. *Coastal Engineering*, 53(9), 749–758. <https://doi.org/10.1016/j.coastaleng.2006.03.006>
- O'Donoghue, T., Pokrajac, D., & Hondebrink, L. J. (2010). Laboratory and numerical study of dambreak-generated swash on impermeable slopes. *Coastal Engineering*, 57(5), 513–530. <https://doi.org/10.1016/j.coastaleng.2009.12.007>
- Posanski, D. (2018). *STENCIL GWK experiments May - June 2018 Net transport rates analysis - Preliminary version*.
- Pritchard, D., & Hogg, A. J. (2003). Suspended sediment transport under seiches in circular and elliptical basins. *Coastal Engineering*, 49(1–2), 43–70. [https://doi.org/10.1016/S0378-3839\(03\)00046-2](https://doi.org/10.1016/S0378-3839(03)00046-2)
- Puleo, J. A., Beach, R. A., Holman, R. A., & Allen, J. S. (2000). Swash zone sediment suspension and transport and the importance of bore-generated turbulence. *Journal of Geophysical Research: Oceans*, 105(C7), 17021–17044. <https://doi.org/10.1029/2000jc900024>
- Randall, R. B. (2008). Spectral Analysis and Correlation. In *Handbook of Signal Processing in Acoustics* (pp. 33–52). Springer New York. https://doi.org/10.1007/978-0-387-30441-0_3
- Reniers, A. J. H. M., Gallagher, E. L., Macmahan, J. H., Brown, J. A., Van Rooijen, A. A., Van Thiel de Vries, J., & Van Prooijen, B. C. (2013). Observations and modeling of steep-beach grain-size variability. *Journal of Geophysical Research: Oceans*, 118(March 2012), 577–591. <https://doi.org/10.1029/2012JC008073>
- Roelvink, D., Mccall, R., Mehvar, S., Nederhoff, K., & Dastgheib, A. (2018). Improving predictions of swash dynamics in XBeach : The role of groupiness and incident-band runup. *Coastal Engineering*, 134(July 2017), 103–123. <https://doi.org/10.1016/j.coastaleng.2017.07.004>
- Roelvink, D., & Reniers, A. (2011). *A Guide to Modeling Coastal Morphology* (Vol. 12). World Scientific. <https://doi.org/10.1142/7712>
- Roelvink, D., Reniers, A. J. H. M., van Dongeen, A., Van Thiel de Vries, J., Mccall, R., & Lescinski, J. (2009). Modelling storm impacts on beaches , dunes and barrier islands. *Coastal Engineering*, 56(11–12), 1133–1152. <https://doi.org/10.1016/j.coastaleng.2009.08.006>
- Roelvink, D., & Stive, M. F. J. (1989). Bar-generating cross-shore flow mechanisms on a beach. *Journal of Geophysical Research*, 94(C4), 4785–4800. <https://doi.org/10.1029/JC094iC04p04785>
- Rooijen, A. A. Van. (2011). Modelling sediment transport in the swash zone. *TU Delft*, MSc Thesis.
- Ruffini, G., Briganti, R., Alsina, J. M., Brocchini, M., Dodd, N., & Mccall, R. (2020). Numerical modeling of flow and bed evolution of bichromatic wave groups on an intermediate beach using nonhydrostatic xbeach. *Journal of Waterway, Port, Coastal and Ocean Engineering*, 146(1). [https://doi.org/10.1061/\(ASCE\)WW.1943-5460.0000530](https://doi.org/10.1061/(ASCE)WW.1943-5460.0000530)
- Smit, P., Stelling, G. S., Roelvink, D., Van Thiel de Vries, J., Mccall, R., van Dongeren, A., ... Jacobs, R. (2009). *XBeach : Non-hydrostatic model Delft University of Technology and Deltares*.
- Teles, V., Chauveau, B., Joseph, P., Weill, P., & Maktouf, F. (2016). CATS – A process-based model for turbulent turbidite systems at the reservoir scale *Comptes Rendus Geoscience* CATS – A process-based model for turbulent turbidite systems at the reservoir scale. *Comptes Rendus Geoscience*, (June). <https://doi.org/10.1016/j.crte.2016.03.002>
- Van der Zanden, J., Fernández-Mora, À., van der A, D., Hurther, D., Cáceres, I., O'Donoghue, T., & Ribberink, J. (2017a). Inclusion of wave breaking turbulence in reference concentration models. *Coastal Dynamics*, 102(4), 24–25. <https://doi.org/10.1002/ejsp.2570>
- Van der Zanden, J., Fernández-Mora, À., van der A, D., Hurther, D., Cáceres, I., O'Donoghue, T., & Ribberink, J. S. (2017b). Inclusion of wave breaking turbulence in reference concentration models. *Coastal Dynamics*, 102(4), 24–25. <https://doi.org/10.1002/ejsp.2570>
- van Rijn, L. C. (2007a). Unified view of sediment transport by currents and waves. I: Initiation of Motion, Bed Roughness, and Bed-Load Transport. *Journal of Hydraulic Engineering*, 133(7),

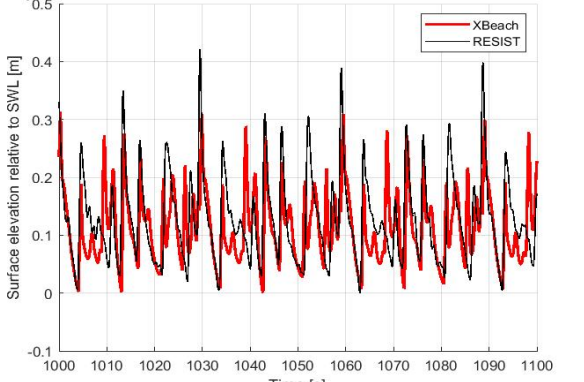
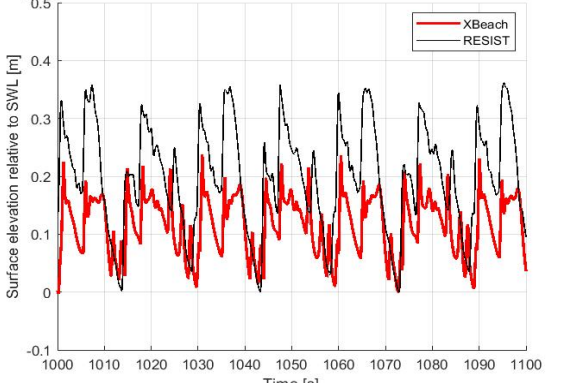
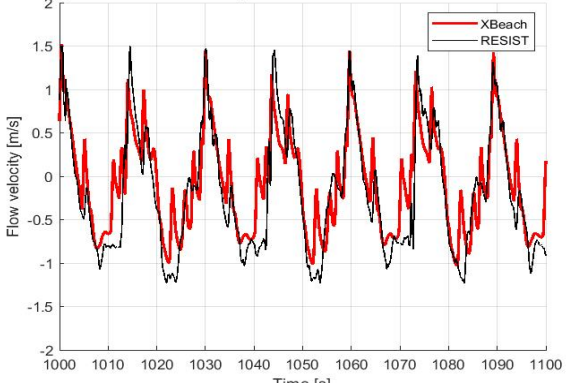
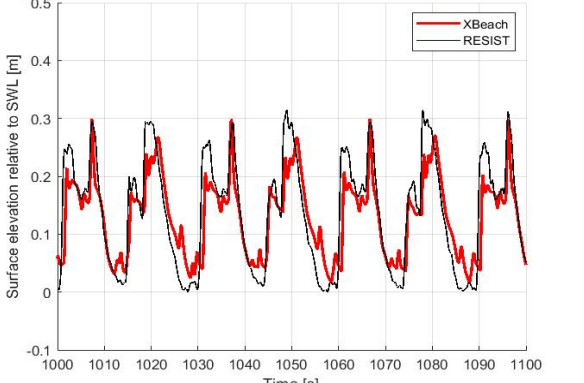
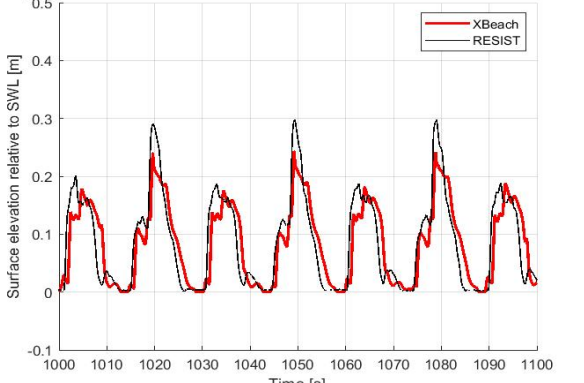
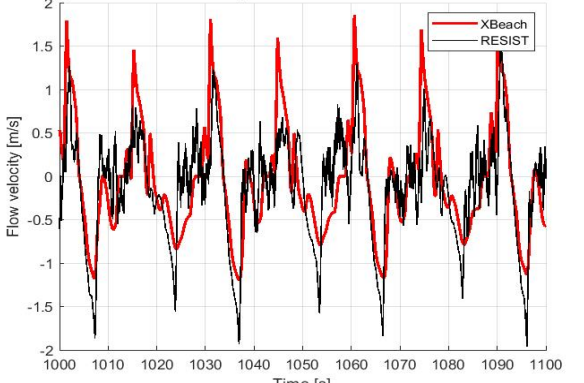
761. [https://doi.org/10.1061/\(ASCE\)0733-9429\(2007\)133:7\(761\)](https://doi.org/10.1061/(ASCE)0733-9429(2007)133:7(761))
- van Rijn, L. C. (2007b). Unified view of sediment transport by currents and waves. II: Suspended Transport. *Journal of Hydraulic Engineering*, 133(7), 776. [https://doi.org/10.1061/\(ASCE\)0733-9429\(2007\)133:7\(776\)](https://doi.org/10.1061/(ASCE)0733-9429(2007)133:7(776))
- Van Thiel de Vries, J. (2009). Dune erosion during storm surges. *Deltares Select Series*.
- van Weeghel, L. (2020). Literature study. *University of Twente*.
- Zeltkevic, M. (1998, April 15). Forward and Backward Euler Methods. Retrieved April 28, 2020, from http://web.mit.edu/10.001/Web/Course_Notes/Differential_Equations_Notes/node3.html

Appendix A

| Distance from wave paddle [m] | Water level comparison | | Flow velocity comparison | |
|-------------------------------|------------------------|-------|--------------------------|----------------|
| | r ² | nRMSE | r ² | nRMSE |
| 71,8 | 0,35 | 0,216 | - ¹ | - ¹ |
| 74,7 | 0,57 | 0,332 | 0,82 | 0,151 |
| 76,5 | 0,80 | 0,189 | - ¹ | - ¹ |
| 77,5 | 0,81 | 0,174 | 0,67 | 0,149 |

1. There was no ADV present at these locations in the RESIST dataset

The associated graphs are presented on the next page.

| Distance from wave paddle [m] | Water level comparison | Flow velocity comparison |
|-------------------------------|--|---|
| 71,8 | <p>Comparison in water surface elevation between XBeach and RESIST at X=71.8 m</p>  | - |
| 74,7 | <p>Comparison in water surface elevation between XBeach and RESIST at X=74.7 m</p>  | <p>Comparison in flow velocity between XBeach and RESIST at X=74.7 m</p>  |
| 76,5 | <p>Comparison in water surface elevation between XBeach and RESIST at X=76.5 m</p>  | - |
| 77,5 | <p>Comparison in water surface elevation between XBeach and RESIST at X=77.6 m</p>  | <p>Comparison in flow velocity between XBeach and RESIST at X=77.5 m</p>  |

Appendix B

